

Cover Page

Date submitted: 14 January 2025

Reporting Period: Oct 2018 – Oct 2024

Cooperator Contact Information:

Paul Angermeier
Virginia Cooperative Fish and Wildlife Research Unit
Dept. of Fish and Wildlife Conservation
Virginia Tech
Blacksburg, VA 24061-0321
540-231-4501; biota@vt.edu

Cooperator Project Title:

Evaluating Efficacy of Agricultural BMPs

Final Performance Report

By:

Joshua Mouser
Department of Fish and Wildlife Conservation, Virginia Tech, Blacksburg, VA 24061

and

Serena Ciparis
U.S. Fish and Wildlife Service, Virginia Field Office, Gloucester, VA 23061
(Office location: Virginia Tech, Blacksburg, VA 24061)

For:

Charles Rewa
NRCS Resource Inventory and Assessment Division
Beltsville, MD 20705

Progress Summary:

Task 1: *Characterize spatial patterns of conservation practice (CP; best management practices or BMPs in previous reports) implementation and predicted sediment and nutrient loading in the upper Clinch, Powell, and Holston watersheds (CPH).*

We obtained CP data from the Natural Resources Conservation Service (NRCS) and the Virginia Department of Conservation and Recreation (VDNR) for the CPH in southwest Virginia. We also collated data needed to run the Soil and Water Assessment Tool (SWAT) including topography, stream network, land use, soil, climate, streamflow, and water quality. We then calibrated the SWAT+ model for estimated streamflow (m^3/sec), sediment loads (metric tons), nitrogen loads (kg), and phosphorus loads (kg) from 2004–2009 for daily (per d) and monthly (per m) time steps. To calibrate the model, we compared sediment and nutrient loads predicted by the SWAT+ model to values measured in streams within our study area and adjusted model parameters (e.g., the erodibility of the soil) until the predicted values were similar to measured values as indicated by Nash-Sutcliffe efficiency values >0.5 . Adjusting channel width and depth according to a regional model led to the greatest improvements in the SWAT+ model's ability to predict streamflow. Further, increasing the movement rate of water through the soil (i.e., soil hydraulic conductivity) and decreasing the amount of water the soil can hold (i.e., soil-available water capacity) improved model performance for streamflow. We found that reducing channel erodibility from the default of 0.01 to $0.00002 \text{ cm}^3/\text{N-s}$ (i.e., making the bed and bank material of the stream channel less prone to erosion) led to the greatest improvements in estimating sediment loads. Finally, we were unable to determine any parameters that improved predictions for nitrogen and phosphorus loads. After calibration, we assessed the SWAT+ model's ability to predict sediment and nutrient loads from 2010–2021. We found that SWAT+ predicted streamflow well, had mixed success predicting sediment loads, overpredicted nitrogen loads, and did not predict phosphorus loads well.

Task 2: *Analyze the influences of CPs, relative to other watershed features, on predicted sediment and nutrient loads in HUC12s across the upper CPH, excluding those encompassing mainstem rivers and those in the Cumberland Plateau coalfields.*

We extracted landscape data and pollutant yields for each landscape unit from the SWAT+ model. We then used multiple linear regression models to relate landscape data to the estimated pollutant yields. Interestingly, greater proportions of agricultural land within landscape units were associated with declines in sediment (metric tons/ha/yr) and nitrogen (kg/ha/yr) yields and increases in phosphorus yields (kg/ha/yr) but agricultural land use was a weak predictor in all models. In contrast, we found that sediment and nitrogen yields were positively associated with increasing urban land use, but phosphorus yields were negatively associated with increasing urban land use, which suggests that urban lands may be a strong driver of sediment and nitrogen budgets within the SWAT+ model. It is well known that agricultural land use, especially cattle grazing, contributes to excessive sediment loads in our study area; therefore, SWAT+ is not capturing the key pathways through which cattle grazing is contributing sediment to streams (i.e., streambank erosion). We also found that soil erodibility and hydraulic conductivity influence sediment and nutrient yields.

Task 3: *Quantify relations among CP implementation, observed instream water quality and habitat quality, and observed biotic assemblages at the spatial resolution of HUC12s or larger (depending on spatial distribution of existing data).*

We mapped CP installation intensity, sediment yield (metric tons/ha/yr), phosphorus yield (kg/ha/yr), and nitrogen yield (kg/ha/yr) to streams in each HUC-12 watershed of the CPH. We also collected macroinvertebrate and instream data from 31 sites within the Copper Creek, Laurel Creek, Big Moccasin Creek, and Big Cedar Creek HUC-10 watersheds (Clinch River and North Fork Holston River HUC-8 watersheds) from fall 2019 to spring 2022, for a total of 154 collections. We ran mixed-effect linear regression models to determine the effects of water quality, instream habitat, and CPs on the proportion of macroinvertebrate individuals collected classified as Ephemeroptera, Plecoptera, or Trichoptera taxa (EPT). These taxa are intolerant to many anthropogenic impacts on streams. Surprisingly, CP density within a subbasin (number/ha) had a quadratic relationship with proportion of EPT individuals, with increased proportions of EPT individuals at low CP densities and decreased proportions of EPT individuals at high CP densities. To better understand the quadratic relationship, we built several models that represented the pathways through which CPs affect the macroinvertebrate community. First, we assessed the effects of CPs on water quality and habitat using simple linear, exponential decay, and linear plateau models. Then, we assessed effects of water quality and habitat on the macroinvertebrate community using Threshold Indicator Analysis. Overall, CPs tended to improve or stabilize water quality and instream habitat above certain implementation thresholds, and changes in water quality and habitat influenced the structure of the aquatic community. Many of the relationships we observed depended on the amount of agricultural land use within the watershed; therefore, sites were grouped into categories of agricultural extent and CP density, and relationships were explored using Analysis of Variance (ANOVA). Results from the ANOVA confirmed previous results and also revealed that proportion EPT individuals appeared to increase at sites with medium agriculture and high CP density compared to those with medium agriculture and low CP density. Our inability to detect direct effects of CPs on the macroinvertebrate community at high agriculture sites suggests that improvements in water quality and habitat due to CP implementation have not been large enough or occurring for a long enough time to produce measurable effects.

Task 4: *Quantify cost-effectiveness of CP implementation in HUC12s across the upper CPH, excluding those encompassing mainstem rivers and those in the Cumberland Plateau coalfields.*

We were unable to complete task 4 because the SWAT+ model was unable to simulate the effects of cattle grazing, precluding our ability to create realistic scenarios of CP implementation.

Section 5: Management implications

We combined the results from all tasks to map the landscape units where CPs are most likely to achieve the greatest biotic response. We overlaid maps showing the landscape units with greatest sediment yields, medium amounts of agricultural land use, and areas where additional CPs could overcome implementation thresholds. We identified 148 landscape units that would most benefit from additional CP installation in terms of achieving desirable biotic responses.

Task 1: *Characterize spatial patterns of CP implementation and predicted sediment and nutrient loading in the upper CPH.*

- 1. Consult databases maintained by state and federal agencies to compile a complete database of all agricultural CPs (including cost, type, location, date, and dimensions) implemented in the upper CPH. Expected sediment and nutrient reductions by CPs also will be summarized.*
- 2. Compile publicly available data on other watershed features (e.g., soils, topography, land use, precipitation) needed to run SWAT models. SWAT models will be calibrated with discharge and turbidity data available from the U.S. Geological Survey (USGS).*
- 3. Use SWAT to estimate stream discharge and sediment and nutrient loads at daily time-steps for all HUC12s in the upper CPH, excluding those encompassing mainstem rivers and those in the Cumberland Plateau coalfields.*

Task 1.1:

Caveats:

Due to recent policy changes, the VDCR was unable to provide georeferenced CP data after 2021. Therefore, the VDCR data were only used for site selection for task three and were excluded from data analyses in task three.

Methods:

We obtained CP databases from the NRCS and the VDCR, then trimmed those databases to retain only CPs that influence water quality. In addition to practice code and name, the VDCR database contained practice completion date and lifespan, and the NRCS database contained applied spatial extent of each practice. We determined the goal of each practice from the VDCR cost share manual (VDCR 2019) and the NRCS conservation practice standards (NRCS 2019a). We removed practices from both databases that were either not focused on agricultural management, or not aimed at sediment or nutrient reduction. We then determined the expected pollutant reductions and the implementation cost for fencing and prescribed grazing because these are common CPs that provide a useful contrast for the scenarios described in task 2.1 of the 2023 report.

Results:

The NRCS database had almost ten times the number of records as the VDCR database. The VDCR database contained 39 unique CPs that were implemented 7,149 times. The most common CPs implemented by the VDCR were stream exclusion with grazing management ($n = 2,355$), riparian forest buffer ($n = 1,057$), woodland buffer filter area ($n = 1,051$), small grain and mixed cover crop ($n = 883$), and harvestable cover crop ($n = 571$). The NRCS database contained 92 unique CPs, which have been implemented 68,391 times. The most common CPs were prescribed grazing ($n = 10,296$), fencing ($n = 9,565$), watering facilities ($n = 7,878$), pipeline installation ($n = 6,122$), nutrient management ($n = 5,073$), access control ($n = 4,095$), forage harvest management ($n = 2,631$), and brush management ($n = 2,521$). Fencing with an associated riparian buffer is expected to reduce nitrogen, phosphorus, and sediment by 41%, 34%, and 46%, respectively and have a total annualized cost of \$284 per acre (Chesapeake Bay Program 2020). Prescribed grazing is not quite as effective as fencing (nitrogen reduction = 10%, phosphorus

reduction = 24%, and sediment reduction = 30%) but total annualized costs are only \$16 per acre (Chesapeake Bay Program 2020).

Task 1.2:

Methods/Results:

We compiled topography, stream network, land use, soil, climate, streamflow, and water quality data to run and calibrate the SWAT+ model (Table 1.2.1). Topography data (30-m resolution) were obtained from the National Elevation Dataset (NED; USGS 2019a). Stream network data were downloaded from the National Hydrography Dataset Plus Version 2 (NHD+; U.S. Environmental Protection Agency [USEPA] and USGS 2012) to assist with watershed delineation. We downloaded both the State Soil Geographic (STATSGO) and Soil Survey Geographic Database (SSURGO) soil layers (NRCS 2019b). The SSURGO layer is finer resolution than STATSGO, which can improve model estimates for streamflow and pollutant loading; however, improved estimates should be weighed against computation time and project objectives (Wang and Melesse 2006, Bhandari et al. 2018). We used the STATSGO layer because SSURGO frequently caused QGIS to crash and resulted in SWAT+ run times in excess of two days. We obtained land-use data from the 2016 National Land Cover Database (USGS 2019b). Climate data were obtained from the PRISM Climate Group (2020) for the centroid of each HUC-12 watershed. Streamflow data were obtained from each of the USGS gages in the upper CPH to calibrate the SWAT+ model (USGS 2020). We downloaded total nitrogen, total phosphorus, and total suspended solid collection data from the Virginia Department of Environmental Quality (VDEQ) database (VDEQ 2021). All geospatial layers were converted to the coordinate reference system NAD 83 UTM zone 17 and clipped to the upper CPH. These data will be archived on the Landscape Partnership portal.

Table 1.2.1. Data sources compiled to run and calibrate the Soil and Water Assessment Tool+.

Data	Source	Website	Accessed
Topography	The National Elevation Dataset	https://tinyurl.com/yce3bft7	18 June 2020
Stream network	National Hydrography Dataset Plus Version 2	https://tinyurl.com/y4st74vh	10 January 2020
Land use	National Land Cover Database	https://www.mrlc.gov/data	25 April 2019
Soil	Soil Survey Geographic Database; State Soil Geographic Database	https://tinyurl.com/yc4r4zdh	21 July 2020
Climate	Parameter-elevation regressions on independent slopes model	https://prism.oregonstate.edu/	4 August 2020
Streamflow	U.S. Geological Survey current water data for Virginia	https://tinyurl.com/yyew8asr	4 December 2020
Water quality	Virginia Department of Environmental Quality	https://tinyurl.com/2p86s7v2	10 December 2021

Task 1.3:

Caveats:

In contrast to the proposal text, we modeled sediment and nutrient dynamics within all HUC-12 watersheds in the CPH and **did not** exclude mainstem rivers and watersheds draining the coalfields because it is much simpler to lump everything together in a single SWAT+ model. The mainstem and coalfield areas, however, were excluded when we selected sites for the biological surveys.

We used SWAT+ to model pollutant yields rather than SWAT because SWAT+ offers several advantages compared to SWAT. SWAT+ was recently released to facilitate model maintenance, improve future code modifications, and foster collaborations among researchers (Bieger et al. 2017). Most importantly, the updated model allows greater flexibility in how water is routed through the environment by dividing subbasins into upland and floodplain landscape units (LSUs; Figure 1.3.1; Bieger et al. 2017), allowing for a more nuanced understanding of pollutant sources from the landscape. Because SWAT+ is relatively new, few studies ($n = 23$) have used a SWAT+ model for modeling pollutants, compared to SWAT ($n = 2,071$; Gassman 2023).

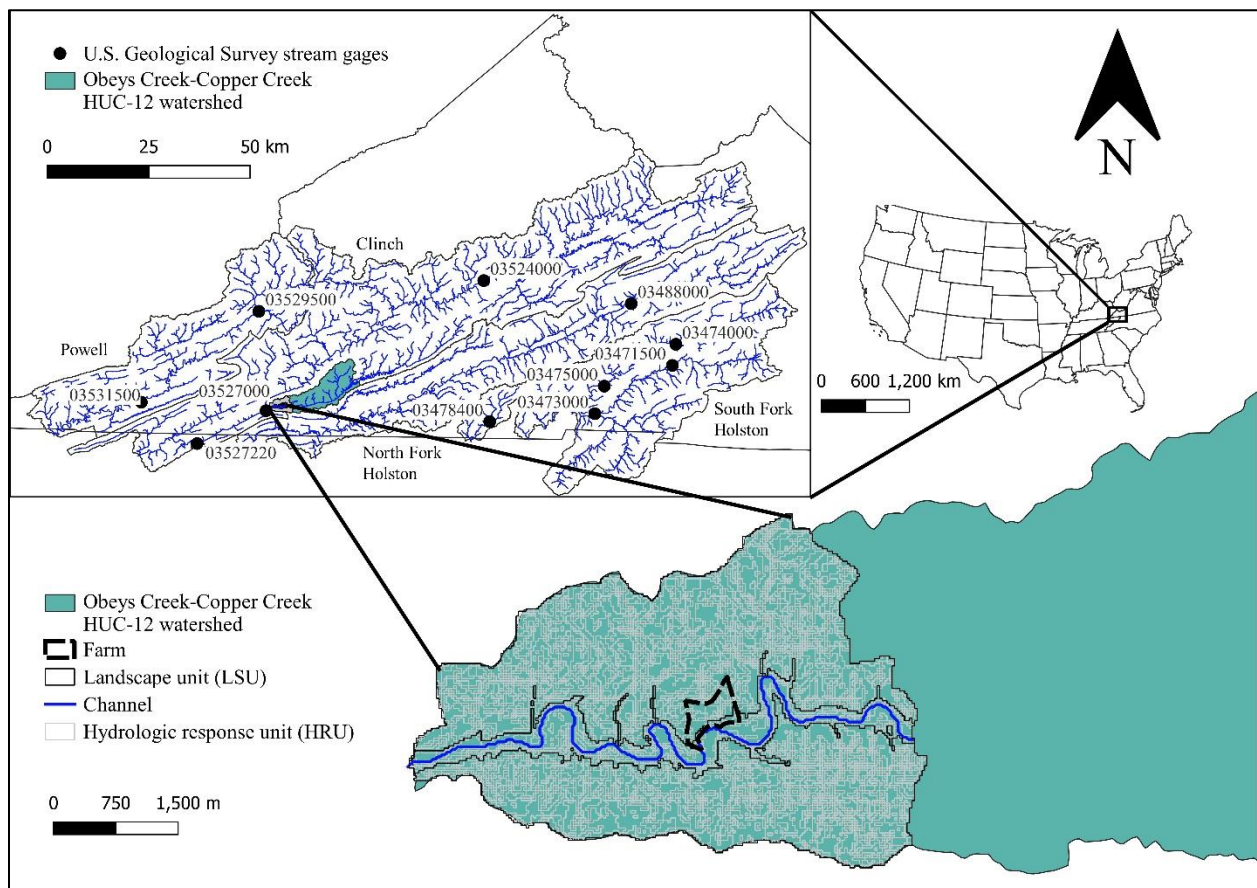


Figure 1.3.1. Illustration of the various spatial scales at which output from the Soil and Water Assessment Tool+ (SWAT+) can be summarized to understand sediment and nutrient yields and loads. SWAT+ estimates sediment (metric tons/ha), nitrogen (kg/ha), and phosphorus (kg/ha) yields from hydrologic response units, which can be summarized at a variety of spatial scales,

including farms and landscape units. Pollutant yields are routed to channels which become instream loads. Landscapes units are divided into upland and floodplain units in SWAT+, which is an improvement upon SWAT that lumped upland and floodplain units into a single subbasin. Data from the U.S. Geological Survey stream gages and Virginia Department of Environmental Quality long-term water quality stations (locations coincide with the gages) were used to calibrate and validate the SWAT+ model.

Methods:

We used the QSWAT+ interface (Dile et al. 2023; version 2.3.5) to prepare the data collected in task 1.2 for the SWAT+ model, which was run through the SWAT+ editor (Tech 2023; version 2.2.2). Stream channels were created when 2 km² (or 2,222 cells) drained to a cell in the NED layer. The NHD+ stream network was used to assist with channel creation. Channel geometry was calculated based on watershed drainage area using parameters from regional models (Bieger et al. 2015), where channel width (m) = $2.79 \times \text{drainage area}^{0.42}$ (km²) and depth (m) = $0.23 \times \text{drainage area}^{0.29}$ (km²). Further, we updated channel slope values that were 0 (i.e., these slope values were unrealistic) based on the average slope from the upstream and downstream channels. Subbasins were created around each channel and those smaller than 25% of the mean subbasin area were merged. Next, we defined the hydrological response units (HRUs) by dividing the slope-range of the watershed into five equal classes, adding the soil and land-use data, and setting the HRU thresholds to zero.

After the watershed was defined, the data were imported into the SWAT+ editor where climate data were added, and model parameters were defined using the default methods. We then calibrated the model for each gage in the upper CPH for streamflow (m³/sec), sediment loads (metric tons), nitrogen loads (kg), and phosphorus loads (kg) at daily (per d) and monthly (per m) time steps. To reduce the amount of time to complete calibration, the model was only run from 2004–2009 with a two-year warmup period. After calibration was complete, we ran the model from 1998–2021 with a three-year warmup period and validated the model for the same variables from 2010–2021. We used the Nash-Sutcliffe efficiency (NSE) to evaluate model performance for both calibration and validation; NSE values > 0.50 indicate satisfactory model performance for monthly time steps (Moriassi et al. 2007). Model fit was also evaluated by plotting measured pollutant and streamflow values against those estimated by the SWAT+ model and calculating correlation coefficients.

We first calibrated the model for streamflow. We assessed the sensitivity of the SWAT+ model to changing the curve number, surface runoff lag coefficient, baseflow recession coefficient, available water content, soil evaporation compensation factor, return flow threshold, groundwater revap coefficient, deep aquifer recharge, plant uptake compensation factor, soil hydraulic conductivity, and Manning's n for the channel using the SWAT+ Toolbox (James 2022; version 1.0.2). Then, we calibrated the model against measured streamflow values using the dynamically dimensioned search algorithm in the SWAT+ Toolbox to determine the best values for the most sensitive parameters.

We calibrated the model for landscape and instream sediment processes separately. We first converted point measurements of total suspended solid concentrations (mg/L) collected by VDEQ (2022) to sediment loads (metric tons/day) by multiplying the concentration by the daily discharge and converting the units. Then, a linear relationship was developed between streamflow and sediment load at each VDEQ monitoring station and used to predict daily sediment loads from the daily streamflow data at each monitoring station. Then, we removed the effects of instream processes from the model by setting channel erosion and the channel cover factor to zero.

After we removed instream processes, we assessed effects of changing the Universal Soil Loss Equation (USLE) cover and practice factors and adding a grazing operation. The USLE cover factor was changed from 0.005 to 0.5 and the USLE practice factor from 1 to 100 (i.e., unrealistically high numbers) to see if those changes influenced predicted daily sediment loads. We consulted a local Soil and Water Conservation District to determine the following parameters for the grazing operation: grazing occurring all year, default beef fertilizer, dry weight of biomass removed by grazing daily = 22.5 kg/ha, dry weight of biomass removed by trampling daily = 15 kg/ha, dry weight of manure deposited daily = 5.7 kg/ha, and minimum plant biomass for grazing to occur = 500 kg/ha. We expect 55% of the sediment load to come from the landscape (Noe et al. 2022); therefore, measured values were multiplied by 0.55 and compared to predicted values.

After the model was calibrated for landscape sediment processes, instream processes were turned back on, and a sensitivity analysis was run using the SWAT+ Toolbox. We determined which parameters (i.e., channel erodibility, channel cover, the effect of peak flow rate on sediment routing in the subbasin, and the exponent and linear parameters for calculating channel sediment routing) had the greatest influence on the model so we could reduce the number of parameters included in the calibration process. Finally, we calibrated the model manually using the most sensitive parameters identified by the SWAT+ Toolbox. We completed the calibration manually because the SWAT+ Toolbox was unable to display very small values for soil erodibility.

The model was calibrated for daily (per d) and monthly (per m) nitrogen (kg) and phosphorus (kg). We first converted point measurements of total nitrogen (mg/L) and total phosphorus (mg/L) to loads (kg/day) following a similar process as for sediment. Then, we developed a linear relationship between streamflow and nitrogen and phosphorus loads at each VDEQ monitoring station and used the relationships to predict daily nitrogen and phosphorus loads at each monitoring station. We assessed the influence of adjusting three parameters on the SWAT+ model's ability to estimate nitrogen loads: 1) adding the previously described cattle grazing operation, 2) increasing the initial concentration of nitrogen in the aquifer to 1000 mg/L (i.e., an unrealistic number that reflects potential legacy nitrogen stored in the aquifer), and 3) changing the ratio of nitrogen in the surface runoff versus nitrogen that percolates into the soil to 1 (i.e., all the nitrate is in the surface runoff). We did not change parameters for phosphorus because the initial predictions seemed reasonable (Figure 1.3.7).

Results:

We successfully calibrated the model for streamflow (Figures 1.3.2 and 1.3.3, Table 1.3.1). We found that the soil’s available water capacity (i.e., how much water the soil can hold) and soil hydraulic conductivity (i.e., the rate of water movement through the soil) had the most influence on streamflow predictions. Decreasing the soil’s available water content by 0.26 mm and increasing the soil hydraulic conductivity by 24.48 mm/hr were most effective in improving performance of the SWAT model. These variables may improve the model because they increase lateral flow through the soil, which could be an important contributor to high-flow events in the upper CPH because of the karst topography in the region. After calibration, the SWAT model generally predicted streamflow well and predictions were above or near the NSE cutoff of 0.50 (Table 1.3.1). The only location where NSE values were much below 0.50 was USGS gage 03529500, located in Big Stone Gap, Virginia (Figure 1.3.3). At most gages, SWAT+ overpredicted streamflow at low measured streamflow but underpredicted streamflow at high measured streamflow (Figures 1.3.2 and 1.3.3). Highly correlated ($r > 0.86$) log-transformed predicted and measured monthly streamflow at all gages also indicated good model fit.

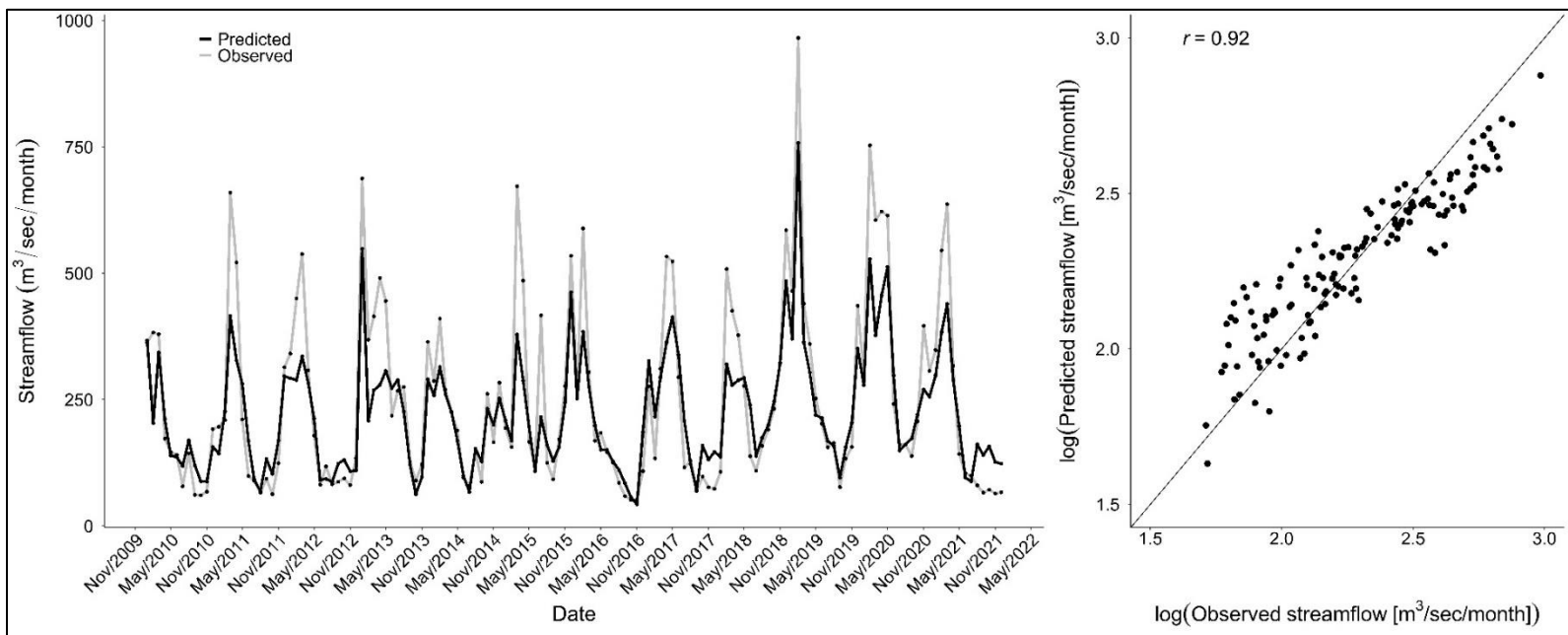


Figure 1.3.2. Streamflow ($m^3/sec/month$) observed at U.S. Geological Survey gage 03475000 (Middle Fork Holston River near Meadowview, Virginia, United States) compared to streamflow predicted by the Soil and Water Assessment Tool+. The Nash-Sutcliffe efficiency (NSE) for streamflow predictions at this gage was the second best of all gages and indicated good fit (0.76). Streamflow predictions were similar for most other gages except for 03529500 (Table 1.3.1, Figure 1.3.3).

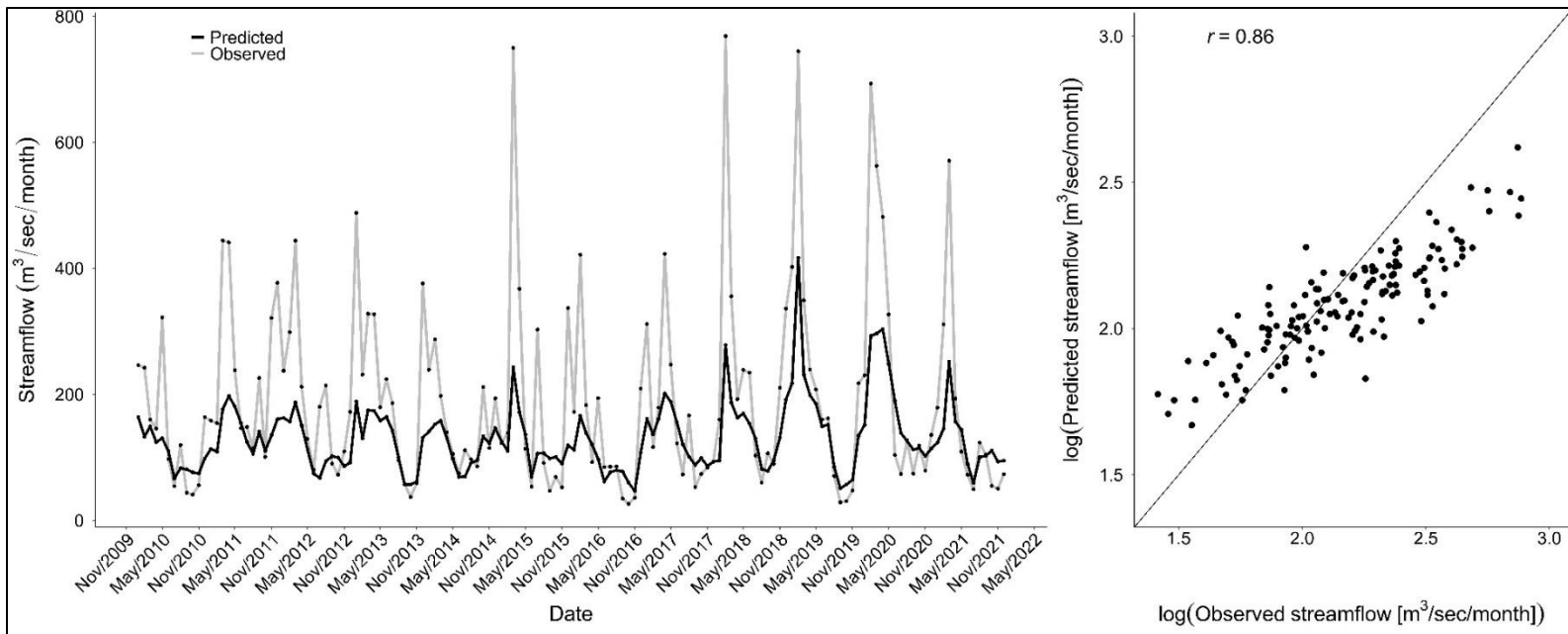


Figure 1.3.3. Streamflow ($\text{m}^3/\text{sec}/\text{month}$) observed at U.S. Geological Survey gage 03529500 (Powell River at Big Stone Gap, Virginia, United States) compared to streamflow predicted by the Soil and Water Assessment Tool+. The Nash-Sutcliffe efficiency (NSE) for streamflow predictions at this gage was worse than all other gages and indicated unsatisfactory fit (0.34). Streamflow predictions at all other gages had NSE values near or above 0.5, indicating good fit (Table 1.3.1, Figure 1.3.2).

Table 1.3.1. Results of the SWAT model calibration* (Cal; 2004–2009) and validation (Val; 2010–2021) for streamflow (m³/sec), sediment loads (metric tons), nitrogen loads (kg), and phosphorus loads (kg) for daily (D; per/d) and monthly (M; per/m) timesteps at 11 gages** in the upper CPH. There were negligible differences between calibration and validation for nitrogen; therefore, results are shown for the entire modeling period (1998–2021). Lat = latitude; Lon = longitude

Gage	Lat	Lon	Streamflow				Sediment				Nitrogen		Phosphorus			
			D		M		D		M		D	M	D		M	
			Cal	Val	Cal	Val	Cal	Val	Cal	Val	Val	Val	Cal	Val	Cal	Val
3531500	36.662	-83.095	0.52	0.57	0.50	0.49	0.26	0.13	0.10	-0.03	-0.24	-0.91	-31.34	-199.44	-6.78	-63.57
3529500	36.869	-82.775	0.41	0.45	0.40	0.34	0.23	0.27	-0.53	0.27	-0.33	-1.21	-7.04	-103.25	-0.44	-33.12
3527220	36.573	-82.939	0.49	0.50	0.64	0.45	-	-	-	-	-	-	-	-	-	-
3524000	36.945	-82.155	0.43	0.59	0.46	0.53	-0.02	-0.03	-0.46	-0.51	-0.26	-1.25	-4.14	-194.57	-0.36	-39.98
3527000	36.649	-82.750	0.41	0.54	0.48	0.54	-0.07	-0.04	-0.47	-0.31	-0.18	-0.76	-0.07	-102.57	-1.30	-39.54
3488000	36.897	-81.746	0.48	0.55	0.57	0.58	0.36	0.28	0.41	0.25	-0.28	-0.91	-134.20	-1138.90	-30.32	-399.90
3475000	36.713	-81.819	0.39	0.38	0.66	0.76	0.28	0.21	0.37	0.27	-0.50	-1.58	-161.22	-548.15	-15.59	-135.52
3474000	36.807	-81.622	0.50	0.63	0.63	0.73	0.29	0.32	0.21	0.46	-0.81	-2.40	-182.56	-2355.79	-18.93	-525.72
3473000	36.652	-81.844	0.55	0.59	0.66	0.63	0.30	0.24	0.39	0.27	-0.25	-1.18	-100.68	-577.05	-22.61	-264.46
3478400	36.632	-82.134	-2.25	-0.63	0.40	0.80	-0.75	0.21	0.16	0.40	-0.63	-1.30	-260.18	-139.44	-23.37	-27.42
3471500	36.760	-81.631	0.29	0.48	0.56	0.65	-6.84	-1.22	-16.80	-5.02	-0.34	-1.37	-957.27	-2813.24	-204.11	-1095.52

*For calibration, the model period was truncated and run only for 2004–2009.

**Gage 3527220 lacked associated sediment, nitrogen, and phosphorus data.

We calibrated the SWAT+ model for sediment dynamics with mixed success (Figures 1.3.4 and 1.3.5, Table 1.3.1). We found that the SWAT+ model initially predicted sediment loads that were several orders of magnitude too high. When we turned off the instream component of sediment processes, the SWAT+ model underpredicted sediment loads, especially at high-flow events. We attempted to improve predictions by increasing the effect of land use on soil erodibility (i.e., increasing the USLE cover and practice factors); however, these changes had little effect on the model at reasonable upper limits. Additionally, adding a grazing schedule had little effect on the model output. Based on visual interpretation of the data and the inherent uncertainty in the point estimates, we felt that model performance for the upslope component was adequate, and there was little we could do to improve the model further. Additionally, we had already observed that instream processes could compensate for the underprediction from the landscape.

The sensitivity analysis revealed that channel erodibility was the parameter that had the most influence on the model. Therefore, we focused on changing the channel erodibility factor and found that setting the channel erodibility factor to $0.00002 \text{ cm}^3/\text{N-s}$ led to model predictions that were fairly close to the measured values for many gages (Table 1.3.1). However, predicted sediment loads were too high during most months at gages in the Powell and Holston river watersheds (Figure 1.3.4) but too low in the Clinch River watershed (Figure 1.3.5). Log-transformed predicted sediment load was strongly correlated with log-transformed observed sediment load at all gages ($r > 0.81$), but the SWAT+ model tended to overestimate low observed values of sediment load and underestimate high observed values of sediment load (Figure 1.3.4; Figure 1.3.5). Overall, we felt the SWAT+ model did an adequate job of predicting sediment loads and the results could be used to identify watersheds that contribute high sediment yields, while acknowledging that predictions for the Clinch River are underestimated.

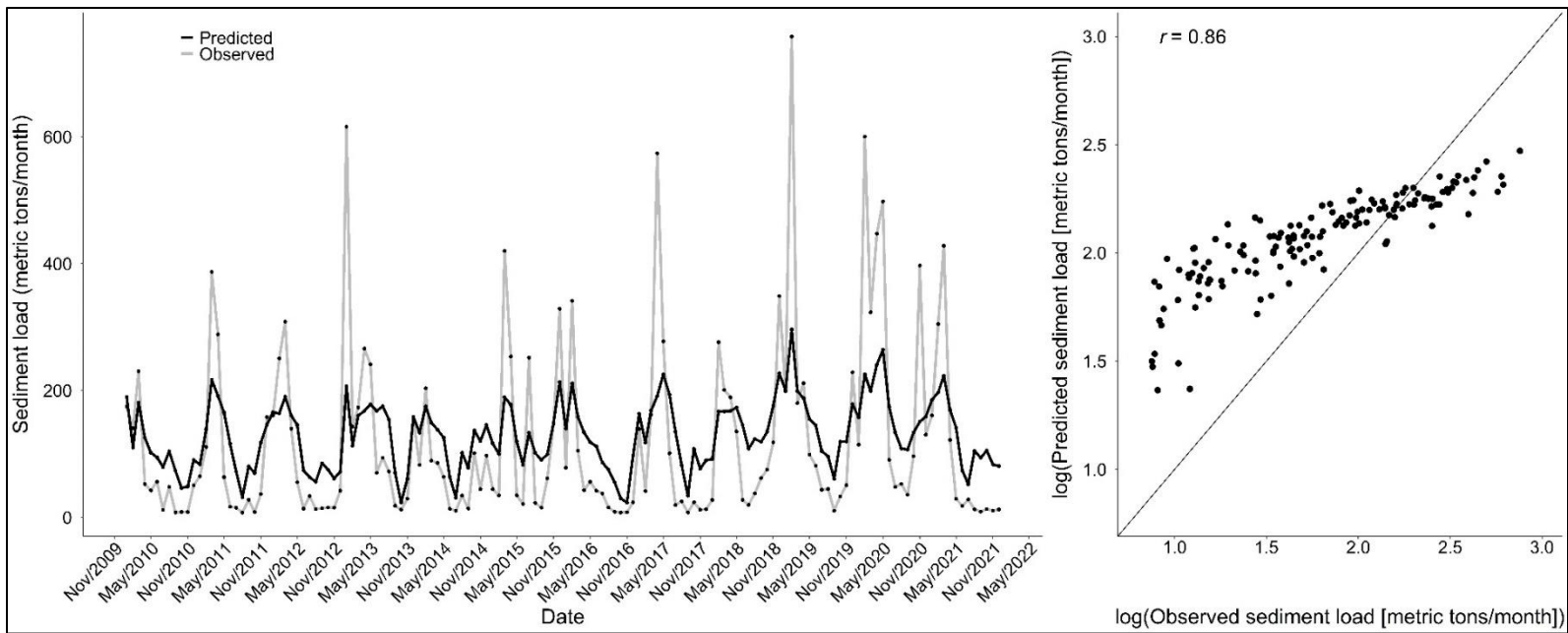


Figure 1.3.4. The sediment load (metric tons/month) observed at Virginia Department of Environmental Quality water quality monitoring station 6CMFH033.40 located near U.S. Geological Survey gage 03474000 (Middle Fork Holston River at Seven Mile Ford, Virginia, United States) compared to the sediment load predicted by the Soil and Water Assessment Tool+. The Nash-Sutcliffe efficiency for sediment load predictions at this gage was better than all other gages but indicated unsatisfactory fit (0.46). Sediment load predictions were similar at all other gages except those in the Clinch River (Table 1.3.1, Figure 1.3.5).

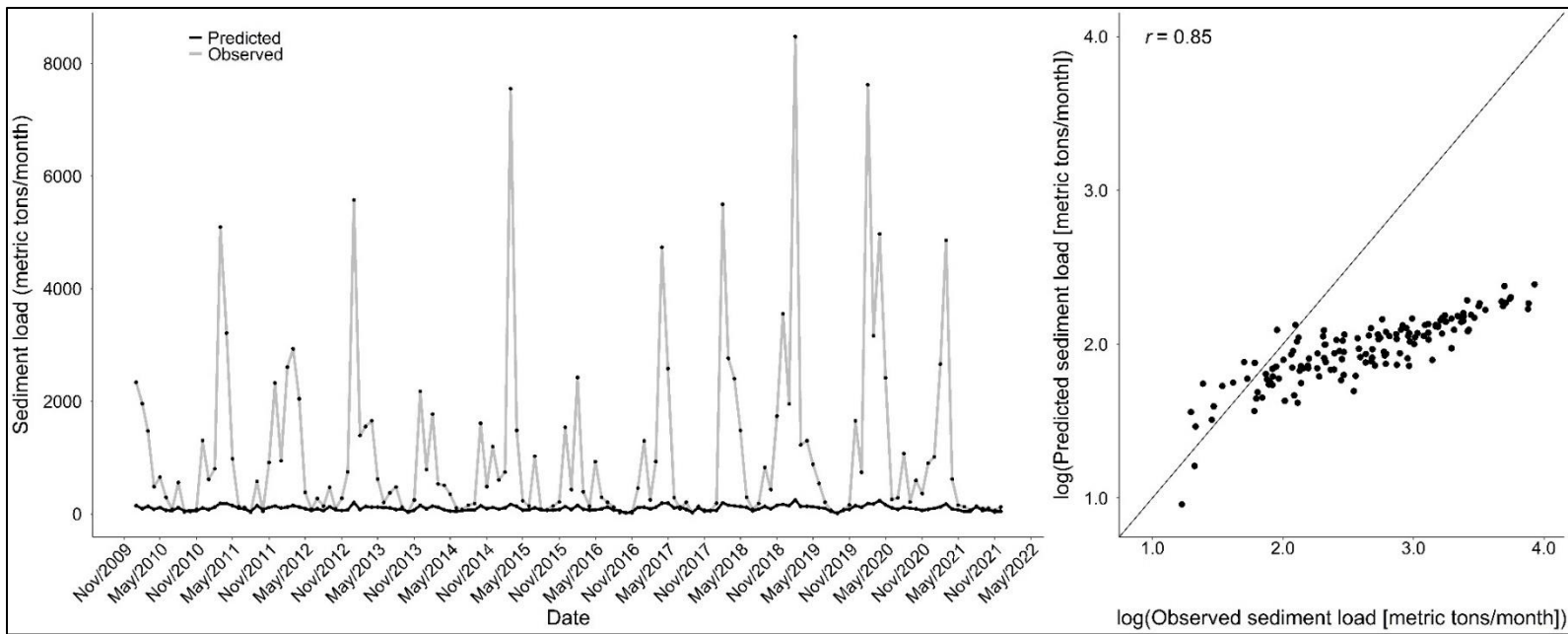


Figure 1.3.5. The sediment load (metric tons/month) observed at Virginia Department of Environmental Quality water quality monitoring station 6BCLN271.50 located near U.S. Geological Survey gage 03524000 (Clinch River at Cleveland, Virginia, United States) compared to the sediment load predicted by the Soil and Water Assessment Tool+. The Nash-Sutcliffe efficiency for sediment load predictions were worse at this gage than all other gages and indicated unsatisfactory fit (-0.51). Sediment predictions extremely underestimated measured values at both gages in the Clinch River (Table 1.3.1).

The SWAT+ model did not predict total nitrogen well (Table 1.3.1, Figure 1.3.6). None of the parameters that we evaluated (i.e., adding cattle grazing, increasing the initial concentration of nitrogen in the aquifer, and changing the nitrogen ratio in the surface runoff) influenced the model output for nitrogen loads. The SWAT+ model likely underpredicted nitrate: the output was about 60% nitrate and 40% organic nitrogen, but values observed in streams are typically closer to 80% nitrate and 20% organic nitrogen (VDEQ 2021). At all gages, the SWAT+ model greatly underpredicted total nitrogen loads (kg/month) compared to measured values (Figure 1.3.6). Only results for the validation period are shown because we observed only small differences between calibration and validation. Despite the SWAT+ model greatly underpredicting nitrogen loads, high correlations ($r = 0.71$) among log-transformed predicted and measured values at all but one gage ($r = 0.53$) show that the model has promise to accurately predict nitrogen loads if parameters can be adjusted to increase predicted loads. When we increased the amount of manure deposited within the grazing operation to completely unrealistic levels, (i.e. 4,000 kg/cow/ha/day), predictions were closer to measured values, which suggests there may be something amiss with the way SWAT+ models nitrogen.

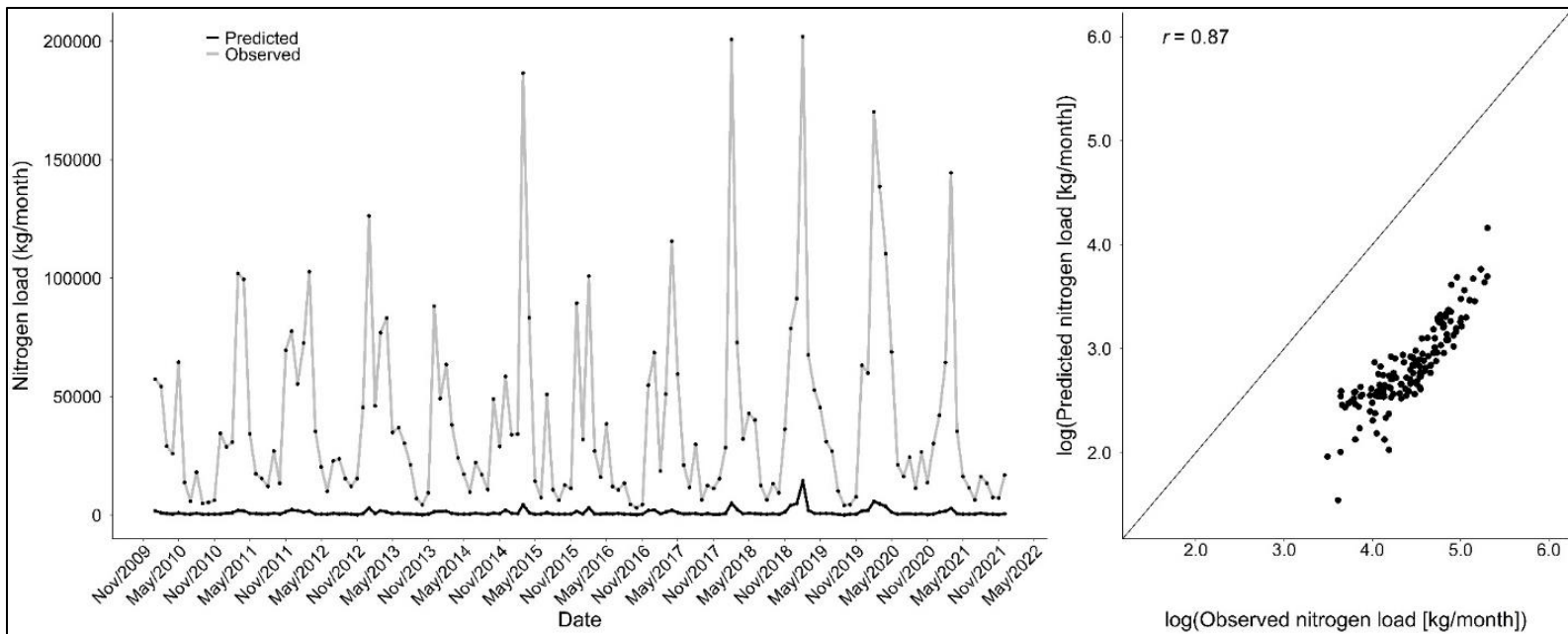


Figure 1.3.6. The total nitrogen load (kg/month) observed at Virginia Department of Environmental Quality water quality monitoring station 6BPOW138.91 located near U.S. Geological Survey gage 03531500 (Powell River near Jonesville, Virginia, United States) compared to the nitrogen load predicted by the Soil and Water Assessment Tool+. Because measured nitrogen loads were greatly underpredicted by the SWAT+ model, the Nash-Sutcliffe efficiency (NSE) indicated unsatisfactory fit for this gage (-0.91) and all other gages (Table 1.3.1).

The SWAT+ model also did not predict total phosphorus well (Figures 1.3.7 and 1.3.8, Table 1.3.1). Phosphorus estimates were close to observed values for the truncated model on which we performed calibration, except for a few high-flow events (Figure 1.3.7); therefore, we felt that changing parameters would not improve phosphorus estimates. Thus, we proceeded without changing parameters in the model for phosphorus. However, when the model was run for the entire time period (1998–2021), phosphorus estimates during high-flow events were extremely too high (Figure 1.3.8), which may indicate the model is accumulating phosphorus throughout the modeling period. Log-transformed predicted total phosphorus loads were highly correlated ($r > 0.76$) with log-transformed observed total phosphorus loads at most gages and moderately correlated ($r = 0.68$) at one gage.

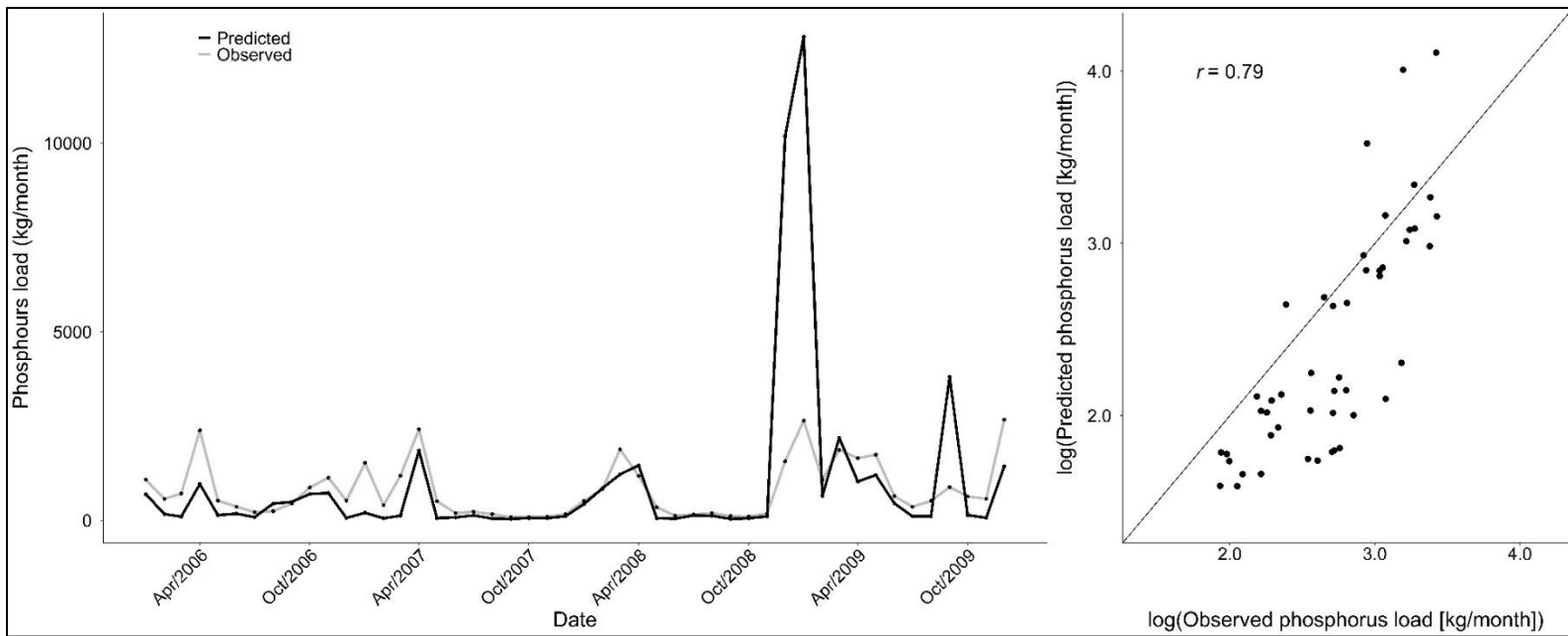


Figure 1.3.7. The total phosphorus load (kg/month) observed at Virginia Department of Environmental Quality water quality monitoring station 6BPOW138.91 located near U.S. Geological Survey gage 03531500 (Powell River near Jonesville, Virginia, United States) compared to the phosphorus load predicted by the Soil and Water Assessment Tool+ for the calibration period. This Nash-Sutcliffe efficiency (NSE) for phosphorus load predictions was the fourth best for this gage and indicated unsatisfactory fit (-6.78). Poor NSE values were largely driven by greatly overpredicting phosphorus during a few months and most locations, with measured values showing results similar to those shown in Figure 1.3.7, so we did not change parameters within the model for phosphorus.

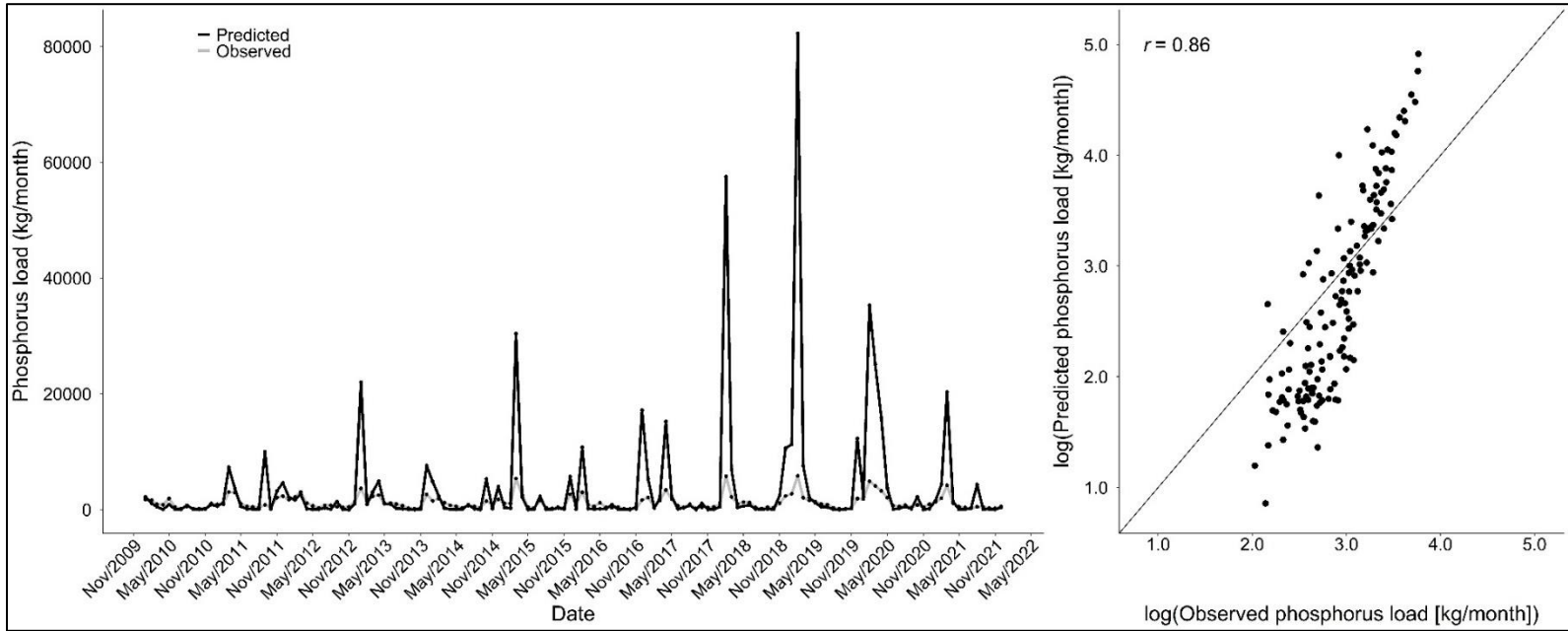


Figure 1.3.8. The total phosphorus load (kg/month) observed at Virginia Department of Environmental Quality water quality monitoring station 6BPOW138.91 located near U.S. Geological Survey gage 03531500 (Powell River near Jonesville, Virginia, United States) compared to the phosphorus load predicted by the Soil and Water Assessment Tool (SWAT+) for the validation period. Because the SWAT+ model greatly overpredicted phosphorus loads at high measured levels of phosphorus, but underpredicted phosphorus at low measured levels, the Nash-Sutcliffe efficiency indicated unsatisfactory fit at this gage (-63.57) and all other gages Table 1.3.1).

Task 2: Analyze the influences of CPs, relative to other watershed features, on predicted sediment and nutrient loads in HUC12s across the upper CPH, excluding those encompassing mainstem rivers and those in the Cumberland Plateau coalfields.

1. Interpret SWAT model outputs to distinguish the cumulative effects of CPs versus other watershed features on sediment and nutrient loading in HUC12s of the upper CPH. In particular, assess influences of soil characteristics (e.g., erodibility, texture), topography (e.g., standard deviation and length of slope), agricultural land use, impervious land cover, forest land cover, and CPs on sediment and nutrient loading. These potential influences will be examined for entire HUC12s. For the two focal watersheds (e.g., Copper Creek), these influences also will be examined for riparian networks (i.e., land within 100 m of a stream) within HUC12s. Relative influences of CPs on sediment and nutrient loads will be derived by comparing outputs of selected scenarios run through the calibrated SWAT model, wherein specific scenarios include or exclude the presence of existing CPs. For instance, an installed riparian buffer can be represented in a model run by adjusting the input FILTERW parameter for riparian-filter width, which influences sediment and nutrient loading via effects on hydrologic responses.

Task 2.1:

Caveats:

We examined the influence of landscape features on sediment (metric tons/ha/yr) and nutrient yields (kg/ha/yr) from the landscape for the entire CPH (instead of just the two watersheds proposed) and at the landscape unit (LSU) resolution rather than the HUC-12 resolution. We chose the finer resolution because LSUs are divided into upslope and floodplain units (Figure 1.3.1), which facilitates assessment of sediment and nutrient yields to both units (Bieger et al. 2017). The division of LSUs into upslope and floodplain units also allows us to use three linear models rather than the six proposed in the 2022 annual report. We expect results at the LSU resolution to readily scale up to coarser resolutions. We were also unable to examine the relative influence of CPs on sediment and nutrient yields because the SWAT+ model was unable to accurately model cattle grazing in southwest Virginia (see Task 1.3 and Tasks 1 and 2 Discussion).

Methods:

We used three multiple linear regression models to assess effects of watershed features on average annual sediment and nutrient yields from LSUs. The response variable in each respective model was the average annual sediment yield (metric tons/ha/yr), phosphorus yield (kg/ha/yr), and nitrogen yield (kg/ha/yr) for each LSU created in SWAT+. Nitrogen yield was calculated as the sum of the organic nitrogen transported in surface runoff and the nitrate transported in surface runoff. Phosphorus yield was calculated as the sum of the organic phosphorus in the surface runoff, the soluble phosphorus in the runoff, and the mineral phosphorus attached to the soil. We included landscape position (i.e., floodplain or upslope) as a categorical predictor variable and suppressed the intercept (Table 2.1.1). We also included proportion urban land cover, proportion forest land cover, proportion agricultural land cover, soil hydraulic conductivity, soil erodibility, and slope as predictor variables (Table 2.1.1). Lastly, we explored

all two-way interactions among the predictor variables. We used the *stats* package in the software R (R Core Team 2023) to build the linear models.

Table 2.1.1. Descriptions of each predictor variable used in multiple linear regression models to assess effects of watershed features on average annual sediment yields (metric tons/ha/yr), nitrogen yields (kg/ha/yr), and phosphorus yields (kg/ha/yr).

Variable	Description
Floodplain	Categorical variable that indicates the landscape unit is adjacent to the stream channel (see Figure 1.3.1).
Upslope	Categorical variable that indicates the landscape unit is not adjacent to the stream channel (see Figure 1.3.1).
Urban	Proportion of urban land cover within the landscape unit
Forest	Proportion of forested land cover within the landscape unit
Agriculture	Proportion of agricultural land cover within the landscape unit
Hydraulic conductivity (mm/hr)	Rate of water movement through the soil
Soil erodibility ([metric tons·ha·hr]/[ha·MJ·mm])	Universal Soil Loss Equation soil erodibility factor
Slope (%)	Average slope of the landscape unit

Results:

Our SWAT+ model contained 4,428 landscape units with varying landscape conditions and sediment and nutrient yields. The upslope land use was 20% agriculture, 69% forested, and 6% urban, whereas the floodplain land use was 27% agriculture, 47% forested, and 20% urban. The mean slope for upslope and floodplain LSUs was 31% and 14%, respectively. Floodplain LSUs had a mean hydraulic conductivity of 80.70 ± 26.82 mm/hr whereas upslope LSUs had a mean hydraulic conductivity of 82.91 ± 22.08 mm/hr. The mean soil erodibility for upslope and floodplain LSUs was 0.33 ± 0.04 metric tons·ha·hr/ha·MJ·mm and 0.32 ± 0.04 metric tons·ha·hr/ha·MJ·mm, respectively. The average sediment, nitrogen, and phosphorus yields for upslope LSUs were 1.82 metric tons/ha/yr, 0.32 kg/ha/yr, and 0.76 kg/ha/yr, respectively. The average sediment, nitrogen, and phosphorus yields for floodplain LSUs were 2.87 metric tons/ha/yr, 0.95 kg/ha/yr, and 1.34 kg/ha/yr, respectively.

Several watershed features were related to pollutant yields (Tables 2.1.2, 2.1.3, 2.1.4). We dropped the predictor variables slope and forest because they were highly correlated ($r > 0.6$) with several other predictor variables. The three models explained 61%, 81%, and 76% of the variation in sediment, nitrogen, and phosphorus yield, respectively. Surprisingly, the proportion of agricultural land in a LSU was negatively associated with both sediment and nitrogen yield (Figure 2.1.1) but agriculture was a weak predictor in both models (Tables 2.1.2 and 2.1.3). The influence of agricultural land use on nitrogen yield depended on the landscape position (Figure 2.1.2). In contrast, phosphorus yield was positively correlated with agricultural land (Figure 2.1.3). These results may indicate that the SWAT+ model is not accurately representing cattle grazing and the model may require further changes to how agricultural land use is modeled

within SWAT+ (see Tasks 1 and 2 Discussion). Sediment and nitrogen yields were positively associated with increasing urban land use, phosphorus yields were negatively associated with increasing urban land use, and urban land use was a strong predictor of sediment and nitrogen yields (Tables 2.1.2, 2.1.3, 2.1.4) suggesting that urban lands are a major driver of sediment and nitrogen budgets within the SWAT+ model. As expected, increasing soil erodibility increased sediment, nitrogen, and phosphorus yields, and the effect of soil erodibility depended on landscape position. Hydraulic conductivity negatively affected sediment, nitrogen, and phosphorus yields, which may be because greater conductivity leads to more water moving through the soil (as opposed to over the soil surface), where sediment and nutrients are captured or stored in the soil profile or groundwater. In contrast, increased soil erodibility and hydraulic conductivity had negative and positive effects on phosphorus yields, respectively, but these relationships were not apparent when the relationships were plotted on a graph.

Table 2.1.2. Results of a multiple linear regression model used to determine factors (Table 2.1.1) that influence sediment yield (metric tons/ha/yr) in the upper Clinch, Powell, and Holston watersheds for 4,428 landscape units. Overall, the model explained 61% of the variation in phosphorus yield and the partial R^2 in the table shows how much of the residual variance each coefficient explains. The intercept was suppressed so the results for both floodplain and upslope landscape units can be easily interpreted. SD refers to standard deviation.

Coefficient	Estimate \pm SD	<i>p</i>-value	R^2
Hydraulic conductivity	-0.23 \pm 0.04	< 0.01	0.08
Urban	1.73 \pm 0.05	< 0.01	0.18
Floodplain	2.05 \pm 0.06	< 0.01	0.20
Upslope	3.39 \pm 0.07	< 0.01	0.37
Agriculture	-0.37 \pm 0.04	< 0.01	0.02
Soil erodibility	0.92 \pm 0.05	< 0.01	0.06
Upslope X urban	1.59 \pm 0.10	< 0.01	0.06
Upslope X soil erodibility	-0.70 \pm 0.08	< 0.01	0.02

Table 2.1.3. Results of a multiple linear regression model used to determine factors (Table 2.1.1) that influence nitrogen yield (kg/ha/yr) in the upper Clinch, Powell, and Holston watersheds for 4,428 landscape units. Overall, the model explained 81% of the variation in nitrogen yield and the partial R² in the table shows how much of the residual variance each coefficient explains. The intercept was suppressed so the results for both floodplain and upslope landscape units can be easily interpreted. SD refers to standard deviation.

Coefficient	Estimate ± SD	p-value	R²
Hydraulic conductivity	-0.04 ± 0.01	< 0.01	0.01
Urban	0.48 ± 0.01	< 0.01	0.51
Floodplain	0.75 ± 0.01	< 0.01	0.59
Upslope	0.54 ± 0.01	< 0.01	0.43
Agriculture	-0.21 ± 0.01	< 0.01	0.12
Soil erodibility	< 0.01 ± 0.01	0.82	<0.01
Upslope X agriculture	0.12 ± 0.01	< 0.01	0.02
Upslope X soil erodibility	-0.04 ± 0.01	< 0.01	<0.01

Table 2.1.4. Results of a multiple linear regression model used to determine factors (Table 2.1.1) that influence phosphorus yield (kg/ha/yr) in the upper Clinch, Powell, and Holston watersheds for 4,428 landscape units. Overall, the model explained 76% of the variation in phosphorus yield and the partial R² in the table shows how much of the residual variance each coefficient explains. The intercept was suppressed so the results for both floodplain and upslope landscape units can be easily interpreted. SD refers to standard deviation.

Coefficient	Estimate ± SD	p-value	R²
Hydraulic conductivity	-0.17 ± 0.01	< 0.01	0.04
Urban	-0.13 ± 0.01	< 0.01	0.02
Floodplain	1.36 ± 0.01	< 0.01	0.64
Upslope	0.80 ± 0.01	< 0.01	0.34
Agriculture	0.17 ± 0.01	< 0.01	0.06
Soil erodibility	0.31 ± 0.01	< 0.01	0.11
Upslope X urban	0.14 ± 0.02	0.01	0.01
Upslope X soil erodibility	-0.04 ± 0.01	0.04	<0.01
Upslope X hydraulic conductivity	0.20 ± 0.02	<0.01	0.02

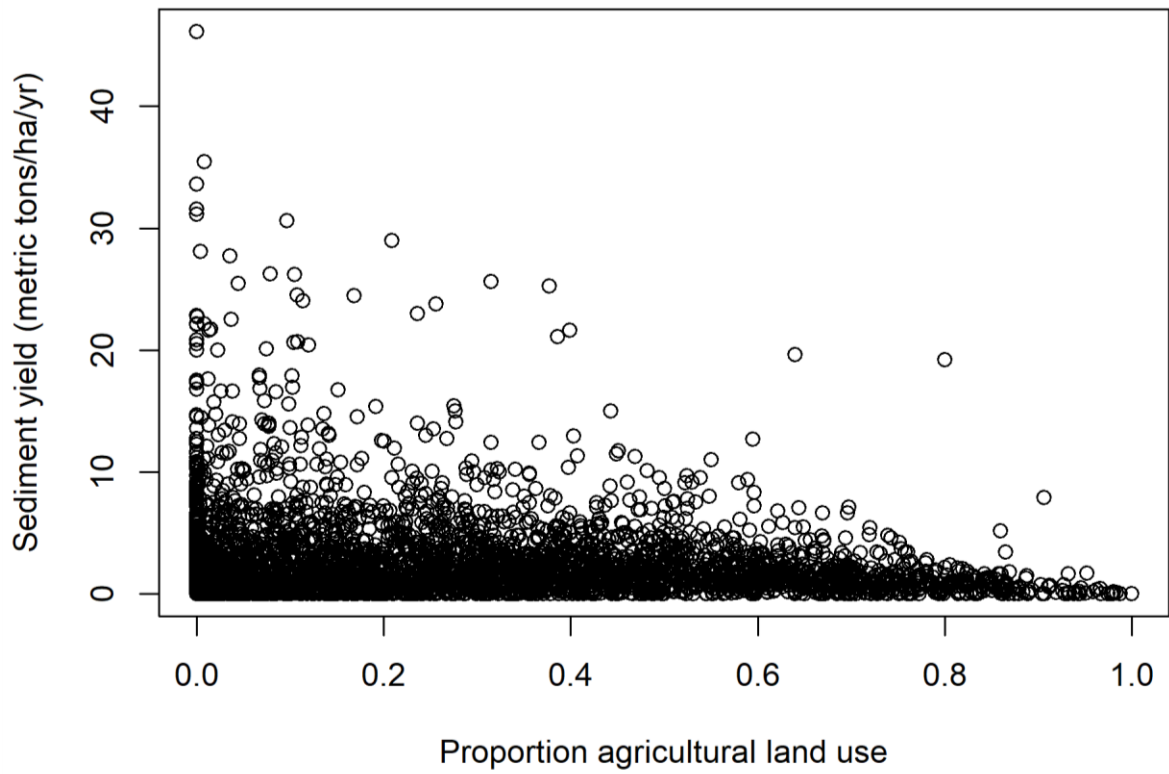


Figure 2.1.1. The relationship ($r = -0.60$) between proportion of agricultural land use and sediment yield (metric tons/ha/yr) as predicted by the Soil and Water Assessment Tool for 4,428 landscape units.

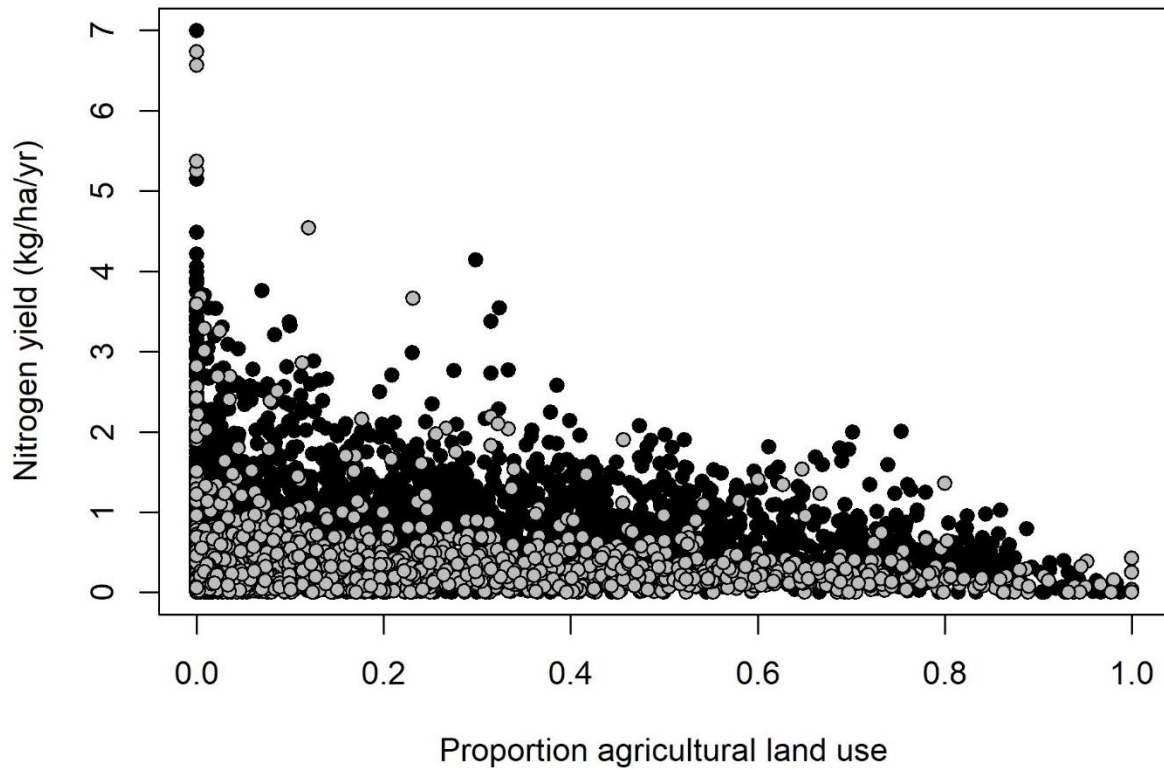


Figure 2.1.2. The relationship between proportion of agricultural land use and nitrogen yield (kg/ha/yr) as predicted by the Soil and Water Assessment Tool for 4,428 landscape units. A multiple linear regression model indicated that the relationship varied by landscape position, so the points are identified as being derived from upslope (grey) or floodplain (black) units. Nitrogen yield was more strongly associated with the amount of agricultural land use within floodplain units ($r = -0.33$) than upland units ($r = -0.07$).

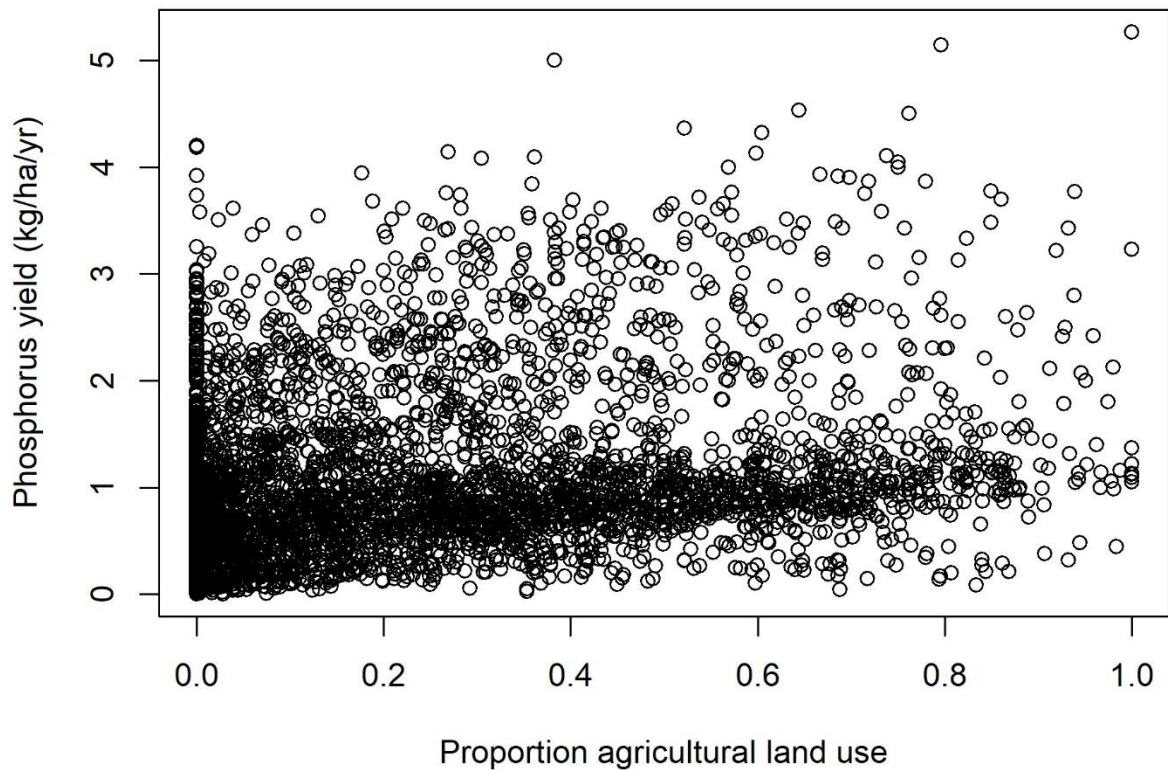


Figure 2.1.3. The relationship ($r = 0.28$) between proportion of agricultural land use and phosphorus yield (kg/ha/yr) as predicted by the Soil and Water Assessment Tool for 4,428 landscape units.

Tasks 1 and 2 Discussion:

We encountered several challenges in building a SWAT+ model to estimate sediment and nutrient loads in the upper CPH. We outline these challenges, steps we took to overcome those challenges, and directions for future research that could lead to a better SWAT+ model.

A preliminary SWAT+ model gave sediment estimates that were over 100 times too high because channels were too wide and deep based on the default parameters for calculating channel morphology. Therefore, we replaced the parameters with regional estimates from Bieger et al. (2015). The widths and depths of headwater streams were still too large, resulting in overestimation of sediment concentrations in headwater streams despite replacing the default parameters with regional estimates. For example, the SWAT+ model provided daily annual sediment estimates that averaged 140.72 mg/L for the sites that we sampled for task 3.4, but the average of our measured values was only 4.23 mg/L (Table 3.4.2). Because sediment concentrations were too high in headwater streams, we could not compare sediment concentrations among watersheds at finer scales (e.g., HRUs and LSUs) but we felt that comparisons among watersheds at coarser scales (e.g., HUC-12) would be appropriate because sediment concentrations would be aggregated. **We suggest that future studies carefully check**

stream width and depth for streams of all sizes. Further, parameters used to calculate channel morphology need to be defined for the specific area of interest (i.e., rather than broader regions) and encompass streams of all sizes before building SWAT+ models.

The influence of choices regarding watershed delineation, geospatial layers, and HRU thresholds are rarely discussed within tutorials or manuals; therefore, we often made decisions based on the best available data, what was feasible, and consultation with SWAT experts from the USDA Agricultural Research Service. Watershed creation involves choices including thresholds for creating channels, if a stream layer (and which one) should be used to assist in channel delineation, and landscape delineation thresholds. For example, we used a threshold of 2 km² to delineate channels because a larger threshold resulted in substantially fewer channels and a smaller threshold did not add any major channels. Building the SWAT+ model also includes the choice of geospatial layers (e.g., topography, soil, and land-use data) to create the watershed and run the model. For example, we used the STATSGO soil layer instead of SSURGO because SSURGO frequently caused QGIS to crash and resulted in SWAT+ run times greater than two days. There are also several choices when creating HRUs. We decided not to remove HRUs from our final model because we felt that more HRUs would be more representative of the watershed and would allow for better CP scenarios (Her et al. 2015). However, after building our model, we learned that having too many HRUs significantly slows model runs and makes calibration more difficult (Jeffery Arnold, USDA Agricultural Research Station, 21 March 2024, written communication). Ideally, we would run SWAT+ using different model inputs, assess the effects on model output, and repeat the process until the best inputs are chosen; however, there are too many parameter choices to complete this in a reasonable project timeline. **We suggest that future studies focus on quantifying the most appropriate model inputs.**

We also had problems with the software available, especially calibration software. Because SWAT+ was relatively new when we started the project, we encountered several instances where the terms and units in the graphical user interface (GUI) did not match those in the user manual (e.g., the GUI displayed the units for nitrate in the aquifer as kg but the user manual showed mg/L). Luckily, these problems became less pervasive as the software evolved and will hopefully not be a major issue moving forward. In addition to SWAT+ software, we had difficulty with the calibration software. We first used SWATCUP to calibrate the model. The coding language makes this a difficult software to use. Further, it was difficult to code for the desired parameters because many had different names than those used by SWAT+. Lastly, we encountered instances where the SWATCUP output did not match the output from SWAT+. The support team was responsive but somewhat dismissive of our problem. After much trial and error, we discovered that a file was being copied incorrectly by the software. The SWAT+ toolbox was much easier to implement because it is a GUI but was limited in its capability. **We suggest that future studies use the SWAT+ toolbox for calibration, but more work is needed to improve its functionality.**

The SWAT+ model had difficulty accurately modeling sediment loads in streams of the upper CPH. We found that higher values for channel erodibility led to better sediment estimates in the

Clinch River basin compared to other watersheds, especially in larger channels. Therefore, sediment estimates could be improved if the SWAT+ model was divided into separate models for the Clinch, Powell, and Holston river watersheds. Developing a separate model for each watershed would allow for unique watershed-specific adjustments to parameters such as channel erodibility but require greater time for calibration. **We suggest that future research carefully weigh the pros (e.g., decreased calibration time) and cons (e.g., a single parameter may not represent the entire watershed) of modeling large watersheds using a single SWAT+ model.**

Poor sediment estimates may also result from limitations in how SWAT+ models sediment loss from the landscape. We found that as the proportion of agricultural land use within a watershed increases, the sediment yield decreases (Figure 2.1.1) but is well known that sediment from agricultural land use is a pervasive problem in southwest Virginia (VDEQ 2004, 2009, 2014). SWAT+ may not be accurately capturing the pathways through which cattle grazing influences sediment yields in southwest Virginia. SWAT+ uses the USLE equation to model sediment loss, which assumes overland flow (Boomer et al. 2008). But many pastures in southwest Virginia are vegetated, with eroding streambanks acting as key sources of fine sediment. If the destabilizing effects of cattle grazing on streambanks were included in SWAT+, it may make for a more realistic model and allow for scenario analyses assessing the effects of altering grazing operations (e.g., rotational grazing and excluding cattle from riparian areas), which was initially a goal of this research. **We suggest that future studies develop model extensions that capture streambank erosion pathways of sediment deposition within streams.**

The SWAT+ model unsatisfactorily predicted nitrogen in our study area. Our SWAT+ model initially greatly underpredicted total nitrogen loads, which was likely due to underprediction of nitrate. Increasing the initial concentration of nitrate in the aquifer, changing the nitrate percolation coefficient, and adding a cattle grazing operation did not improve nitrogen estimates. Similarly, Singh et al. (2023) and Buhr et al. (2022) found that nitrogen estimates were not sensitive to the nitrate percolation coefficient. Factors that nitrogen estimates were sensitive to include the humus mineralization of active organic nutrients (Singh et al. 2023) and denitrification exponential rate coefficient (Buhr et al. 2022, Singh et al. 2023). SWAT+ may not accurately represent nitrogen movement within the karst system of the CPH, the cattle grazing operation is not accurately simulating nitrogen deposition on the landscape, or SWAT+ is unable to account for legacy nitrogen, which can be stored in the groundwater for decades (Hamilton 2012). **Extensions already developed for SWAT, such as SWAT-MODFLOW-RT3D (Wei et al. 2019), may help improve nitrogen estimates for SWAT+.**

The SWAT+ model also unsatisfactorily predicted phosphorus. It was strange that the SWAT+ model reasonably predicted phosphorus for the calibration period but not the validation period — especially considering that there were not major differences in sediment estimates between the two periods and phosphorus is typically associated with sediment. Legacy phosphorus could be accumulating in the streambed and resuspended during high-flow events (Wallington et al. 2024). We did not spend much time attempting to improve phosphorus estimates because we were more concerned about sediment. **Future studies might improve phosphorus estimates by**

using extensions (e.g., SWAT+P.R&R) that more accurately capture the role of instream processes on phosphorus transport within a watershed (Wallington and Cai 2023) or by adjusting some of the following parameters: phosphorus enrichment ratio for loading with sediment, the phosphorus availability index, or the parameters affecting instream phosphorus (e.g., local settling rate for organic phosphorus).

Task 3: *Quantify relations among CP implementation, observed instream water quality and habitat quality, and observed biotic assemblages at the spatial resolution of HUC12s or larger (depending on spatial distribution of existing data).*

- 1. Based on the SWAT-based analyses above, develop maps (at HUC12 resolution) to represent spatial variation in sediment loading, nutrient loading, and CP implementation across the upper CPH.*
- 2. Consult databases maintained by state and federal agencies to compile a complete geo-referenced database on water quality, habitat quality, and biotic conditions at HUC12 resolution across the upper CPH.*
- 3. Select two focal watersheds, each comprising multiple HUC12s, to conduct more in-depth analyses and field studies. Focal watersheds will be selected after consultation with state and federal biologists; selections will be based on availability of supplemental data on water/habitat quality and on the presence of priority at-risk aquatic species. One of these watersheds will be the Copper Creek watershed in the Clinch River drainage. Preliminary candidates for the other watershed include Middle Fork Holston River and Wallen Creek (tributary to Powell River).*
- 4. Quantify effects of land management, including CPs, on instream conditions by surveying water quality, streambank stability, benthic habitat quality, and benthic macroinvertebrates (BMIs) at 10 sites per focal watershed (20 sites total). Sites will be selected to represent the full range of predicted sediment and nutrient loading in HUC12s across the respective focal watersheds. Sites will be 150-200 m long, encompassing two contiguous riffle/pool complexes. The downstream end of each site will be >200 m upstream of the confluence with the receiving stream. Instream surveys will be conducted in August-October to match VDEQ biomonitoring schedules. Water samples will be collected quarterly during base-flow conditions for one year to represent seasonal variation. Concentrations of total nitrogen, total phosphorus, and coliforms will be measured, as well as conductivity and turbidity. A modified USGS protocol (Fitzpatrick et al. 1998) will be used to characterize streambank and channel conditions. BMIs will be sampled via the VDEQ protocol (VDEQ 2008). Briefly, riffles will be sampled at base flow with a D-frame dip net, then a 110-organism sub-sample will be sorted and identified to genus in the laboratory. The eight metrics associated with the Virginia Stream Condition Index (VSCI) will be calculated (VDEQ 2008). We will use aerial imagery to “ground-truth” CPs reportedly installed in focal watersheds. Instream data will be summarized as dependent variables in regression analyses to assess responses to watershed features, such as CP implementation, predicted sediment loading, topography, and land use. In these analyses, we will examine responses of individual measures (e.g., embeddedness) as well as multi-metric indices (e.g., VSCI) and component metrics.*
- 5. Provide a detailed outline and discussion of the proposed database, how it should operate, and the inputs required.*

Task 3.1:*Results:*

We used the results from the SWAT+ model (see Task 1.3) to create maps of yearly pollutant yields from HUC-12 watersheds in the upper CPH. Conservation practices are especially concentrated in the Big Moccasin Creek-North Fork Holston River, Copper Creek, Laurel Creek-North Fork Holston River, Little River, Rowland Creek-South Fork Holston River, Middle Fork Holston River, and Wallen Creek-Powell River HUC-10 watersheds (Figure 3.1.1). Sediment yield (metric tons/ha/yr) was high in the Abrams Creek-North Fork Holston River, Dumps Creek-Clinch River, Middle Fork Holston River, North Fork Clinch River-Clinch River, Stony Creek-Clinch River, Swords Creek-Clinch River, and Wallen Creek-Powell River Guest River HUC-10 watersheds. Nitrogen yield (kg/ha/yr) was high in the Dumps Creek-Clinch River, Laurel Creek-South Fork Holston River, Middle Fork Holston River, North Fork Clinch River-Clinch River, South Fork Powell River-Powell River, Stony Creek-Clinch River, and Swords Creek-Clinch River HUC-10 watersheds (Figure 3.1.3). Lastly, phosphorus yield (kg/ha/yr) was high in the Abrams Creek-North Fork Holston River, Laurel Creek-South Fork Holston River, Dumps Creek-Clinch River, Middle Fork Holston River, Rowland Creek-South Fork Holston River, Tumbling Creek-North Fork Holston River, and Wallen Creek-Powell River HUC-10 watersheds (Figure 3.1.4).

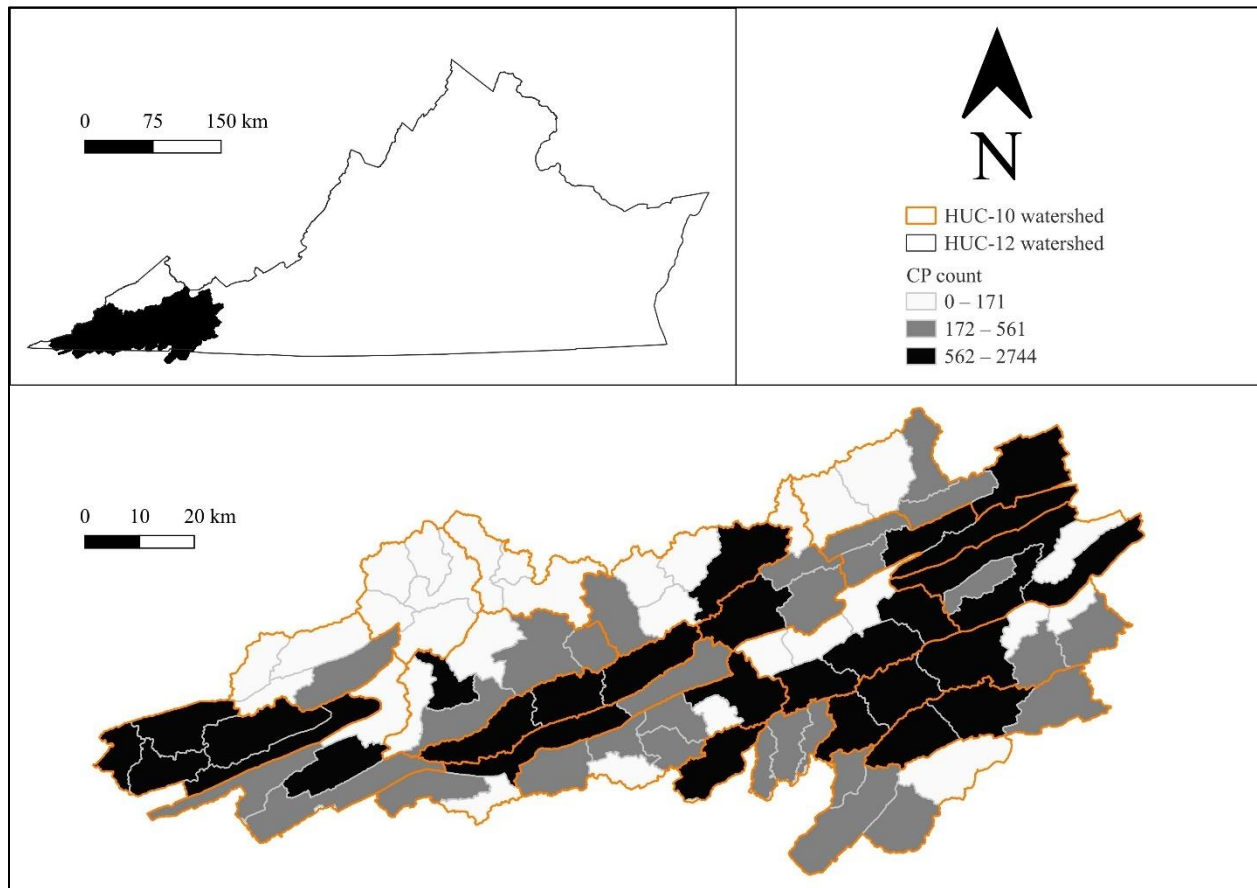


Figure 3.1.1. The distribution of agricultural conservation practices (CPs) implemented by the Virginia Department of Conservation and Natural Resource Conservation Service in the upper Clinch, Powell, and Holston watersheds (see task 1.1 for a description of the CP databases). HUC-12 watersheds were categorized as low, medium, or high CP count, with an equal number of watersheds in each bin.

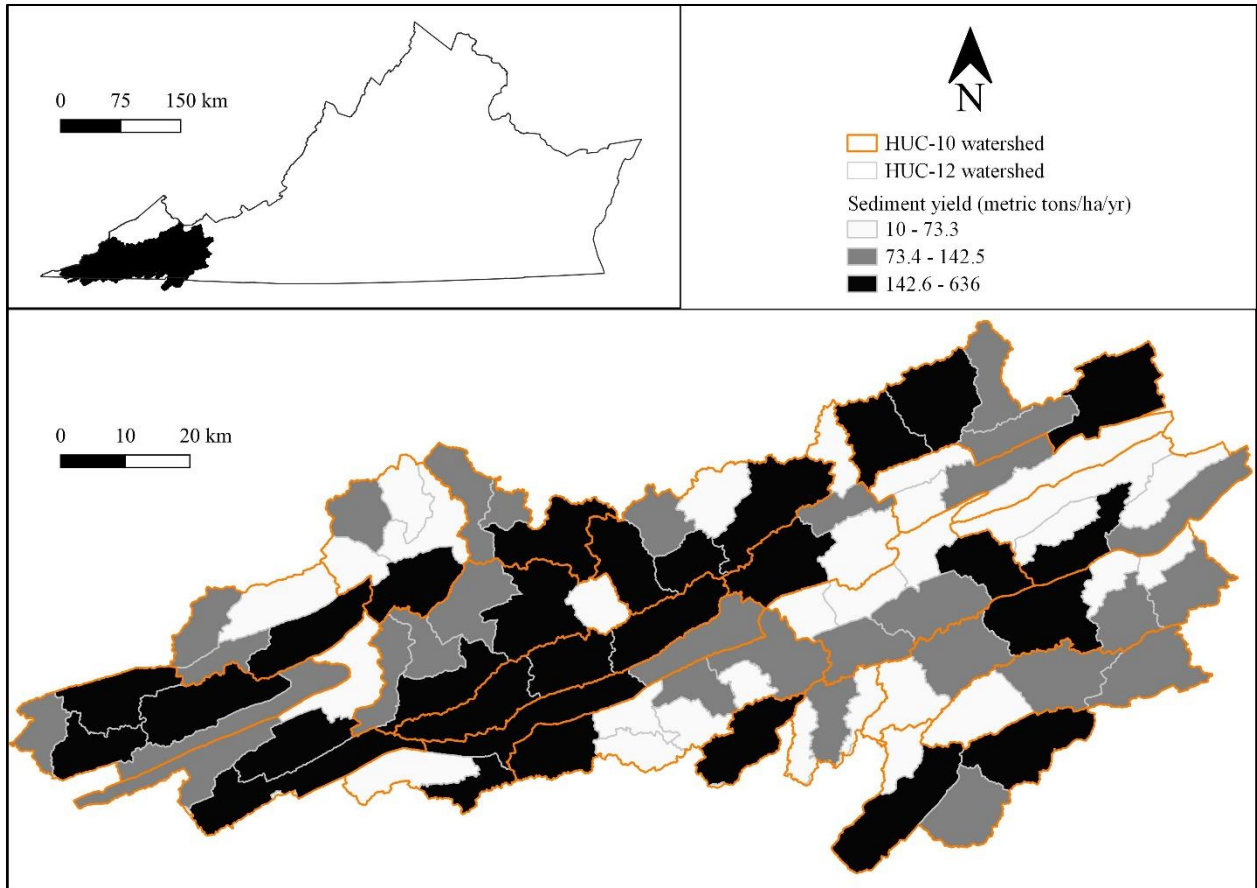


Figure 3.1.2. The mean annual sediment yield (metric tons/ha/yr) delivered to the stream in each HUC-12 watershed in the upper Clinch, Powell, and Holston watersheds as predicted by the Soil and Water Assessment Tool+ model described in task 1.3. HUC-12 watersheds were categorized as low, medium, or high sediment yield, with an equal number of watersheds in each bin.

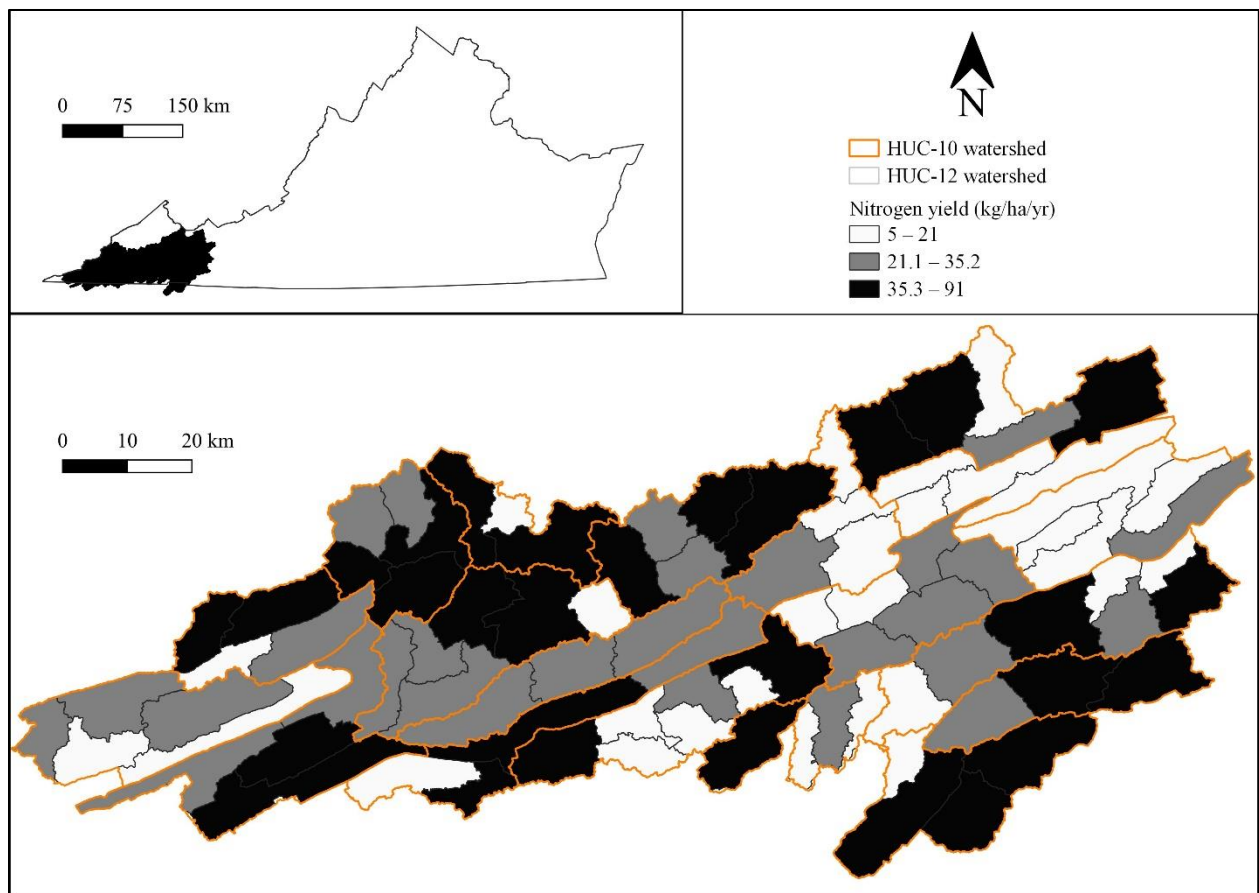


Figure 3.1.3. The mean annual nitrogen yield (kg/ha/yr) delivered to the stream in each HUC-12 watershed in the upper Clinch, Powell, and Holston watersheds as predicted by the Soil and Water Assessment Tool+ model described in task 1.3. HUC-12 watersheds were categorized as low, medium, or high nitrogen yield, with an equal number of watersheds in each bin.

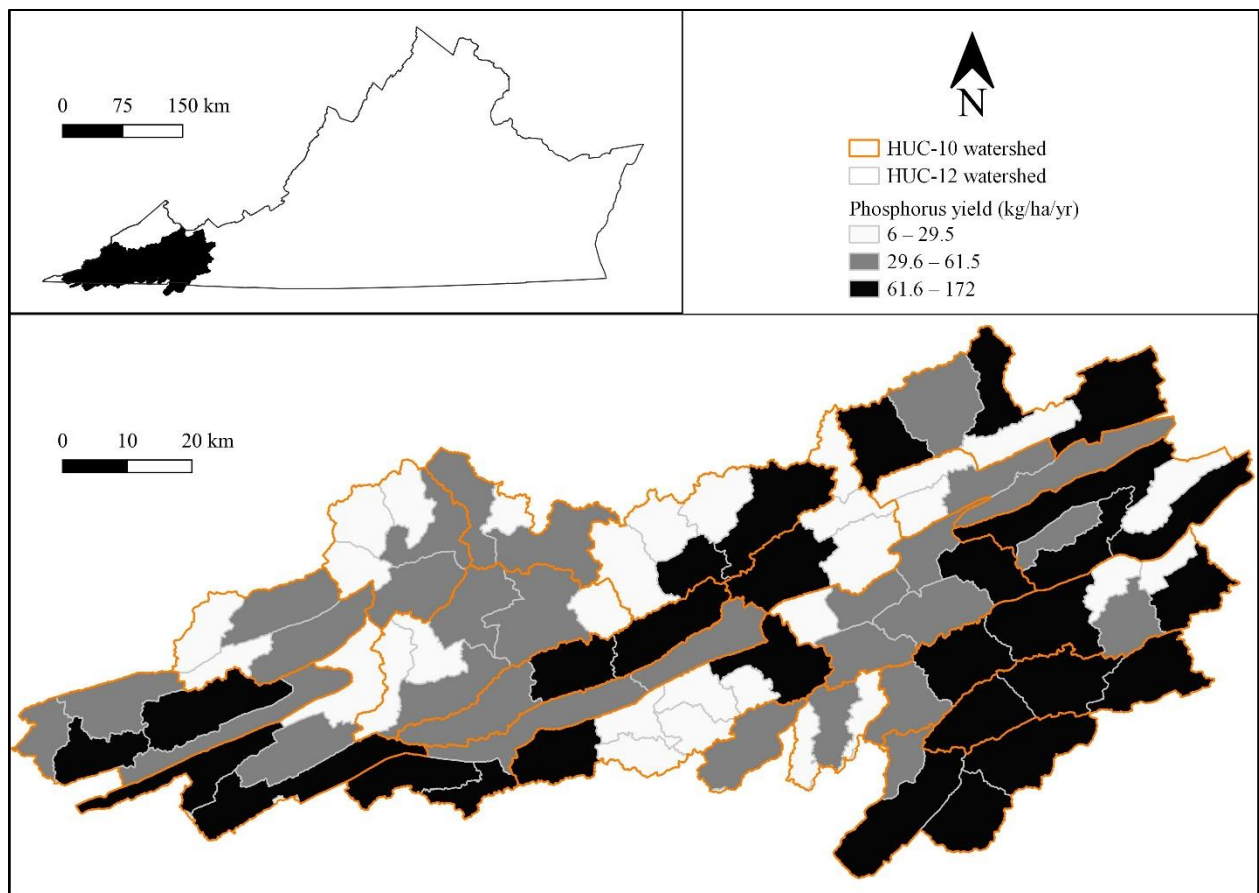


Figure 3.1.4. The mean annual phosphorus yield (kg/ha/yr) delivered to the stream in each HUC-12 watershed in the upper Clinch, Powell, and Holston watersheds as predicted by the Soil and Water Assessment Tool+ model described in task 1.3. HUC-12 watersheds were categorized as low, medium, or high phosphorus yield, with an equal number of watersheds in each bin.

Task 3.2:

Caveats:

We completed approximately half of this task (as proposed) but did not use the compiled data in further analyses. We felt that increasing the number of sampling locations (from 20 to 31; see task 3.3) along our gradients of sediment yield and CP implementation provided more insight regarding the influence of CPs on stream health (i.e., completing project objectives) than any coarse-scale analysis we might derive from the existing data maintained by agencies. We expected such data to be fraught with temporal and spatial biases and confounding factors, thereby rendering interpretation of analytical results ambiguous. Thus, with concurrence from NRCS, we left this task incomplete.

Results:

We obtained macroinvertebrate collection data from TVA and VDEQ. The TVA dataset contains 168 unique collections from the Clinch-Powell drainages from 2000–2015. The VDEQ dataset

contains 65 unique collections from the entire upper CPH from 2001–2016. Various water quality data are available for many of the VDEQ collections.

Task 3.3:

Caveats:

We chose to select five HUC-10 watersheds (rather than the single HUC-10 proposed) so that we could capture a broader range of sediment yield and CP installation intensity in our analyses.

Methods:

We selected 31 sites within the Copper Creek, Laurel Creek, Tumbling Creek, Big Moccasin Creek, and Big Cedar Creek HUC-10 watersheds for intensive study (Figure 3.3.1, Table 3.3.1). Copper Creek is within the Clinch River HUC-8 watershed, whereas Laurel Creek, Tumbling Creek, Big Moccasin Creek, and Big Cedar Creek are within the North Fork Holston HUC-8 watershed. A previous study in the Copper Creek watershed (Martin 2019) delineated 87 subbasins and we chose a subset of those that represented a range of potential sediment yield (tons/ha) and CP implementation intensity. We first removed all subbasins that were $< 0.5 \text{ km}^2$ and those that drained to segments $\geq 3^{\text{rd}}$ order (Strahler). For each subbasin, we determined the number of CPs, the percentage riparian agricultural use (i.e., within a 30-m buffer around the stream), and potential sediment yield as determined from the SWAT model described in Martin (2019). Each subbasin was then ranked as high, medium, or low for each category. We removed all subbasins that were ranked as low agricultural use and those with medium CP count or potential sediment yield. We chose 3–4 sites that fit in each of the following categories: “low sediment yield, high CP count”; “low sediment yield, low CP count”; “high sediment yield, high CP count”; “high sediment yield, low CP count”. Based on our ranking scheme and a visit to potential sampling locations, we selected an initial 15 subbasins for intensive study in the Copper Creek watershed in autumn 2019. We selected a single site per subbasin within 200 m of the pour point so that instream data could easily be matched with SWAT+ output. In autumn 2020, we repeated the ranking scheme for the entire CPH using data from a preliminary SWAT+ model for the entire CPH. The expanded SWAT+ model revealed that all but two sites within the Copper Creek watershed were now in the category “high sediment yield, high CP count”, so we focused on picking 5–6 sites for each of the other three categories. After visiting the potential sites, we selected an additional 16 for intensive study.

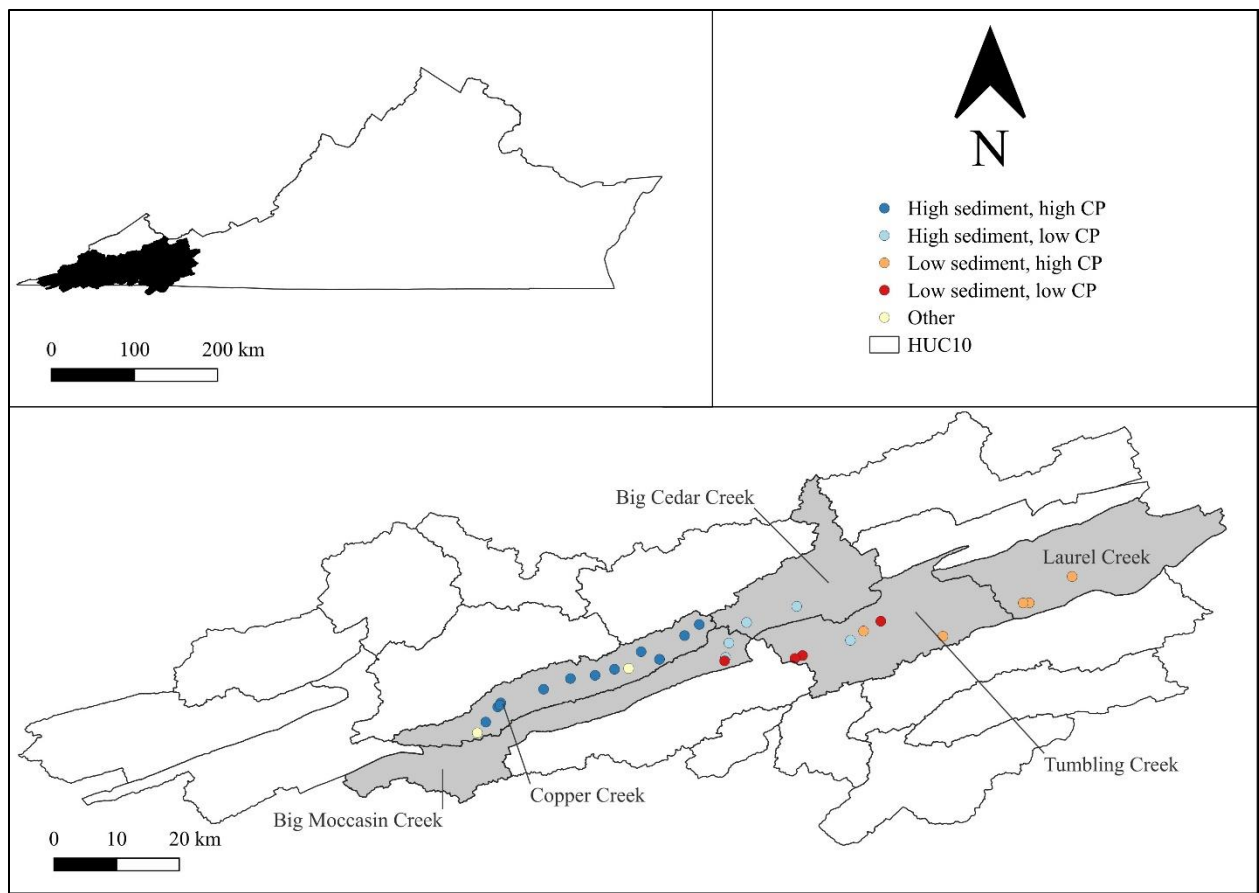


Figure 3.3.1. Spatial distribution of the 31 sites we chose for intensive study. Sites were chosen to represent a range of sediment yields (metric tons/ha/yr) and conservation practice (CP) installation intensity.

Table 3.3.1. We chose 31 sites in the Copper Creek, Laurel Creek, Tumbling Creek, Big Moccasin Creek, and Big Cedar Creek HUC-10 watersheds for intensive study. The table reports the site identification code (ID), subbasin number assigned by SWAT (SB), stream name and order (Ord) derived from the National Hydrography Dataset, and the latitude (Lat) and longitude (Lon) of the site. Also provided are the average annual sediment yields (Sed) of the subbasins from 2001–2019 (tons/ha/yr), number of conservation practices within the subbasin (CP), percent agriculture (Ag) within the riparian area of the subbasin, and the corresponding ranks of each.

ID	SB	Name	HUC10	Ord	Lat	Lon	Sed	Rank	CP	Rank	Ag	Rank
BC-LC678	678	Little Cedar Creek	Big Cedar Creek	3	36.8658	-82.1145	17.86	High	0	Low	18	Med
BC-MB584	584	Mountain Branch	Big Cedar Creek	2	36.8945	-82.0254	23.48	High	0	Low	35	High
BC-WB666	666	Willis Branch	Big Cedar Creek	3	36.8658	-82.1145	23.76	High	0	Low	54	High
BM-NF734	734	North Fork Moccasin Creek	Big Moccasin	2	36.8294	-82.1458	16.65	High	0	Low	31	High
BM-NF832	832	North Fork Moccasin Creek	Big Moccasin	3	36.8037	-82.1519	23.44	High	0	Low	64	High
BM-SF836	886	South Fork Moccasin Creek	Big Moccasin	1	36.7976	-82.1535	1.31	Low	0	Low	33	High
CC-AB29	637	Amos Branch	Copper Creek	1	36.7661	-82.4277	21.12	High	124	High	33	High
CC-CC05	1707	Copper Creek	Copper Creek	2	36.8426	-82.2247	26.75	High	120	High	41	High
CC-CC44	921	Culbertson Creek	Copper Creek	2	36.7472	-82.4755	26.40	High	157	High	32	High
CC-FB75	1264	Flower Branch	Copper Creek	1	36.6696	-82.5935	3.25	Med	30	High	36	High
CC-GC24	823	Grassy Creek	Copper Creek	1	36.7827	-82.3493	21.07	High	38	High	34	High
CC-JB25	875	Jessee Branch	Copper Creek	2	36.7719	-82.3839	27.97	High	125	High	66	High
CC-LC16	712	Little Copper Creek	Copper Creek	2	36.8003	-82.2693	18.95	High	200	High	58	High
CC-MC14	752	Moll Creek	Copper Creek	1	36.8139	-82.3021	39.33	High	30	High	57	High
CC-MC22	837	Moll Creek	Copper Creek	2	36.7842	-82.3242	18.08	High	14	Med	37	High
CC-OC56	1010	Obeys Creek	Copper Creek	2	36.7229	-82.5517	28.01	High	68	High	38	High
CC-PB64	1141	Peters Branch	Copper Creek	1	36.7157	-82.5571	31.82	High	79	High	38	High
CC-PC67	1171	Plank Camp Creek	Copper Creek	2	36.6888	-82.5784	34.14	High	29	High	32	High
CC-SB58	1102	Strong Branch	Copper Creek	1	36.7190	-82.5531	30.98	High	97	High	34	High
CC-UC03	621	Unnamed	Copper Creek	1	36.8623	-82.1986	19.89	High	178	High	33	High
CC-UC15	808	Unnamed	Copper Creek	1	36.8003	-82.2693	14.48	High	38	High	70	High
LC-CB576	576	Crewey Branch	Laurel Creek	2	36.9008	-81.6117	0.21	Low	48	High	48	High
LC-UC559	559	Unnamed	Laurel Creek	1	36.9006	-81.6223	0.00	Low	156	High	45	High
LC-UC756	754	Unnamed	Laurel Creek	2	36.8413	-81.7652	0.70	Low	78	High	59	High

LC-W0422	422	White Oak Branch	Laurel Creek	2	36.9475	-81.5353	0.63	Low	41	High	40	High
TC-BC868	868	Brumley Creek	Tumbling Creek	3	36.8070	-82.0150	0.01	Low	0	Low	27	High
TC-EF639	639	East Fork Wolf Creek	Tumbling Creek	2	36.8506	-81.9063	1.44	Low	29	High	15	Med
TC-RM582	582	Rich Mountain Creek	Tumbling Creek	1	36.8681	-81.8757	0.26	Low	0	Low	20	Med
TC-SH803	803	Steel Hollow	Tumbling Creek	1	36.8070	-82.0150	1.80	Low	0	Low	11	Med
TC-UC792	792	Unnamed	Tumbling Creek	1	36.8020	-82.0284	0.62	Low	0	Low	5	Med
TC-WF1719	1719	West Fork Wolf Creek	Tumbling Creek	3	36.8342	-81.9297	17.41	High	0	Low	30	High

Task 3.4:

Caveats:

Instead of sampling >200 m upstream of confluences, we selected sites as close to confluences as possible, so we can more easily link findings to the SWAT+ output. Also, to save on travel costs and directly link water quality and macroinvertebrate data, we collected water quality samples only twice per year rather than quarterly. Rather than using aerial imagery to ground-truth CPs, we used landowner surveys (Mouser 2024, Chapter 3) to characterize the condition of CPs. We proposed using path analysis to continue exploring indirect effects that CPs have on biota through their effects on water and habitat quality; however, we were unable to develop informative path models that fit the data. Finally, we did not include results of the boosted regression tree models in this report because the information was largely redundant with information from other models. The boosted regression tree models were initially built to explore non-linear relationships between CPs, landscape variables, water quality, and instream habitat and biota. The effects of CPs, agricultural land use, and total nitrogen on biota were similar to those found in Figures 3.4.1, 3.4.2, and 3.4.3, respectively.

Methods:

We collected data on water quality, instream condition, and habitat from the 31 sites described for task 3.3 (Table 3.4.1). Temperature (°C), pH, conductivity (µS/cm), dissolved oxygen (mg/L), and discharge (m³/sec) were collected at each site during autumn 2019, 2020, and 2021 and during spring 2020, 2021, and 2022. Starting spring 2020, we conducted pebble counts (Wolman 1954) and measured embeddedness as indicators of instream habitat during each collection period. Pebble counts were conducted by measuring the intermediate axis on 100 substrate particles selected from a riffle. The median particle size was determined for each collection event at each site (D50). Embeddedness was measured on the same particles by measuring the entire height of the particle perpendicular to the stream bed and the depth of the embedded plane. The depth of the embedded plane was then divided by the entire height of the particle and averaged across all particles measured at a site during a collection event (hereafter measured embeddedness). In spring 2022, we visually estimated bank stability (score 0–10 for each bank then summed, where 0 means 100% of the bank has erosional scars and 10 means 0% of the bank has erosional scars) and embeddedness (score 0–20, where 0 means gravel, cobble, and boulder particles are 100% surrounded by fine sediment and 20 means gravel, cobble, and boulder particles are 0% surrounded by fine sediment; hereafter visual embeddedness). These estimated habitat indices were assessed over an entire site, following the USEPA rapid habitat assessment protocol for high-gradient streams (Barbour et al. 1999, Appendix A-1). During each sampling period except spring 2020 we collected water quality samples. Water quality sampling was not conducted in spring 2020 because of because of laboratory closures due to COVID-19. We collected 1000 ml of water for total suspended solid samples (TSS), 250 ml for both total nitrogen (TN) and total phosphorus (TP) samples, and 100 ml of water for bacteria samples (total fecal coliform bacteria and *E. coli* bacteria). Water samples were stored on ice and returned to the Water Quality Laboratory at Virginia Tech within 24 hours for analysis.

To collect benthic macroinvertebrates, we kicked a total of 3 m² of riffle habitat into a D-frame net (Barbour 1999). Macroinvertebrate samples were stored in 100% ethanol. Macroinvertebrate

samples were identified to genus by an independent contractor that maintains Society for Freshwater Science genus-level certification. We summarized macroinvertebrate collections using the Virginia Stream Condition Index (VSCI; Burton and Gerritsen 2003) and by the proportion of individuals classified as Ephemeroptera, Plecoptera, or Trichoptera minus individuals in the pollution-tolerant family Hydropsychidae (hereafter EPT).

We collated landscape variables (i.e., slope and agriculture) that might influence stream health. We extracted the slope of each subbasin (%) from the SWAT+ model built for Task 1.3. We also calculated the percent agricultural land use within the subbasin containing our site by calculating the number of pixels for each NLCD land use category within the buffer (USGS 2019b), dividing the number of pixels for both hay/pasture and row crop land use by the total number of pixels, and multiplying by 100. We felt that these two variables might account for variation in the aquatic community not explained by our other variables.

We characterized the condition of CPs by surveying landowners as part of another study funded by the Global Change Center at Virginia Tech (Mouser 2024, Chapter 3). We mailed surveys to 889 landowners that asked if they still used their CPs after their cost-share contracts ended. The surveys were also used to identify landowner characteristics that influence continued use of CPs after contracts ended. Results from the survey were used to retain expired CPs in the analysis according to the level of persistence reported in the surveys.

We developed mixed-effect linear regression models to explore the effects of water quality, instream habitat, and CPs on aquatic biota. We built the regression models using the *lme4* package (Bates et al. 2015) in R (R Core Team 2023). Our response variables for the mixed-effect linear regression models were the VSCI and EPT. Our predictor variables in the mixed-effect linear regression models included CP density within the subbasin, CP density squared (to capture potential quadratic effects), average subbasin slope, all the habitat variables, and all the water quality variables (Table 3.4.1). All water quality variables were natural log-transformed to reduce the influence of outliers and to approximate a normal distribution. Similarly, CP density, D50, and slope were square root-transformed. Each variable was also scaled and centered to have a mean of zero and standard deviation of one. All variables were checked for correlations to avoid collinearity; none were highly correlated. Lastly, we included site, watershed, and season as random variables in the model to account for spatial and seasonal autocorrelation. We expected that CPs would first influence water quality and habitat, both of which would eventually shape the aquatic assemblage, and these relationships would be constrained by landscape conditions; therefore, we explored these relationships separately using the models described below.

Table 3.4.1. Descriptions of each predictor variable used in the regression models that assess effects of landscape variables, water quality, instream habitat, and conservation practices (CPs) on aquatic biota.

Variable	Description
CP density (CPs/ha)	Number of CPs within the subbasin containing the site divided by the area of the subbasin
CP density ² (CPs/ha)	Number of CPs within the subbasin containing the site divided by the area of the subbasin squared
Slope (%)	Average slope of the subbasin containing the site
Agriculture	Percent agricultural land use within the subbasin containing the site
Measured embeddedness (%)	Average height of the embedded plane divided by the entire height for 100 particles collected at each site
Visual embeddedness (unitless)	Visual estimate from 0–20, where 0 indicates the substrate particles at the site are 100% surrounded by fine sediment and 20 indicates 0%
D50 (mm)	Median length of the intermediate axis measured on 100 substrate particles collected at each site
Bank stability (unitless)	Visual estimate from 0–10 for each streambank (summed), where 0 indicates 100% of the bank has erosional scars and 10 indicates 0% of the bank has erosional scars
Total suspended solids (mg/L)	Concentration of suspended solids in the water at each site
Total nitrogen (mg/L)	Concentration of nitrogen in the water at each site
Total phosphorus (mg/L)	Concentration of phosphorus in the water at each site
<i>E. coli</i> (most probable number/100 ml)	Concentration of <i>E. coli</i> bacteria in the water at each site
Fecal coliform (most probable number/100 ml)	Concentration of fecal coliform bacteria in the water at each site

We modeled relationships among CP density, landscape variables, habitat variables, and water quality variables using simple linear, exponential decay, and linear plateau models. Because sampling multiple times at the same site resulted in pseudoreplication and a random effect could not be added to these types of models, we calculated the mean of each variable for each site (i.e., reducing the data to 31 rows). We calculated the arithmetic mean for all variables except *E. coli* bacteria, and instead calculated the geometric mean, which is more appropriate for left-skewed data. We then calculated correlations among all variables and found that TP was significantly correlated with TSS and *E. coli* bacteria was significantly correlated with fecal coliform bacteria; therefore, we focus on TSS and *E. coli* bacteria going forward. Likewise, we dropped measured embeddedness from the following analyses because having two measures of embeddedness was redundant and initial analyses did not reveal any significant relationships with measured embeddedness. We visually assessed for outliers using boxplots and a plotting Cook’s distance values. The plots revealed potential outliers for N, TSS and *E. coli* bacteria but we chose not to remove the outliers for N and TSS because their distribution was similar to non-outliers and their removal did not significantly change the model outputs described below. However, the outlier for *E. coli* bacteria did not follow the general pattern and came from a site that had consistently higher values than other sites (presumably because of constant cattle access at one of our smallest sites), so it was removed. Simple linear regression models were built using the lm

function from the *stats* package in R (R Core Team 2023). We used the functions *asymptotic_ineg* and *linear_plateau* from the *AgroReg* package (Shimizu and Goncalves 2023) to build the exponential decay and quadratic plateau models. We used visual inspections of relationships, model coefficient *p*-values, and indices of the proportion variation explained (i.e., R^2 and pseudo- R^2) to determine which model best explained the influence of CP density on each variable. None of those models could adequately explain the relationship between CP density and visually estimated embeddedness or CP density and bank stability, so we used the function *chgptm* from the package *chngrpt* to model a breakpoint regression with two disjunct flat lines (Fong et al. 2017).

We explored the relationship between macroinvertebrate community and water quality and habitat using Threshold Indicator Taxa Analysis (TITAN; Baker et al. 2023). We removed taxa with less than five observations and ran TITAN using 500 bootstrapped runs. We determined the values at which the macroinvertebrate community exhibits two threshold responses — one where taxa respond negatively and one where taxa respond positively — to changes in water quality and habitat based only on “high purity” taxa (i.e., taxa that are consistently assigned the same response direction) and “high reliability” taxa (i.e., taxa that consistently achieve a *p*-value < 0.05).

Because many of the relationships between conservation practice density and water quality, habitat, and biota were not significant and depended on agricultural land use, we further explored these relationships using ANOVA. First, we assigned each site to 1 of 5 bins: high subbasin agricultural land use, low CP density ($n = 4$); high agriculture, high CP ($n = 9$); medium agriculture, high CP ($n = 9$); medium agriculture, low CP ($n = 3$); or low agriculture, low CP ($n = 6$). We then built ANOVA models with the response variables TN, TSS, *E. coli*, bank stability, embeddedness, VSCI, proportion EPT, and EPT taxa and site classification as the treatment. Finally, we tested for differences between categories using Tukey’s test.

Results:

The instream data collected were quite variable across sites (Table 3.4.2). Most collections ($n = 88$) were dominated by pebble substrates (i.e., $5 \text{ mm} \leq D50 \leq 64 \text{ mm}$); however, a single collection was dominated by bedrock (i.e., $D50 < 1 \text{ mm}$ and substrate predominately bedrock) and 53 collections were dominated by cobble (i.e., $65 \text{ mm} \leq D50 \leq 256 \text{ mm}$). Measured embeddedness ranged from 8.20–48.34% (mean \pm standard deviation: $23.56 \pm 8.61\%$) and visually estimated embeddedness ranged from 9–18 (12.60 ± 2.41). Visually estimated bank stability ranged from 4–18 (13.79 ± 3.53). Total suspended solids ranged from <0.10–44.80 mg/L ($4.23 \pm 5.60 \text{ mg/L}$), TN ranged from <0.08–4.65 mg/L ($1.27 \pm 0.77 \text{ mg/L}$), and TP ranged from <0–0.01 mg/L ($0.03 \pm 0.04 \text{ mg/L}$). Most total coliform bacteria samples had values greater than the laboratory could measure ($n = 84$); however, measurable values ranged from 435.2–2,416.17 (1596.28 ± 632.95 most probable number/100 ml). Measurable values for *E. coli* ($n = 124$) ranged from 6.30–2,416.17 (439.43 ± 546.19 most probable number/100 ml). The VSCI for each site ranged from 34.05–81.04 (65.10 ± 9.15). The proportion of individuals classified as EPT taxa ranged from 0–0.87 (0.37 ± 0.20).

Table 3.4.2. Results of the instream data collection. ID = site identification code, Date = date the data were collected, Temp = water temperature (°C), DO = dissolved oxygen (mg/L), SPC = specific conductivity (µS/cm), Q = discharge (m³/sec), D50 = median substrate size (mm), Emb = embeddedness (%), TSS = total suspended solids (mg/L), Coli = total fecal coliform bacteria (most probable number/100 ml), Ecoli = total *E. coli* bacteria (most probable number/100 ml), TN = total nitrogen (mg/L), TP = total phosphorus (mg/L), Emb2 = visually estimated embeddedness, Stab = bank stability, VSCI = Virginia Stream Condition Index, EPT = proportion of macroinvertebrate individuals classified as Ephemeroptera, Plecoptera, or Trichoptera minus individuals in the family Hydropsychidae.

ID	Date	Temp	DO	SPC	pH	Q	D50	Emb	TSS	Coli	Ecoli	TN	TP	Emb2	Stab	VSCI	EPT
BC-MF584-A20	24 Oct 20	15.6	8.47	267.2	8.9	0.023	38	21.84	10.04	>2419.2	1553.07	1.78	0.05	12	14	54.65	0.14
BC-MF584-A21	22 Oct 21	13.3	9.41	302.1	7.97	0.017	78	26.63	40.31	1011.10	137.40	1.97	0.12	12	14	59.74	0.16
BC-MF584-SP21	15 May 21	9.6	10.53	264.5	8.23	0.020	80	26.62	10.38	1011.10	524.70	1.55	0.05	12	14	52.80	0.09
BC-MF584-SP22	01 May 22	14	9.54	251	7.93	0.028	30	37.60	13.83	>2419.2	727.00	1.53	0.05	12	14	66.83	0.25
BC-UC678-A20	24 Oct 20	15.7	9	333.2	8.92	0.025	1	12.59	2.40	>2419.2	2419.17	1.54	0.02	15	10	68.26	0.20
BC-UC678-A21	22 Oct 21	14.1	9.44	374.2	8.29	0.008	90	19.97	4.49	>2419.2	2419.17	1.50	0.03	15	10	50.62	0.13
BC-UC678-SP21	15 May 21	12.3	9.96	296.3	8.28	0.031	30	21.26	2.30	>2419.2	1413.60	1.37	0.01	15	10	68.66	0.37
BC-UC678-SP22	01 May 22	13.3	10.48	295	7.95	0.026	40	20.75	3.31	>2419.2	866.40	1.29	0.01	15	10	70.69	0.44
BC-WB666-A20	25 Oct 20	15	9.52	311.6	8.79	0.022	35	15.79	3.46	2419.2	1046.2	1.24	BD	12	16	53.60	0.12
BC-WB666-A21	22 Oct 21	13.3	9.58	339	8.1	0.013	20	27.31	4.25	>2419.2	866.40	1.27	0.01	12	16	54.38	0.11
BC-WB666-SP21	15 May 21	11.7	9.98	323.9	8.18	0.022	58	19.60	3.65	>2419.2	161.60	1.05	0.01	12	16	49.91	0.23
BC-WB666-SP22	01 May 22	13.2	10.1	317.9	7.86	0.016	60	21.44	4.62	>2419.2	579.40	1.05	0.01	12	16	49.37	0.07
BM-NF734-A20	24 Oct 20	17.2	9.73	365.9	8.74	0.021	22	14.25	1.89	>2419.2	365.40	1.13	0.02	10	16	51.50	0.18
BM-NF734-A21	22 Oct 21	15.1	9.82	400	8.12	0.003	50	11.77	13.96	>2419.2	228.20	1.18	0.07	10	16	64.79	0.14
BM-NF734-SP21	15 May 21	13.7	11.06	371.4	8.15	0.007	25	18.73	4.22	960.60	344.40	0.70	0.02	10	16	59.76	0.21
BM-NF734-SP22	01 May 22	17.7	14.09	341.3	8.21	0.006	30	22.64	2.50	1011.10	360.90	1.23	0.03	10	16	65.56	0.28
BM-NF832-A20	08 Nov 20	11.1	8.72	395.5	8.75	0.041	90	14.70	4.05	>2419.2	>2419.2	1.82	0.02	13	4	63.95	0.14
BM-NF832-A21	22 Oct 21	15.4	9.28	421.8	8.43	0.008	110	23.80	4.79	1011.10	1011.10	1.91	0.06	13	4	59.47	0.11
BM-NF832-SP21	15 May 21	19.3	10.94	372.7	8.56	0.015	70	31.09	3.08	>2419.2	>2419.2	0.99	0.02	13	4	51.80	0.24
BM-NF832-SP22	01 May 22	19.7	10.68	345.6	8.37	0.013	70	16.05	1.56	>2419.2	>2419.2	0.98	0.03	13	4	58.37	0.15
BM-SF886-A20	24 Oct 20	15.5	9.57	305	8.75	0.008	28	12.47	2.17	>2419.2	365.40	0.30	0.02	11	13	56.68	0.21
BM-SF886-A21	22 Oct 21	13.8	9.15	345.9	8.09	0.002	40	17.08	3.65	>2419.2	435.20	0.80	0.04	11	13	56.46	0.20
BM-SF886-SP21	15 May 21	14.8	11.3	263.7	8.44	0.015	35	22.82	4.54	2419.17	193.50	0.22	0.02	11	13	67.13	0.34

BM-SF886-SP22	01 May 22	17.9	12.42	301.4	8.21	0.008	30	36.28	3.39	>2419.2	579.40	0.54	0.04	11	13	59.30	0.34
CC-AB29-A19	10 Nov 19	12.8	9.19	238.6	8.06	0.065	-	-	0.30	>2419.2	>2419.2	1.21	0.00	16	14	56.27	0.24
CC-AB29-A20	01 Nov 20	13.2	8.73	306.8	8.08	0.107	50	12.44	0.86	>2419.2	488.40	1.95	0.04	16	14	53.48	0.12
CC-AB29-A21	23 Oct 21	13.3	9.39	328.8	7.38	0.053	40	35.38	0.67	920.80	77.10	1.17	0.01	16	14	48.98	0.12
CC-AB29-SP20	16 May 20	14	9.49	266.1	8.16	0.206	70	12.74	-	-	-	-	-	16	14	61.39	0.66
CC-AB29-SP21	16 May 21	13	9.05	308.4	7.56	0.120	65	21.55	0.50	1299.65	58.10	1.23	0.01	16	14	64.94	0.40
CC-AB29-SP22	02 May 22	13.7	10.44	289.2	7.3	0.048	40	32.75	0.30	1413.60	159.70	1.29	BD	16	14	49.97	0.50
CC-CC05-A19	10 Nov 19	11.6	9.03	333	8.11	0.055	-	-	5.55	2419.17	77.10	2.18	0.02	12	12	57.26	0.37
CC-CC05-A20	31 Oct 20	13	9.15	311.5	8.26	0.244	27	24.47	6.46	>2419.2	461.1	2.25	0.01	12	12	58.97	0.23
CC-CC05-A21	22 Oct 21	13.6	8.76	349.4	7.84	0.027	15	43.51	4.05	>2419.2	>2419.2	2.48	0.04	12	12	61.63	0.30
CC-CC05-SP20	16 May 20	13.4	9.7	271.2	8.38	0.191	30	16.55	-	-	-	-	-	12	12	61.76	0.21
CC-CC05-SP21	15 May 21	14.4	10.14	336.4	8.02	0.078	20	20.92	3.38	>2419.2	1413.60	1.70	0.01	12	12	64.91	0.55
CC-CC05-SP22	01 May 22	13	10.4	242.2	7.71	0.077	25	30.17	1.17	1011.10	61.30	1.62	BD	12	12	73.80	0.58
CC-CC44-A19	10 Nov 19	12.2	8.78	311	8.76	0.041	-	-	1.26	>2419.2	686.7	1.46	0.01	10	18	67.68	0.24
CC-CC44-A20	01 Nov 20	13.9	9.61	314.8	8.98	0.142	63	19.68	2.84	>2419.2	461.1	1.93	0.03	10	18	71.86	0.24
CC-CC44-A21	23 Oct 21	13.9	9.14	333.2	8.21	0.029	50	28.80	0.92	>2419.2	22.30	1.24	0.01	10	18	75.57	0.42
CC-CC44-SP20	15 May 20	16	8.75	256.8	9.01	0.190	23	37.61	-	-	-	-	-	10	18	69.59	0.57
CC-CC44-SP21	16 May 21	13.4	10.19	318.7	8.39	0.099	45	23.72	3.33	2419.17	32.30	1.53	0.01	10	18	68.71	0.65
CC-CC44-SP22	02 May 22	15.7	10.92	320.2	8.12	0.087	60	31.23	2.04	1203.31	272.30	1.40	BD	10	18	72.92	0.47
CC-FB75-A19	17 Nov 19	5.5	12.32	378	8.57	0.003	-	-	0.41	1732.87	6.30	1.47	0.02	12	18	69.50	0.32
CC-FB75-A20	01 Nov 20	11.2	10	325.3	8.95	0.017	55	13.05	1.88	>2419.2	148.3	0.92	BD	12	18	48.11	0.07
CC-FB75-A21	23 Oct 21	12.1	7	400.5	7.93	0.001	30	12.42	2.03	>2419.2	14.30	0.95	0.01	12	18	50.56	0.10
CC-FB75-SP20	15 May 20	12.5	8.96	319.8	8.73	0.012	40	12.29	-	-	-	-	-	12	18	60.62	0.29
CC-FB75-SP21	16 May 21	14.4	8.83	350.1	8.19	0.006	40	8.20	2.29	1011.10	42.80	0.66	0.01	12	18	47.70	0.18
CC-FB75-SP22	02 May 22	13.2	9.77	349.7	7.89	0.011	43	22.92	2.50	2419.17	49.60	0.42	0.01	12	18	58.22	0.23
CC-GC24-A19	10 Nov 19	12.5	10.2	314.1	8.76	0.030	-	-	1.73	>2419.2	727	1.54	0.01	9	17	63.22	0.12
CC-GC24-A20	31 Oct 20	13.5	9.51	301.7	8.73	0.107	16	16.57	11.44	>2419.2	344.8	2.05	0.07	9	17	56.38	0.08
CC-GC24-A21	24 Oct 21	12.6	9.41	337.7	8.05	0.015	20	18.37	1.75	>2419.2	344.80	1.33	0.02	9	17	60.92	0.24
CC-GC24-SP20	16 May 20	16.1	9.28	271.6	8.78	0.120	20	9.34	-	-	-	-	-	9	17	61.02	0.21
CC-GC24-SP21	15 May 21	16.9	9.26	314.6	8.38	0.045	15	21.98	1.64	>2419.2	313.00	1.51	0.01	9	17	64.83	0.33
CC-GC24-SP22	02 May 22	19	9.72	292.1	8.16	0.047	15	31.92	3.47	>2419.2	1732.87	1.42	0.02	9	17	72.90	0.44

CC-JB25-A19	17 Nov 19	13	9.54	310.6	8.18	0.056	-	-	0.11	435.20	6.30	1.83	0.01	10	17	46.01	0.13
CC-JB25-A20	08 Nov 20	13	9.48	314.9	8.07	0.087	65	20.42	0.57	920.80	53.80	2.34	0.01	10	17	55.42	0.16
CC-JB25-A21	23 Oct 21	13	9.4	328.5	7.33	0.049	30	48.34	0.62	2419.17	64.40	1.79	BD	10	17	55.00	0.16
CC-JB25-SP20	15 May 20	13.2	9.43	271.5	8.18	0.242	30	38.68	-	-	-	-	-	10	17	55.42	0.21
CC-JB25-SP21	16 May 21	12.9	9.37	329.9	7.58	0.136	55	34.41	BD	613.10	228.20	2.01	0.01	10	17	68.09	0.38
CC-JB25-SP22	02 May 22	13.2	10.6	324.7	7.39	0.139	50	39.93	0.10	960.60	313.00	2.39	BD	10	17	74.60	0.61
CC-LC16-A19	10 Nov 19	7.2	12.08	396	8.86	0.060	-	-	2.10	1986.3	109.5	1.89	0.03	13	14	56.96	0.24
CC-LC16-A20	31 Oct 20	13.1	10.45	354.9	8.91	0.254	60	9.50	7.83	>2419.2	344.4	2.42	0.02	13	14	73.63	0.43
CC-LC16-A21	24 Oct 21	17.4	7.39	357.7	8.32	0.038	50	30.48	9.11	>2419.2	980.40	2.39	0.04	13	14	61.02	0.14
CC-LC16-SP20	16 May 20	22.7	9.07	287.8	9.28	0.132	65	16.97	-	-	-	-	-	13	14	68.23	0.24
CC-LC16-SP21	17 May 21	16.3	10.19	369.8	8.56	0.055	145	12.00	5.74	>2419.2	>2419.2	2.23	0.02	13	14	64.11	0.40
CC-LC16-SP22	03 May 22	23.4	10.51	373	8.24	0.042	80	22.06	1.90	>2419.2	378.40	1.89	0.02	13	14	47.06	0.26
CC-MC14-A19	10 Nov 19	11.2	10.38	307.5	8.6	0.016	-	-	44.80	>2419.2	>2419.2	2.91	0.33	13	16	34.05	0.06
CC-MC14-A20	31 Oct 20	14.4	9.58	256	8.56	0.057	36	28.52	6.34	>2419.2	396.8	1.80	0.03	13	16	67.96	0.31
CC-MC14-A21	24 Oct 21	13.2	9.19	334.8	8.03	0.012	11	39.89	0.10	>2419.2	1203.31	1.38	0.02	13	16	76.54	0.48
CC-MC14-SP20	15 May 20	17.6	9.28	219.8	8.99	0.047	28	35.86	-	-	-	-	-	13	16	63.68	0.70
CC-MC14-SP21	16 May 21	12.4	9.23	304.2	8.12	0.023	45	31.63	10.25	>2419.2	>2419.2	1.83	0.05	13	16	78.44	0.61
CC-MC14-SP22	02 May 22	17.8	9.08	295.3	8.01	0.017	38	21.98	3.27	>2419.2	579.40	1.35	0.02	13	16	67.86	0.87
CC-MC22-A19	10 Nov 19	8.3	11.5	285	8.73	0.101	-	-	1.60	>2419.2	95.8	1.07	0.01	12	9	63.80	0.13
CC-MC22-A20	31 Oct 20	14.1	9.41	264.8	8.84	0.279	73	20.82	5.42	1011.1	601.5	2.37	BD	12	9	73.54	0.15
CC-MC22-A21	24 Oct 21	14.3	9.7	302.6	8.13	0.057	58	24.68	6.67	1011.10	39.30	0.95	0.01	12	9	71.47	0.49
CC-MC22-SP20	16 May 20	15.2	9.8	210	8.98	0.213	60	27.02	-	-	-	-	-	12	9	72.80	0.34
CC-MC22-SP21	16 May 21	12.7	9.37	308.2	8.24	0.131	80	19.06	4.07	>2419.2	78.00	1.39	0.01	12	9	75.12	0.41
CC-MC22-SP22	03 May 22	17.4	10.78	297.6	7.97	0.072	40	32.84	4.63	640.50	51.20	1.06	BD	12	9	83.63	0.70
CC-OC56-A19	17 Nov 19	8.8	10.7	298.5	8.57	0.057	-	-	1.20	>2419.2	1119.85	0.82	0.01	11	14	70.58	0.41
CC-OC56-A20	01 Nov 20	14.2	9.53	293.3	8.9	0.127	70	29.20	5.03	>2419.2	161.6	1.32	BD	11	14	70.56	0.27
CC-OC56-A21	23 Oct 21	13.8	9.43	322.2	8.16	0.078	110	35.97	2.25	2419.17	63.80	0.67	BD	11	14	78.75	0.50
CC-OC56-SP20	15 May 20	15.5	7.49	243.8	8.84	0.193	12	31.25	-	-	-	-	-	11	14	73.21	0.75
CC-OC56-SP21	16 May 21	15.1	9.54	296.6	8.41	0.108	125	25.44	4.18	>2419.2	325.50	0.88	0.01	11	14	67.37	0.56
CC-OC56-SP22	02 May 22	16	10.23	297.7	8.18	0.111	85	21.75	2.54	2419.17	70.30	0.76	BD	11	14	81.86	0.68
CC-PB64-A19	17 Nov 19	7.2	11	314.7	8.87	0.005	-	-	2.18	1553.07	45.70	1.22	0.02	11	8	61.28	0.35

CC-PB64-A20	01 Nov 20	13.1	9.88	298.1	9.05	0.025	60	14.12	4.23	>2419.2	107.1	2.00	BD	11	8	56.85	0.15
CC-PB64-A21	23 Oct 21	12.3	8.59	332.1	8.27	0.001	50	23.17	5.19	>2419.2	63.10	1.00	0.02	11	8	66.74	0.26
CC-PB64-SP20	15 May 20	14.1	7.98	256.7	9.97	0.013	20	27.15	-	-	-	-	-	11	8	67.26	0.58
CC-PB64-SP21	16 May 21	14.7	8.67	293.1	8.37	0.009	50	10.66	3.43	>2419.2	43.50	1.15	0.01	11	8	60.72	0.68
CC-PB64-SP22	02 May 22	13.1	10.69	299.7	8.14	0.012	30	22.82	1.41	1011.10	107.60	0.97	0.02	11	8	67.86	0.45
CC-PC65-A19	10 Nov 19	9.8	9.88	298.7	8.76	0.020	-	-	1.74	>2419.2	55.6	0.71	0.01	12	15	63.77	0.17
CC-PC65-A20	01 Nov 20	12.1	10.07	311.2	9.04	0.074	35	19.95	2.86	>2419.2	80.90	1.32	BD	12	15	69.04	0.17
CC-PC67-A21	23 Oct 21	11.8	8.78	309.5	8.26	0.017	65	38.55	1.17	>2419.2	1732.87	0.52	0.02	12	15	71.06	0.61
CC-PC67-SP20	15 May 20	13.7	8.64	283.6	9	0.071	15	18.00	-	-	-	-	-	12	15	70.44	0.76
CC-PC67-SP21	16 May 21	14.6	9.47	326.5	8.51	0.039	70	34.23	2.45	1986.28	61.30	0.85	0.01	12	15	68.38	0.60
CC-PC67-SP22	02 May 22	13	10.63	333.1	8.24	0.028	50	29.36	1.61	>2419.2	101.90	0.72	BD	12	15	65.38	0.39
CC-SB58-A19	17 Nov 19	10.4	10.29	310	8.81	0.014	-	-	1.03	1986.28	11.00	0.78	0.01	16	16	64.94	0.15
CC-SB58-A20	01 Nov 20	13.8	9.35	97.1	8.96	0.070	95	20.25	4.66	2419.2	104.6	1.24	BD	16	16	71.67	0.17
CC-SB58-A21	23 Oct 21	13.2	8.81	328.1	8.33	0.014	120	33.49	2.32	2419.17	39.90	0.69	BD	16	16	59.23	0.28
CC-SB58-SP20	15 May 20	14.3	8.01	272.1	8.86	0.039	30	34.14	-	-	-	-	-	16	16	65.74	0.61
CC-SB58-SP21	16 May 21	13.3	9.35	237.7	8.39	0.015	113	29.99	3.31	>2419.2	165.80	0.81	0.01	16	16	72.41	0.54
CC-SB58-SP22	02 May 22	14	10.83	324.1	8.19	0.012	60	29.08	1.46	829.70	12.20	0.73	BD	16	16	74.32	0.49
CC-UC03-A19	10 Nov 19	12.4	9.94	340	8.34	0.026	-	-	1.20	>2419.2	61.7	2.15	0.01	11	16	69.08	0.21
CC-UC03-A20	31 Oct 20	12.4	9.5	325.1	8.14	0.089	15	9.25	4.16	>2419.2	166.9	2.39	0.03	11	16	61.54	0.19
CC-UC03-A21	22 Oct 21	13.4	9.01	352	7.77	0.016	15	18.72	4.26	>2419.2	65.00	1.70	0.01	11	16	46.64	0.03
CC-UC03-SP20	16 May 20	12.9	9.39	280	8.53	0.061	20	12.08	-	-	-	-	-	11	16	62.82	0.55
CC-UC03-SP21	15 May 21	14.8	9.24	339.1	7.99	0.036	17	10.87	3.15	>2419.2	172.20	1.96	0.01	11	16	71.88	0.34
CC-UC03-SP22	01 May 22	13.7	10.86	269.1	7.55	0.020	20	24.79	2.01	960.60	222.40	1.90	0.01	11	16	75.32	0.32
CC-UC15-A19	10 Nov 19	9.7	10.73	396.8	8.75	0.013	-	-	2.29	1553.1	108.6	3.76	0.04	16	12	62.16	0.19
CC-UC15-A20	31 Oct 20	14.5	9.78	363	8.69	0.035	30	22.39	8.51	>2419.2	>2419.2	3.49	0.04	16	12	75.38	0.36
CC-UC15-A21	24 Oct 21	15.8	6.44	409.8	8.08	0.006	45	21.83	11.38	>2419.2	488.40	2.49	0.06	16	12	71.60	0.38
CC-UC15-SP20	16 May 20	20	8.6	318.3	8.89	0.041	30	15.88	-	-	-	-	-	16	12	65.89	0.44
CC-UC15-SP21	17 May 21	18.5	9.89	372.7	8.54	0.031	30	20.95	2.47	>2419.2	1732.87	2.63	0.02	16	12	73.99	0.50
CC-UC15-SP22	03 May 22	22.4	9.11	386.9	8.07	0.013	30	23.60	3.89	>2419.2	571.70	4.65	0.05	16	12	69.20	0.41
LC-CB576-A20	23 Oct 20	13.9	9.68	343.6	8.49	0.043	93	31.47	2.89	>2419.2	1203.31	1.15	0.02	16	6	72.52	0.48
LC-CB576-A21	30 Oct 21	13.1	8.61	340.2	7.76	0.062	130	17.30	8.54	960.60	344.40	1.40	0.02	16	6	67.80	0.38

LC-CB576-SP21	22 May 21	14	10.6	337.3	7.97	0.038	130	30.94	1.98	>2419.2	1203.31	1.30	0.03	16	6	74.05	0.70
LC-CB576-SP22	08 May 22	12.4	11.11	297.1	7.52	0.137	125	15.78	3.07	>2419.2	>2419.2	1.06	0.02	16	6	80.96	0.77
LC-UC559-A20	08 Nov 20	16.9	7.96	337	9	0.007	50	22.42	1.21	>2419.2	>2419.2	1.21	0.02	10	16	50.88	0.14
LC-UC559-A21	30 Oct 21	12.5	9.3	281.3	8.29	0.009	70	33.24	0.60	>2419.2	>2419.2	0.68	0.04	10	16	37.96	0.00
LC-UC559-SP21	22 May 21	23.9	5.62	375.3	8.03	0.006	50	35.26	4.97	>2419.2	2419.17	0.87	0.03	10	16	63.85	0.23
LC-UC559-SP22	08 May 22	15.4	11.38	240.8	8.21	0.015	60	33.15	1.44	>2419.2	>2419.2	0.57	0.02	10	16	45.67	0.33
LC-UC754-A20	23 Oct 20	-	8.54	417	8.75	0.006	8	27.57	4.94	816.40	24.30	0.43	0.03	17	14	69.45	0.29
LC-UC754-A21	30 Oct 21	12.6	8.78	374.5	8.05	0.018	80	11.62	7.60	>2419.2	1413.60	1.28	0.04	17	14	73.24	0.43
LC-UC754-SP21	22 May 21	20.2	6.58	345.1	8.31	0.025	40	14.64	6.76	>2419.2	>2419.2	0.84	0.03	17	14	74.71	0.21
LC-UC754-SP22	08 May 22	16	10.42	306.8	8.02	0.015	60	9.87	5.31	>2419.2	410.60	0.48	0.01	17	14	75.47	0.59
LC-WO422-A20	23 Oct 20	11.9	9.5	329	8.82	0.011	60	14.94	2.82	>2419.2	325.50	1.61	0.11	11	8	74.57	0.37
LC-WO422-A21	30 Oct 21	12.5	8.94	401.8	8.27	0.066	110	24.96	5.02	>2419.2	517.20	1.55	0.04	11	8	67.36	0.83
LC-WO422-SP21	22 May 21	14.2	9.92	337.7	8.42	0.018	85	20.37	4.38	>2419.2	1299.65	1.40	0.02	11	8	63.77	0.54
LC-WO422-SP22	08 May 22	11.6	11.13	313.2	7.97	0.113	103	23.40	10.05	>2419.2	>2419.2	1.00	0.03	11	8	68.43	0.58
TC-BC868-A20	08 Nov 20	12.5	10.04	16.4	7.69	0.335	138	10.52	0.20	488.40	11.00	0.08	0.01	18	12	81.04	0.69
TC-BC868-A21	31 Oct 21	11.4	9.72	12.5	5.81	2.095	140	23.70	3.39	1011.10	133.30	BD	BD	18	12	75.59	0.52
TC-BC868-SP21	23 May 21	14.9	9.28	19	7.24	0.214	130	15.97	0.37	1119.85	191.80	0.28	BD	18	12	67.25	0.47
TC-BC868-SP22	12 May 22	13.4	11.3	14.8	6.19	0.853	150	27.54	0.85	1203.31	62.40	0.25	BD	18	12	75.15	0.61
TC-EF639-A20	24 Oct 20	14.3	8.36	157.3	8.46	0.056	70	11.24	0.80	2419.17	37.90	0.19	0.16	16	11	75.33	0.66
TC-EF639-A21	31 Oct 21	13.5	8.77	212	7.79	0.110	55	15.19	1.04	2419.17	116.20	0.41	0.01	16	11	83.22	0.72
TC-EF639-SP21	22 May 21	19.5	9.18	155.8	8.1	0.059	73	36.21	1.23	>2419.2	770.10	0.26	0.01	16	11	69.21	0.43
TC-EF639-SP22	08 May 22	13.9	10.86	120.8	7.54	0.487	80	20.62	4.56	>2419.2	1119.85	0.35	0.02	16	11	66.40	0.55
TC-RM582-A20	23 Oct 20	14.8	8.79	201.9	8.71	0.028	30	23.66	3.47	>2419.2	1553.07	0.20	0.01	10	18	77.22	0.43
TC-RM582-A21	30 Oct 21	12.2	9.21	247.9	7.96	0.047	110	31.93	6.16	>2419.2	83.30	0.42	0.03	10	18	66.40	0.31
TC-RM582-SP21	22 May 21	17.2	8.92	173.6	8.1	0.021	120	37.04	5.67	>2419.2	17.10	0.35	0.02	10	18	71.23	0.56
TC-RM582-SP22	08 May 22	-	11.14	160.9	7.74	0.230	100	33.55	8.75	1011.10	304.40	0.34	0.03	10	18	77.13	0.59
TC-SH803-A20	08 Nov 20	13.7	8.3	27.8	7.77	0.069	43	26.67	1.19	1732.87	90.60	0.14	0.01	10	15	73.06	0.39
TC-SH803-A21	31 Oct 21	12.3	9.01	30.1	6.51	0.130	40	35.49	1.82	960.60	231.00	BD	BD	10	15	61.86	0.41
TC-SH803-SP21	23 May 21	14.7	7.95	26.3	7.33	0.025	70	22.70	0.65	>2419.2	235.90	0.29	0.01	10	15	60.03	0.31
TC-SH803-SP22	12 May 22	13.2	10.82	20.1	6.83	0.117	68	32.28	0.69	1986.28	166.40	0.18	BD	10	15	76.32	0.62
TC-UC792-A20	24 Oct 20	15	8.55	133.8	8.5	0.009	160	23.17	1.96	2419.17	7.40	0.80	0.03	15	18	68.29	0.51

TC-UC792-A21	31 Oct 21	12.2	10.38	124.7	7.55	0.101	190	34.95	16.06	691.00	178.50	1.08	0.04	15	18	68.81	0.54
TC-UC792-SP21	22 May 21	16.2	8.55	114.7	7.82	0.008	180	25.45	7.16	>2419.2	8.40	0.56	0.04	15	18	68.22	0.46
TC-UC792-SP22	08 May 22	12.1	11.82	100	7.44	0.133	180	18.65	11.57	2419.17	228.20	0.64	0.04	15	18	64.71	0.40
TC-WF1719-A20	08 Nov 20	13.9	10.31	38.5	7.82	0.317	73	13.63	1.01	1413.60	344.80	0.18	0.01	13	16	70.35	0.34
TC-WF1719-A21	31 Oct 21	13.4	10.04	55.1	7.28	0.339	100	13.29	2.14	>2419.2	816.40	0.30	0.01	13	16	63.13	0.44
TC-WF1719-SP21	22 May 21	19.9	7.82	52	8.09	0.172	70	19.34	0.76	>2419.2	204.60	0.43	BD	13	16	66.70	0.49
TC-WF1719-SP22	12 May 22	15	11.29	36.3	6.52	0.498	80	19.45	2.30	1986.28	235.90	0.23	BD	13	16	70.33	0.54

“-” = samples/data that were not collected

“BD” = below detection level.

We received responses about 398 CPs from 84 landowners that could be used to characterize continued use of CPs. We found that 84%, 94%, 94% of fencing, watering, and pasture management CPs were reported to still be in use. In contrast, only about 74% of riparian buffers were reported to still be in use.

Counterintuitive results from the mixed-effects regression model revealed that it would be helpful to explore the indirect relationships between CPs and biotic responses (e.g., how CPs influence water quality and how water quality influences biotic responses). The VSCI and EPT responded similarly to the predictor variables, but EPT had stronger relationships, so we only discuss the EPT results (Table 3.4.3). The regression model explained 29% of the variation in EPT. Nitrogen was the only water quality variable related to EPT, and that correlation was negative. Bank stability was also negatively related to EPT, which is opposite of the relationship we would expect. Interestingly, CPs showed a quadratic relationship with proportion EPT, wherein CPs were positively correlated with biotic health at very low levels of CP implementation (0 – ≈ 0.15 CPs/ha) but a negative relationship occurred at higher levels of implementation (Figure 3.4.1). To further explore how CPs influence stream health, we built the models described below.

Table 3.4.3. Results of a mixed-effects linear regression model used to predict the proportion of macroinvertebrate individuals collected at a site that were classified as Ephemeroptera, Plecoptera, or Trichoptera minus individuals in the family Hydropsychidae. Watershed, season, and site were included as random effects. See task 3.4 methods and table 3.4.1 for the descriptions of each parameter.

Parameter	Estimate \pm SE	<i>p</i>-value
Intercept	0.40 \pm 0.06	< 0.01
CP density	0.03 \pm 0.03	0.40
CP density ²	-0.06 \pm 0.02	< 0.01
Slope	0.03 \pm 0.02	0.17
Measured embeddedness	<0.01 \pm 0.01	0.94
Visual embeddedness	0.01 \pm 0.02	0.47
D50	0.01 \pm 0.02	0.51
Bank stability	-0.03 \pm 0.02	0.08
Total nitrogen	-0.05 \pm 0.02	0.03
Total suspended solids	-0.01 \pm 0.02	0.35
Total phosphorus	<0.01 \pm 0.02	0.66
<i>E. coli</i>	-0.01 \pm 0.02	0.49
Fecal coliform	<-0.01 \pm 0.01	0.75

SE = standard error

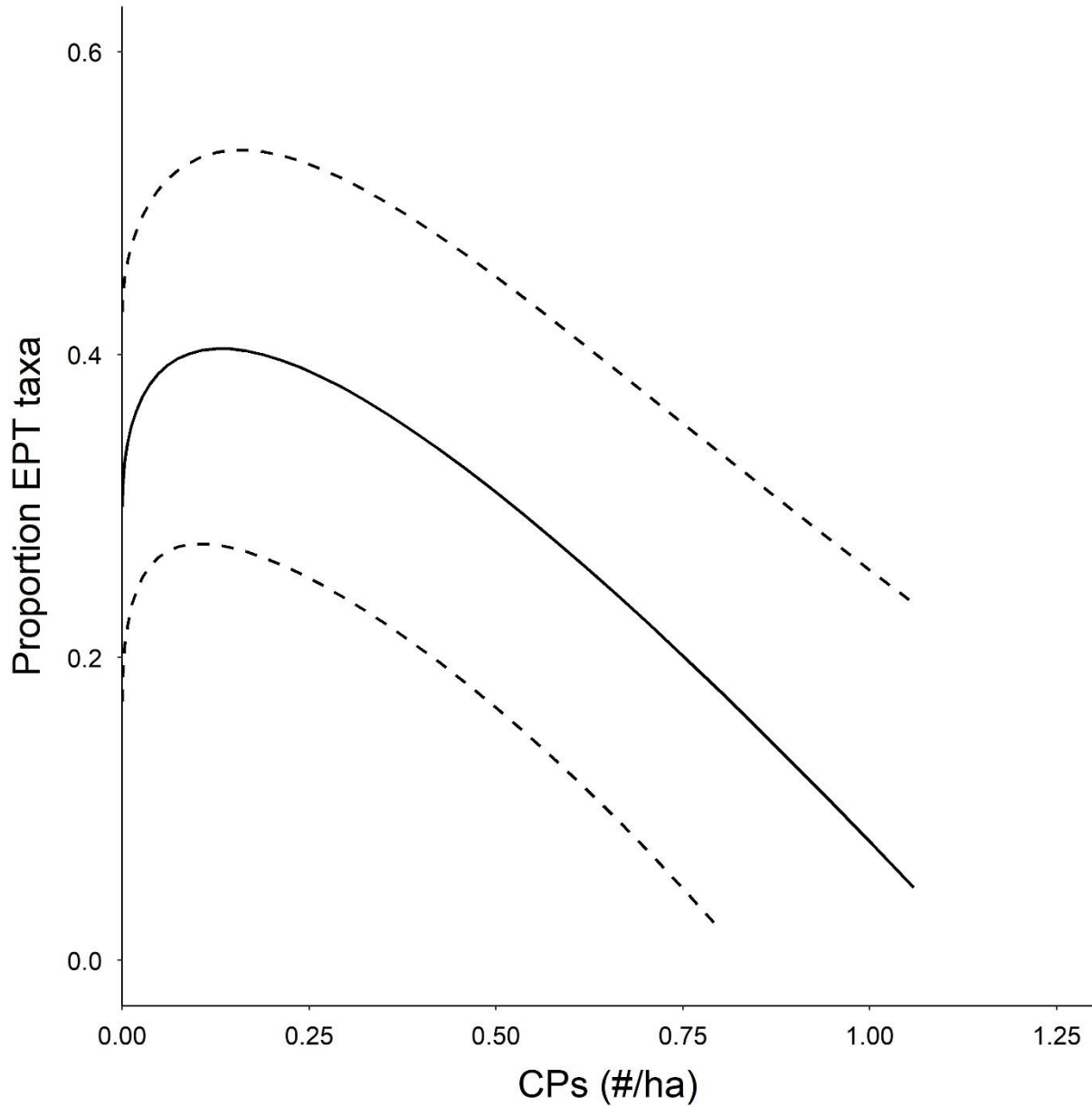


Figure 3.4.1. Relationship between number of conservation practices (CPs) per hectare and proportion of macroinvertebrate individuals collected at a site that were classified as Ephemeroptera, Plecoptera, or Trichoptera minus individuals in the family Hydropsychidae (EPT). The solid line depicts the predicted relationship and the dashed lines are 95% confidence intervals. The relationship was derived from a mixed-effects linear regression model (Table 3.4.3) where all other variables were held at their means. Watershed, season, and site were included as random effects.

Agricultural land use negatively affected water quality and the macroinvertebrate assemblage, but there was no direct relationship between agricultural land use and habitat. The simple linear regression models indicated that agricultural land use was positively related to TN ($p < 0.01$) and *E. coli* ($p < 0.01$) but not TSS ($p = 0.41$), embeddedness ($p = 0.74$), or bank stability ($p = 0.38$).

Slope was negatively related to agriculture ($p < 0.01$), and CPs were positively related with agriculture ($p = 0.08$). Agricultural land use had a negative relationship with proportion EPT ($p < 0.01$), VSCI ($p = 0.09$), and number of EPT taxa ($p < 0.01$).

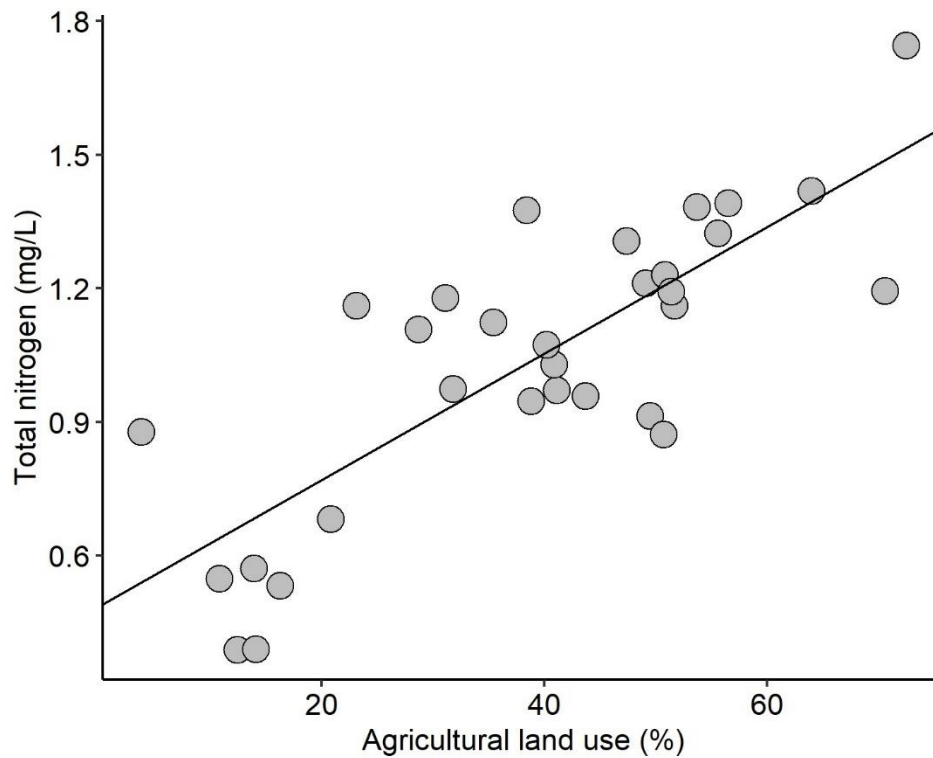


Figure 3.4.2. A simple linear model showed that increasing agricultural land use in 31 watersheds led to increased total nitrogen.

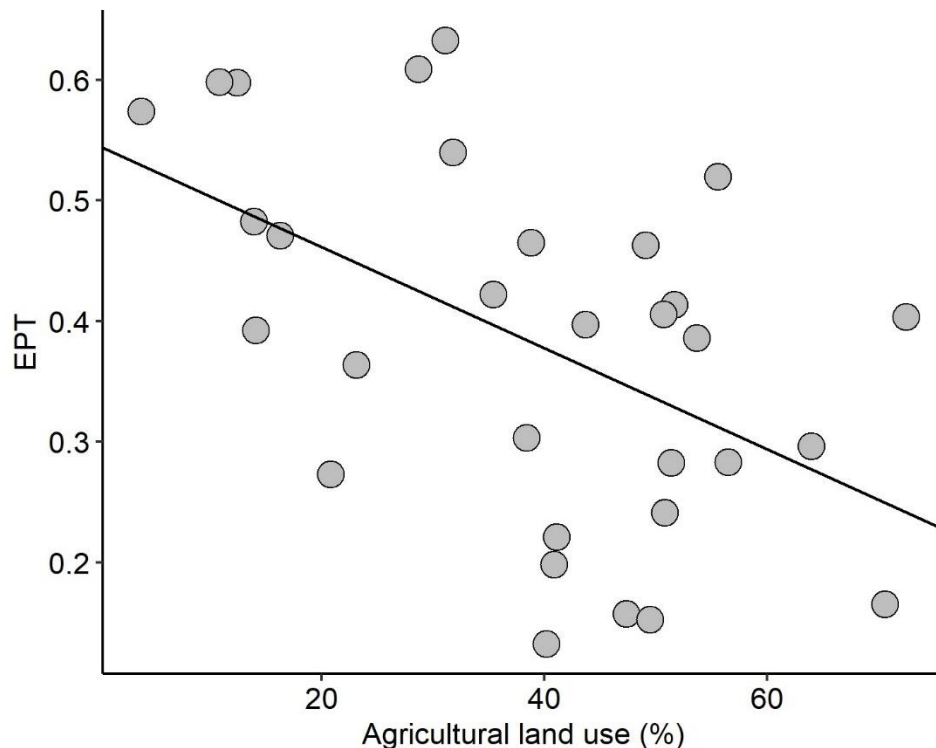


Figure 3.4.3. A simple linear model showed that increasing agricultural land use in 31 watersheds led to decreased proportions of macroinvertebrate individuals collected at a site that were classified as Ephemeroptera, Plecoptera, or Trichoptera minus individuals in the family Hydropsychidae (EPT).

We found that CPs appear to improve or stabilize several water quality and physical habitat measures above certain thresholds of CP density (Figures 3.4.4–3.4.7, Table 3.4.4), but apparent effects of CPs varied widely across physicochemical factors and models, and no model accounted for more than 21% of the variance in a physicochemical factor. The linear plateau model explained the greatest amount of variation (pseudo- $R^2 = 0.21$) in the response of nitrogen to CP density and showed a significant change in slope after the breakpoint (breakpoint = 0.30, p -value = 0.09; Figure 3.4.4). The exponential decay model explained the most variation in the relationship between CP density and TSS (pseudo- $R^2 = 0.05$), *E. coli* bacteria (pseudo- $R^2 = 0.07$), and D50 (pseudo- $R^2 = 0.07$) but the coefficients for the exponents were not statistically significant (Table 3.4.4). Despite poor predictive power of the exponential decay models, higher CP density visually appeared to be associated with lower values of TSS (Figure 3.4.5), *E. coli* bacteria (Figure 3.4.6), and D50. Although we could not calculate R^2 for stepwise regression, it appeared to best explain the relationship between CPs and bank stability (Figure 3.4.7). When CP density was greater than 0.41 CPs/ha, bank stability received an average score of 16.4 and when CP density was below that threshold, bank stability received a score of 12.4 on average (p -

value < 0.01). Our results collectively suggest that increasing CP density leads to improved or stabilized water quality and habitat, but outcomes vary greatly among specific sites.

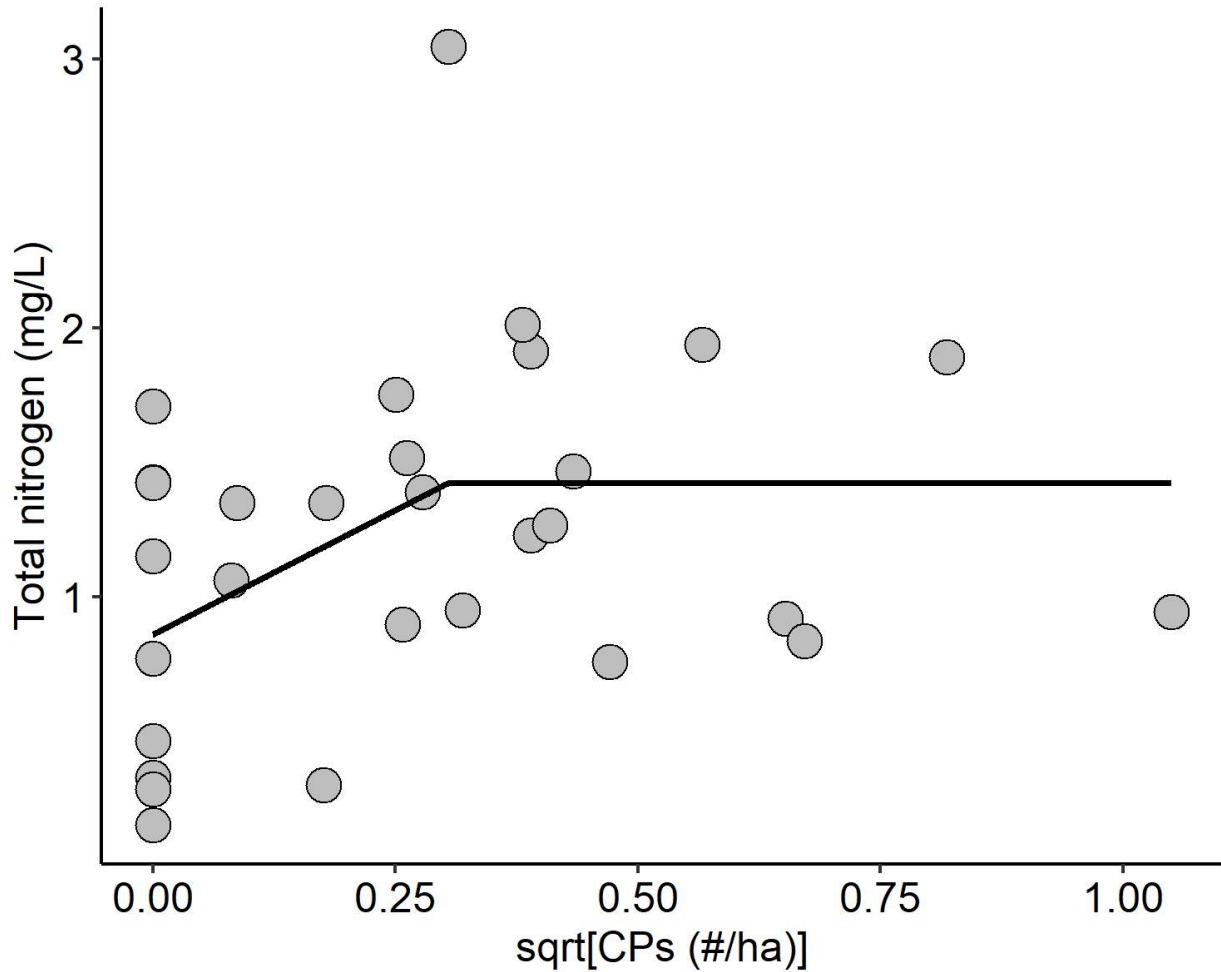


Figure 3.4.4. A linear plateau model showed that total nitrogen in 31 watersheds stops increasing after conservation practices (CPs) reach a density (number per hectare) of $\approx 0.1/\text{ha}$.

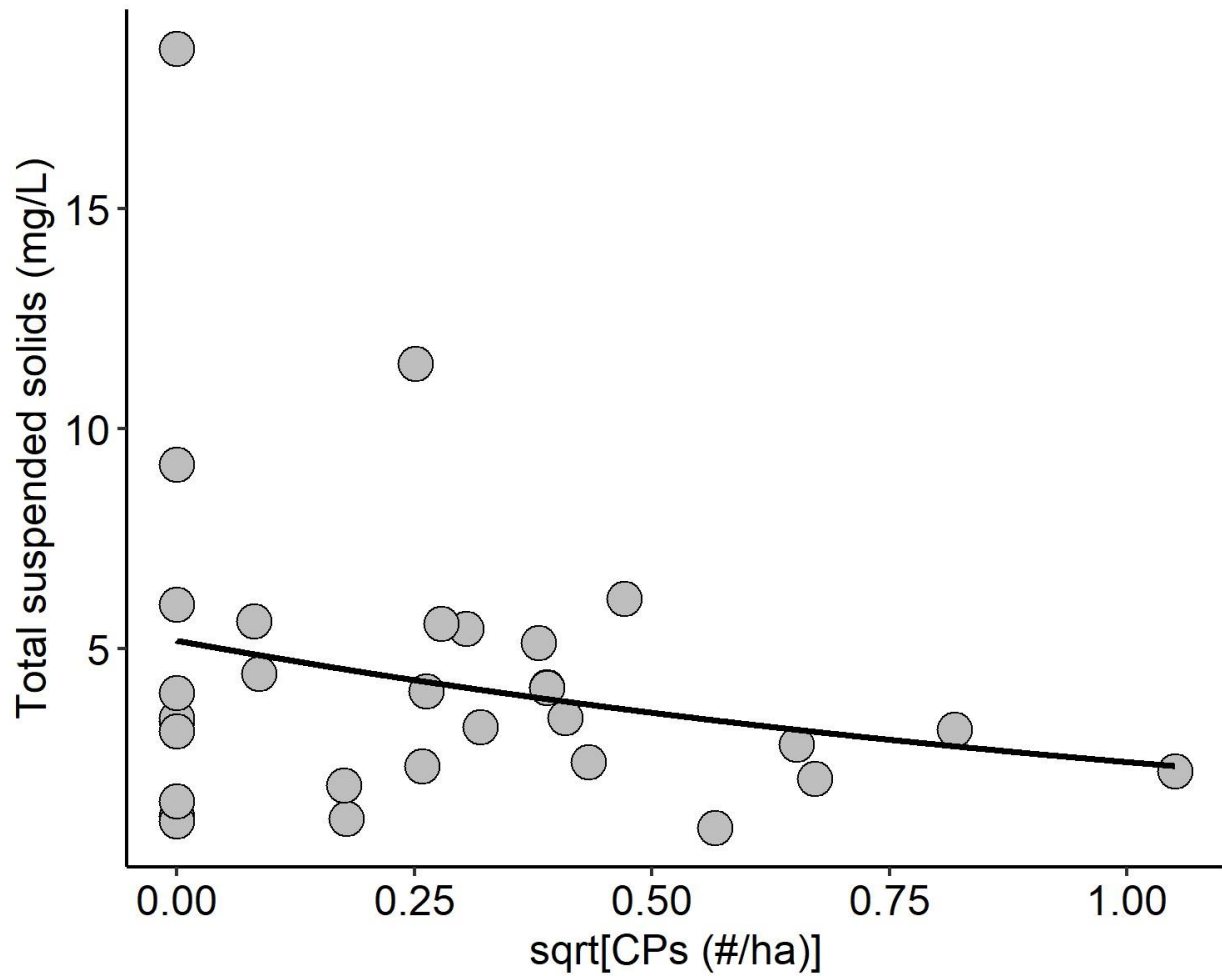


Figure 3.4.5. Increasing density of conservation practices (CPs) appeared to lead to declines in total suspended solids following a pattern of exponential decay. However, the exponential decay model only explains 5% of the variation in the relationship between CP density (number per hectare) and total suspended solids, and the model coefficients are not statistically significant.

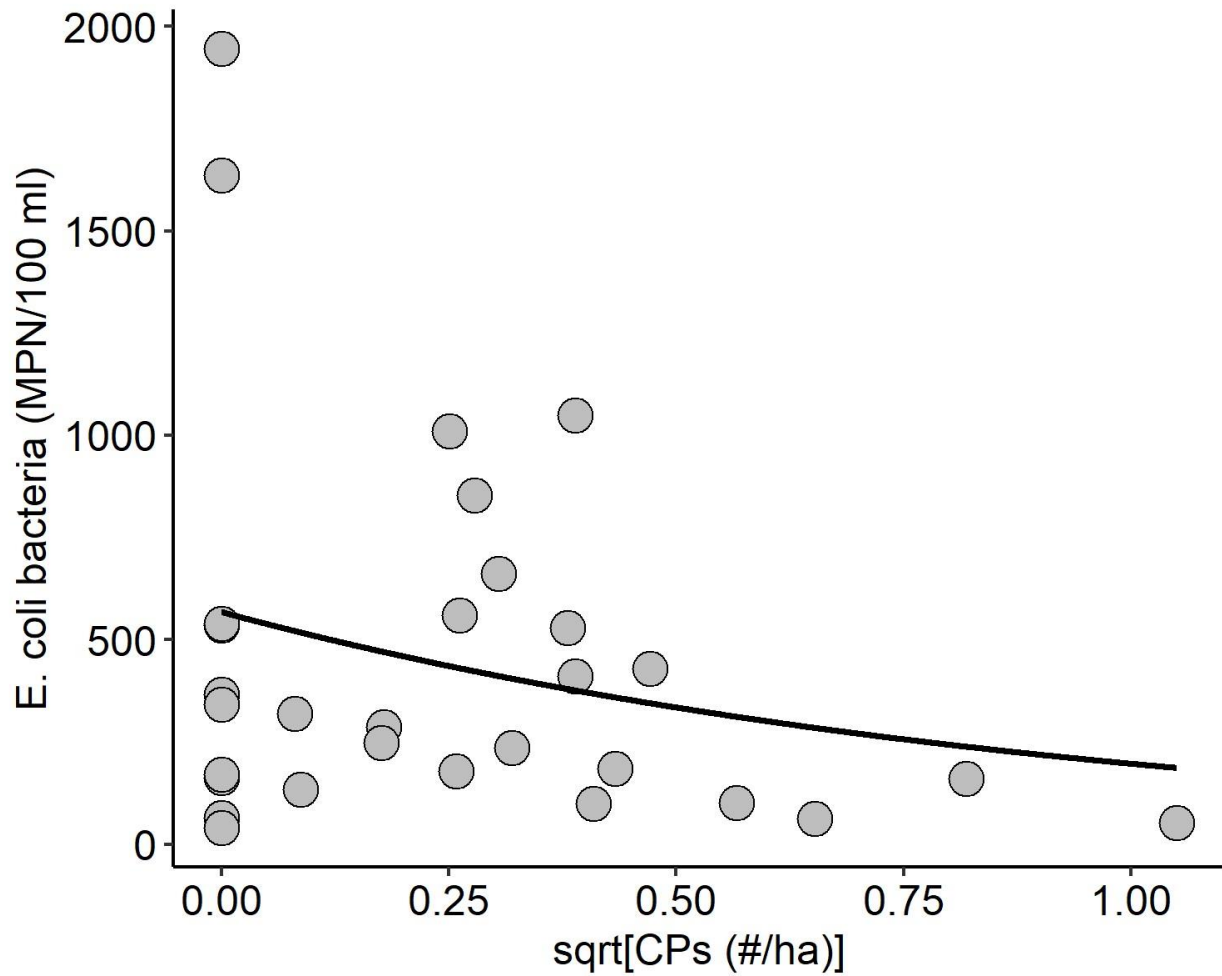


Figure 3.4.6. Increasing density of conservation practices (CPs) appears to lead to declines in *E. coli* bacteria following a pattern of exponential decay. However, the exponential decay model only explains 6% of the variation in the relationship between CP density (number per hectare) and *E. coli* bacteria, and the model coefficients are not statistically significant. MPN = most probable number.

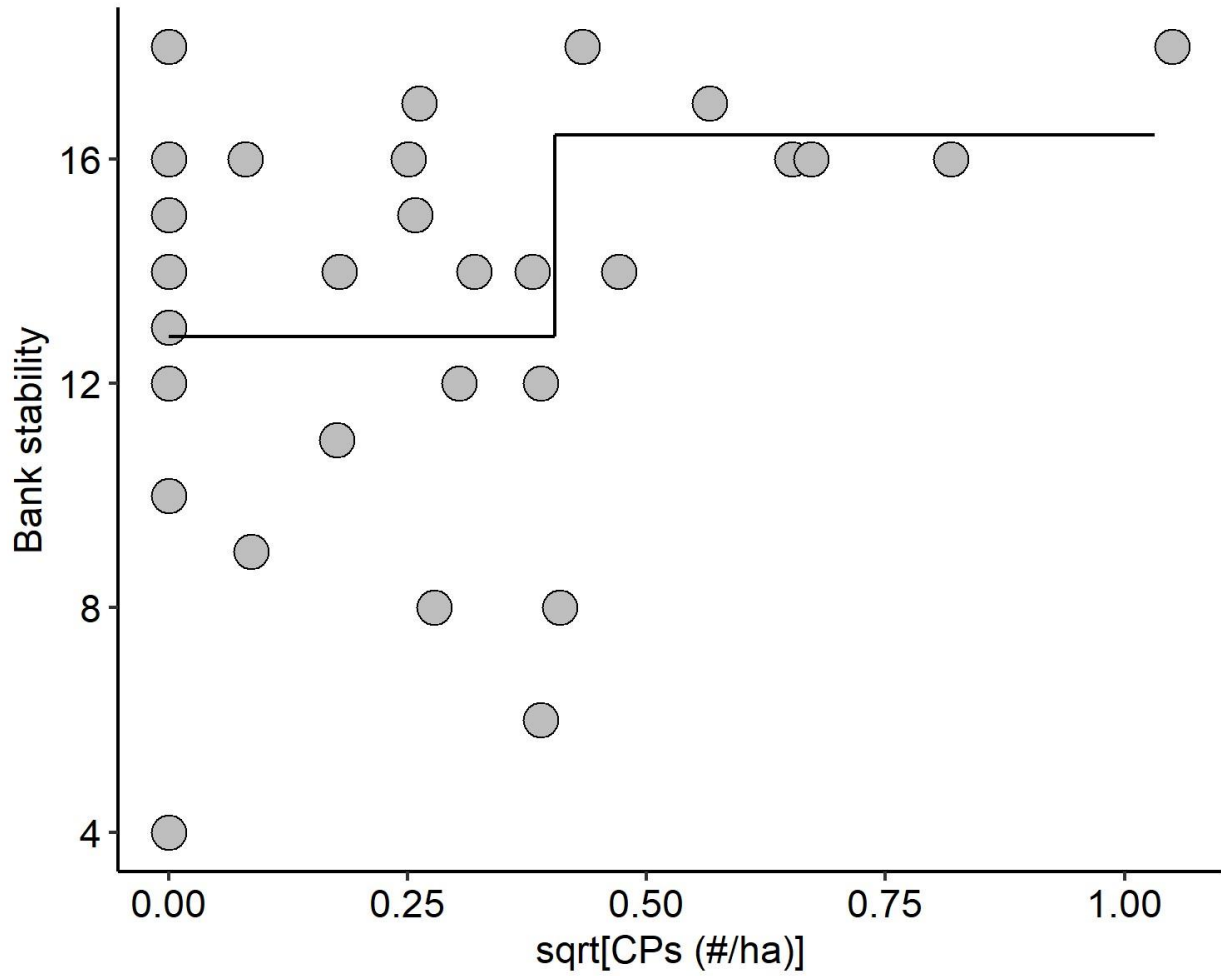


Figure 3.4.7. Streambanks were more stable (average score of 16.4) when conservation practice (CP) density (number per hectare) was greater than $\approx 0.17/\text{ha}$ than when CP density was less than $\approx 0.17/\text{ha}$ (average score of 12.8).

Table 3.4.4. Results of linear, linear plateau, and exponential decay models were used to explain relationships between conservation practice density and water quality and habitat descriptors. NA indicates that a model either did not make sense for the data or produced an error.

Variable	Linear			Linear plateau			Exponential decay		
	Coefficient	<i>p</i> -value	R ²	Breakpoint	<i>p</i> -value	pseudo-R ²	Coefficient	<i>p</i> -value	pseudo-R ²
Total nitrogen	0.67	0.09	0.05	0.30	0.09	0.21	NA	NA	NA
Total suspended solids	-3.07	0.20	0.02	NA	NA	NA	0.75	0.26	0.05
<i>E. coli</i>	-506.00	0.12	0.05	NA	NA	NA	1.06	0.26	0.06
D50	-33.31	0.14	0.04	NA	NA	NA	0.60	0.15	0.07
Visual embeddedness	-0.90	0.60	-0.20	NA	NA	NA	0.07	0.60	0
Bank stability	3.12	0.21	0.02	NA	NA	NA	NA	NA	NA

We found that the macroinvertebrate community exhibited many threshold responses to changes in water quality and habitat. Negative indicator taxa began to decline at values that were often much lower than we measured at most sites for total N (Figure 3.4.8), TSS, total P, and *E. coli* bacteria (Table 3.4.5). Positive indicator taxa began to increase at slightly higher values for the same parameters (Table 3.4.5). The responses for bank stability, visual embeddedness, and D50 should be interpreted inversely because higher values for these parameters are desirable (Table 3.4.5). We urge caution in interpreting the positive responses to *E. coli* bacteria and visually estimated embeddedness. These indicators exhibited wide confidence intervals because we observed only two pure and reliable indicator taxa.

Table 3.4.5. The threshold indicator analysis revealed changepoints (cp), or thresholds, at which the majority of the macroinvertebrate community responded negatively (-) or positively (+) to selected water quality and habitat parameters (i.e., the value of the variable that had the greatest sum for individual taxon responses). Also shown are 95% confidence intervals (ci) based on 5th and 95th percentiles from 500 bootstrap replicates and the number of pure and reliable taxa (*n*) that responded positively or negatively. See table 3.4.1 for descriptions of each variable.

Variable	cp	ci	<i>n</i>
Total nitrogen -	0.65	0.57–1.08	17
Total nitrogen +	1.07	0.81–1.81	11
Total suspended solids -	1.04	0.78–3.45	4
Total suspended solids +	4.72	4.20–8.93	7
Total phosphorus -	0.02	0.01–0.02	8
Total phosphorus +	0.02	0.02–0.05	6
<i>E. coli</i> bacteria -	242.88	67.92–283.66	17
<i>E. coli</i> bacteria +	245.57	242.88–1790.69	13
Visual embeddedness -	13	12–13	2
Visual embeddedness +	12.5	12–17.5	9
D50 -	30	22.95–80	6
D50 +	116.5	65–130	16
Bank stability -	6	5–6	5
Bank stability +	17.5	16–18	6

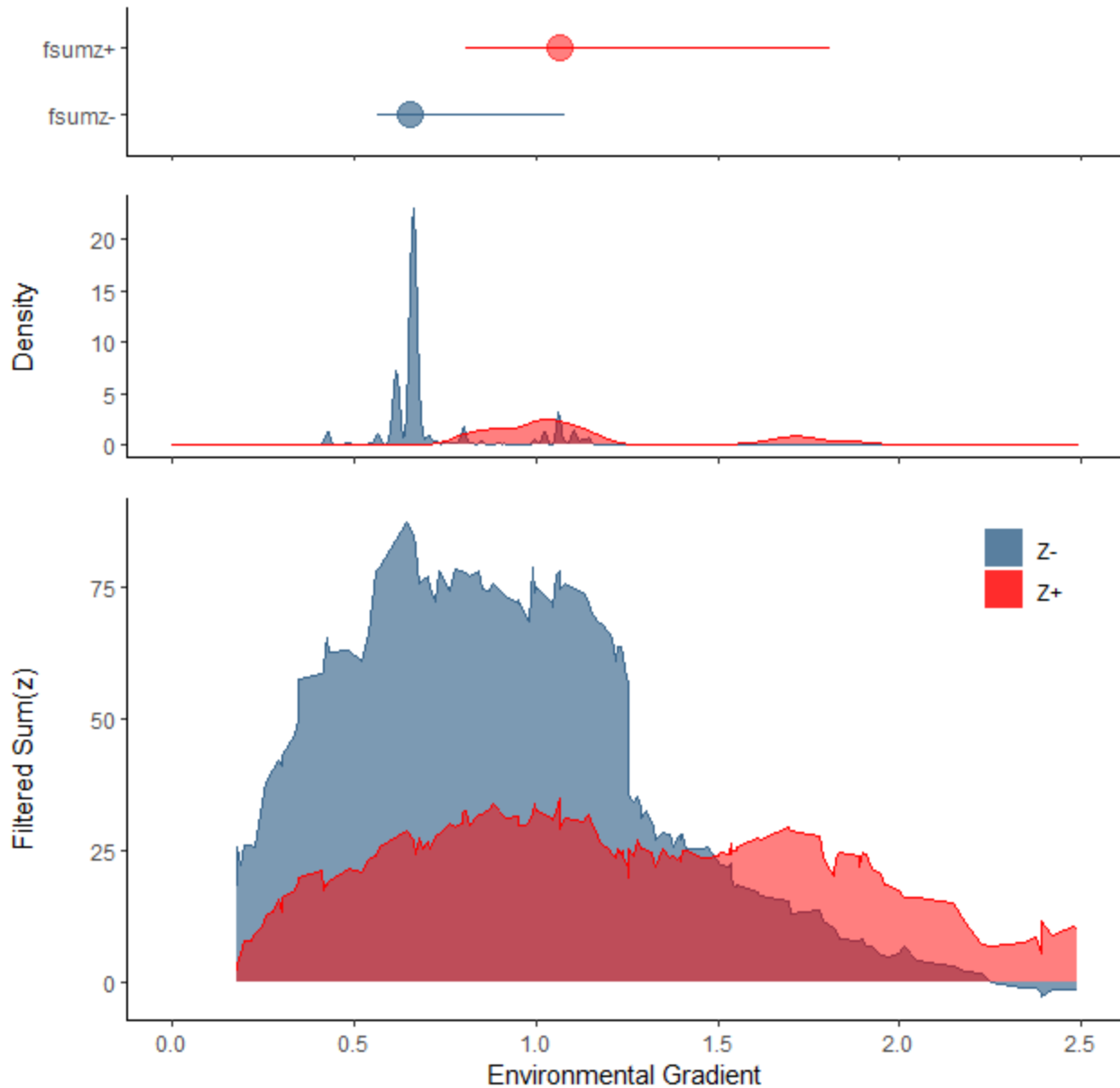


Figure 3.4.8. Example Threshold Indicator Analysis output for assessing the community response to total nitrogen. The top panel represents the estimated change points (positive in red; negative in blue) with 95% confidence intervals (see values in Table 3.4.5). The middle panel displays the probability density of the change points across the 500 bootstrap replicates. The bottom panel displays the magnitude of change among taxa along the environmental gradient (in this example, total nitrogen), where peaks in the values indicate points along the environmental gradient that produce large amounts of change in community structure and are the community change points. Analogous panels are also available for other variables listed in Table 3.4.5.

Comparing categories of CP density and agricultural land use confirmed that increased CP density improves some metrics of water quality and habitat, but those improvements did not translate into changes in the macroinvertebrate assemblage at high levels of agricultural land use (Figure 3.4.9). There were significant differences between sites with low agriculture and low CP density and sites with high agriculture and low conservation practice density for TN (p -value = 0.02), bank stability (p -value = 0.08), and EPT (p -value = 0.01), confirming that agriculture can adversely affect water quality, habitat, and biota. In many cases, CPs seemed to improve instream conditions but not necessarily by statistically significant amounts. For example, bank stability was significantly (p -value = 0.05) better at sites with high agriculture and high CP density than at sites with high agriculture and no practices. Further, *E. coli* and TSS tended to be lower at high-agriculture sites with CPs compared to those without CPs, but those relationships were not significant. Interestingly, there appeared to be higher proportions of EPT at sites with medium agriculture and high CP density compared to those with medium agriculture and low CP density (p -value = 0.03).

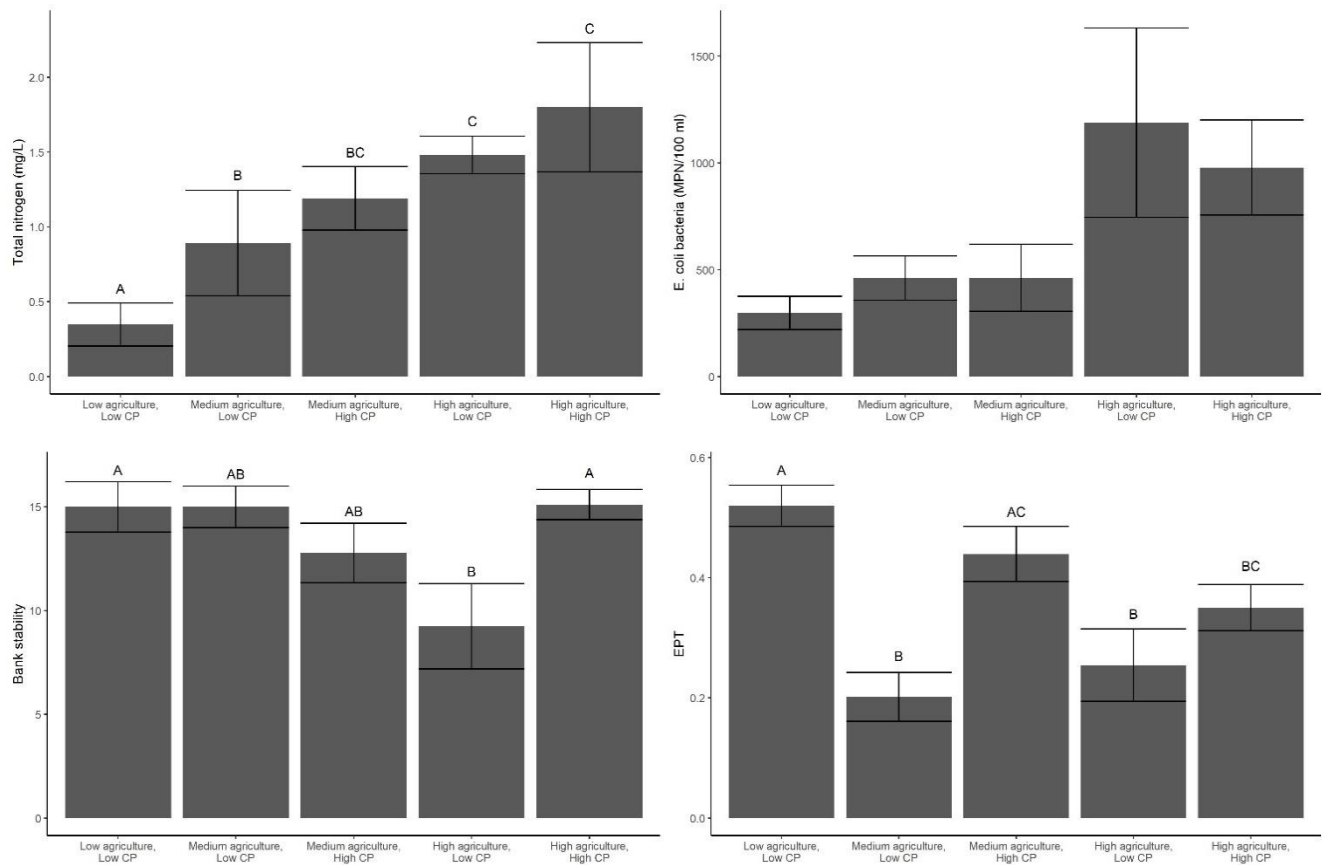


Figure 3.4.9. Results of analysis of variance on categories representing gradients in agricultural land use and conservation practice (CP) density. Bars represent the mean water quality and habitat for each category with 90% confidence intervals. Bars with different letters above them indicate statistically significant ($p < 0.1$) differences in means. No differences were statistically significant for *E. coli* bacteria. EPT = Proportion of individuals collected at each site classified as EPT, minus the pollution-tolerant family Hydropsychidae

The macroinvertebrate community may not have shown a direct positive response to CP installation because improvements in water quality were too small (resulting in non-significant relationships). For example, our results demonstrate that macroinvertebrates begin to respond negatively at 0.65 mg/L of nitrogen but most sites exceed that value. In fact, many of the water quality and habitat parameters exceed the thresholds at which the macroinvertebrate community responds negatively. Perhaps more time (Meals et al. 2010, Hamilton 2012) or a greater number of CPs (or both) in areas contributing the greatest nutrient yields is needed to observe biotic responses to CPs.

Task 3.5:

Caveat:

We omitted task 3.5 because the proposed database (task 3.2) was not needed to complete the core objectives of this study (i.e., understand efficacy of CPs).

Task 4: *Quantify cost-effectiveness of CP implementation in HUC12s across the upper CPH, excluding those encompassing mainstem rivers and those in the Cumberland Plateau coalfields.*

1. *Summarize existing data from state and federal agencies, along with newly collected survey data, to use as dependent variables in regression analyses to estimate relative cost-effectiveness of CP implementation across the upper CPH and within the two focal watersheds. These analyses will be conducted for all CPs combined, as well as individually for the two most common CPs. The depth/extent of these analyses will depend on the availability of NRCS data on expected load reductions and cost-share amounts for specific CP projects.*

Task 4.1

Caveats:

We were unable to complete task 4.1 because we could not accurately model the pathways through which cattle grazing influences sediment yields to streams and, therefore, were unable to develop meaningful, interpretable scenarios.

Task 5: Management implications

Collectively, our findings can be used to prioritize watersheds in the CPH for future CP implementation. Ideally, such prioritizations would be conducted in collaboration with local and regional management agencies. As a starting point for discussion, we suggest that key factors used to prioritize watersheds might include sediment load within the watershed, intensity of agricultural land use, and current CP implementation levels. Using these factors, we identified hypothetical priority locations for CP installation using two different ranking schemes. A spreadsheet with agricultural land use intensity and CP implementation levels for all subbasins will be archived on the Landscape Partnership portal.

Our first hypothetical prioritization aimed to identify locations where CP installation would provide the greatest benefit to biota and included the following steps. First, we used Figure 3.1.2 to identify HUC-12 watersheds that had excessive sediment loads. Ideally, we would use the sediment loads to target LSUs and associated stream channels, but we felt that the sediment results are only valid when aggregated (See Tasks 2 and 3 Discussion). Then, we selected LSUs that had medium amounts of agriculture (i.e., from 25 to 50%) within those HUC-12 watersheds because the ANOVA revealed that medium-agricultural sites could benefit most from CP installation (in terms of biotic responses, Figure 3.4.9). Lastly, we identified which of the selected LSUs already had many CPs (i.e., density > 0.1 CPs/ha) such that installation of several additional CPs would exceed density thresholds needed to improve instream conditions to levels that would no longer limit biota. Ultimately, we identified 155 LSUs that would benefit most from additional CPs in terms of achieving biotic responses (Figure 5.1, Table 5.1).

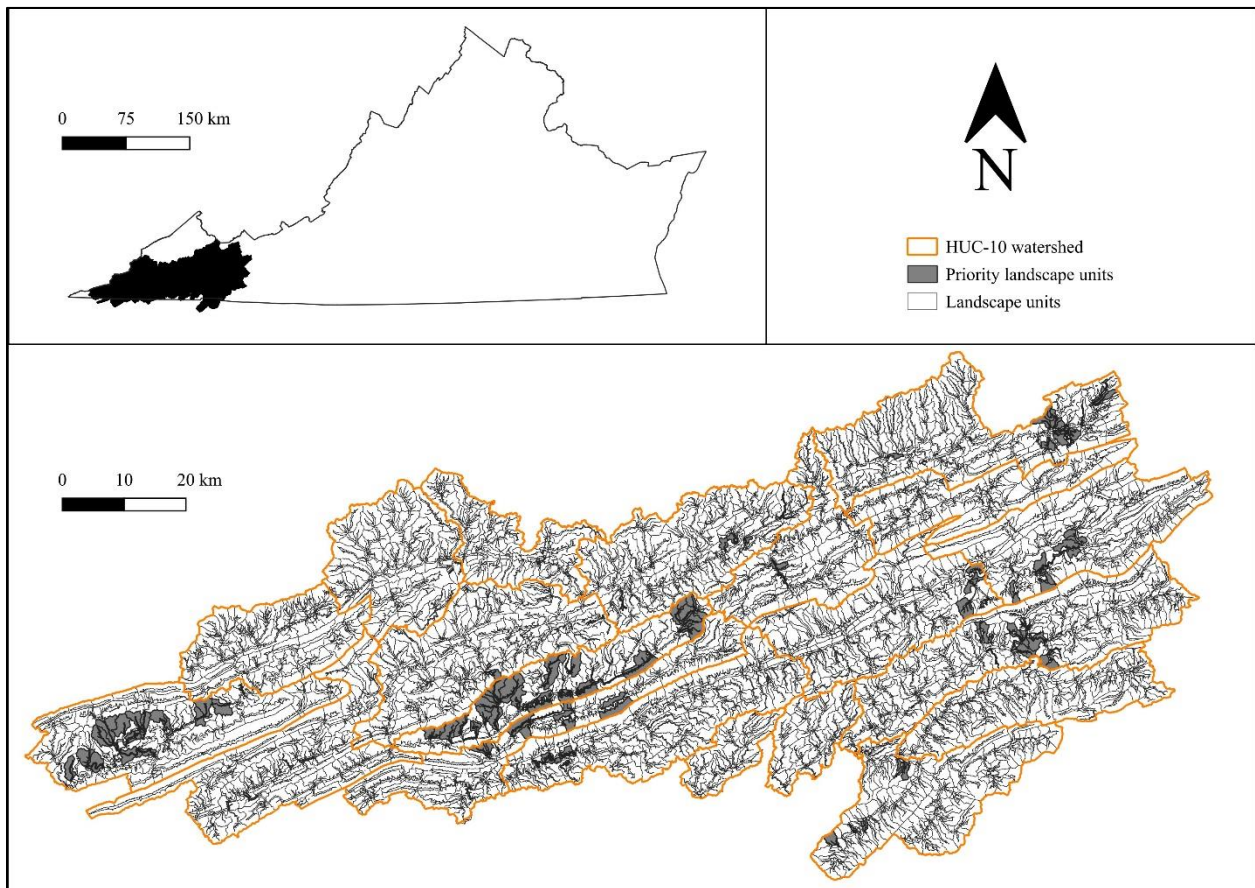


Figure 5.1. Landscape units where installing additional conservation practices could achieve the greatest biotic response. See Table 5.1 for the coordinates of the landscape units.

Table 5.1. Landscape units where greater density (number/hectare) of conservation practices (CPs) could achieve the greatest biotic response. Landscape units with medium percentages of agricultural land use (Ag) and CP density greater than 0.1 present the greatest opportunity to protect aquatic biota.

Latitude	Longitude	Ag	CP	HUC-12
36.64	-82.46	27	0.101	Abrams Creek-North Fork Holston River
36.65	-82.43	28	0.12	Abrams Creek-North Fork Holston River
36.65	-82.43	28	0.144	Abrams Creek-North Fork Holston River
36.63	-82.43	29	0.123	Abrams Creek-North Fork Holston River
36.63	-82.48	36	0.134	Abrams Creek-North Fork Holston River
36.65	-82.44	38	0.13	Abrams Creek-North Fork Holston River
36.64	-82.46	43	0.153	Abrams Creek-North Fork Holston River
36.91	-82.05	25	0.312	Big Cedar Creek-Clinch River
36.9	-82.04	28	0.228	Big Cedar Creek-Clinch River
36.93	-82.06	39	0.181	Big Cedar Creek-Clinch River
36.93	-82.05	46	0.156	Big Cedar Creek-Clinch River
36.69	-82.52	25	0.136	Big Moccasin Creek-North Fork Holston River
36.68	-82.5	27	0.162	Big Moccasin Creek-North Fork Holston River
36.59	-82.61	29	0.185	Big Moccasin Creek-North Fork Holston River
36.72	-82.34	31	0.204	Big Moccasin Creek-North Fork Holston River
36.72	-82.43	42	0.136	Big Moccasin Creek-North Fork Holston River
36.7	-82.43	43	0.27	Big Moccasin Creek-North Fork Holston River
36.65	-82.55	43	1.372	Big Moccasin Creek-North Fork Holston River
36.7	-82.47	44	0.152	Big Moccasin Creek-North Fork Holston River
36.66	-82.57	45	0.208	Big Moccasin Creek-North Fork Holston River
36.65	-82.59	45	0.213	Big Moccasin Creek-North Fork Holston River
36.67	-82.64	25	0.288	Copper Creek
36.74	-82.56	26	0.192	Copper Creek
36.76	-82.35	26	0.141	Copper Creek
36.71	-82.58	26	0.207	Copper Creek
36.74	-82.43	27	0.117	Copper Creek
36.74	-82.4	28	0.135	Copper Creek
36.78	-82.3	29	0.154	Copper Creek
36.75	-82.53	30	0.108	Copper Creek
36.69	-82.62	30	0.259	Copper Creek
36.78	-82.43	31	0.31	Copper Creek
36.68	-82.64	31	0.353	Copper Creek
36.72	-82.58	32	0.179	Copper Creek
36.75	-82.38	33	0.352	Copper Creek
36.77	-82.46	34	0.443	Copper Creek
36.73	-82.43	34	0.297	Copper Creek
36.72	-82.48	34	0.213	Copper Creek
36.87	-82.21	35	0.61	Copper Creek
36.83	-82.2	38	0.307	Copper Creek

36.7	-82.56	38	0.104	Copper Creek
36.84	-82.21	39	0.619	Copper Creek
36.83	-82.21	39	0.182	Copper Creek
36.73	-82.57	39	0.458	Copper Creek
36.67	-82.61	39	0.148	Copper Creek
36.87	-82.2	41	1.781	Copper Creek
36.8	-82.28	41	0.497	Copper Creek
36.69	-82.6	41	0.131	Copper Creek
36.68	-82.66	42	0.644	Copper Creek
36.72	-82.52	43	0.325	Copper Creek
36.74	-82.39	45	0.403	Copper Creek
36.86	-82.21	46	0.168	Copper Creek
36.85	-82.2	48	0.606	Copper Creek
36.76	-82.39	49	0.31	Copper Creek
36.78	-82.42	50	0.486	Copper Creek
36.73	-82.52	50	0.225	Copper Creek
36.96	-82.15	27	0.342	Dumps Creek-Clinch River
36.97	-82.13	31	0.382	Dumps Creek-Clinch River
37.01	-82.04	34	0.322	Dumps Creek-Clinch River
37	-82.03	41	0.328	Dumps Creek-Clinch River
36.87	-82.33	45	0.192	Dumps Creek-Clinch River
36.86	-82.23	46	0.22	Dumps Creek-Clinch River
36.96	-82.11	48	0.616	Dumps Creek-Clinch River
36.93	-82.49	40	0.28	Guest River
36.98	-81.52	28	0.193	Laurel Creek-North Fork Holston River
36.9	-81.56	31	0.16	Laurel Creek-North Fork Holston River
36.91	-81.56	37	0.449	Laurel Creek-North Fork Holston River
36.97	-81.51	41	0.146	Laurel Creek-North Fork Holston River
36.96	-81.52	41	0.326	Laurel Creek-North Fork Holston River
36.93	-81.57	41	0.192	Laurel Creek-North Fork Holston River
36.94	-81.55	42	0.42	Laurel Creek-North Fork Holston River
36.89	-81.62	42	0.364	Laurel Creek-North Fork Holston River
36.93	-81.63	49	0.107	Laurel Creek-North Fork Holston River
36.63	-81.82	28	0.125	Laurel Creek-South Fork Holston River
36.63	-81.82	28	0.598	Laurel Creek-South Fork Holston River
36.53	-81.95	29	0.117	Laurel Creek-South Fork Holston River
36.64	-81.83	30	0.138	Laurel Creek-South Fork Holston River
36.64	-81.82	33	0.461	Laurel Creek-South Fork Holston River
36.54	-81.91	38	0.159	Laurel Creek-South Fork Holston River
36.55	-81.89	42	0.165	Laurel Creek-South Fork Holston River
36.55	-81.89	44	0.184	Laurel Creek-South Fork Holston River
36.55	-81.89	47	0.199	Laurel Creek-South Fork Holston River
36.55	-81.91	49	0.546	Laurel Creek-South Fork Holston River
36.82	-81.66	29	0.362	Middle Fork Holston River
36.8	-81.55	31	0.186	Middle Fork Holston River

36.85	-81.6	35	0.387	Middle Fork Holston River
36.84	-81.62	37	0.23	Middle Fork Holston River
36.84	-81.61	39	0.193	Middle Fork Holston River
36.82	-81.58	39	0.37	Middle Fork Holston River
36.81	-81.55	40	0.289	Middle Fork Holston River
36.84	-81.59	40	0.263	Middle Fork Holston River
36.83	-81.59	40	0.44	Middle Fork Holston River
36.79	-81.56	42	0.232	Middle Fork Holston River
36.81	-81.6	44	0.531	Middle Fork Holston River
36.83	-81.68	45	0.307	Middle Fork Holston River
36.82	-81.6	45	0.101	Middle Fork Holston River
36.84	-81.6	46	0.218	Middle Fork Holston River
36.81	-81.62	47	0.122	Middle Fork Holston River
36.8	-81.66	47	0.264	Middle Fork Holston River
36.64	-82.89	27	0.94	North Fork Clinch River-Clinch River
36.57	-83.04	30	0.212	North Fork Clinch River-Clinch River
36.63	-82.93	35	0.37	North Fork Clinch River-Clinch River
36.58	-83	41	0.159	North Fork Clinch River-Clinch River
36.63	-82.91	43	3.044	North Fork Clinch River-Clinch River
36.68	-82.68	26	0.154	Stony Creek-Clinch River
36.76	-82.56	30	0.151	Stony Creek-Clinch River
36.78	-82.58	48	0.125	Stony Creek-Clinch River
36.77	-82.46	48	0.167	Stony Creek-Clinch River
37.13	-81.53	26	2.184	Swords Creek-Clinch River
37.14	-81.55	27	0.399	Swords Creek-Clinch River
37.13	-81.54	27	0.282	Swords Creek-Clinch River
37.12	-81.51	28	0.39	Swords Creek-Clinch River
37.11	-81.52	28	0.133	Swords Creek-Clinch River
37.18	-81.46	30	0.416	Swords Creek-Clinch River
37.15	-81.5	30	0.148	Swords Creek-Clinch River
37.09	-81.84	33	0.147	Swords Creek-Clinch River
37.17	-81.48	35	0.238	Swords Creek-Clinch River
37.15	-81.56	38	0.25	Swords Creek-Clinch River
37.15	-81.55	38	0.159	Swords Creek-Clinch River
37.2	-81.46	39	0.168	Swords Creek-Clinch River
37.08	-81.79	39	0.204	Swords Creek-Clinch River
37.12	-81.54	43	0.142	Swords Creek-Clinch River
37.18	-81.46	44	0.699	Swords Creek-Clinch River
37.17	-81.48	45	0.275	Swords Creek-Clinch River
37.14	-81.57	46	0.101	Swords Creek-Clinch River
37.11	-81.56	48	0.26	Swords Creek-Clinch River
36.92	-81.69	32	0.21	Tumbling Creek-North Fork Holston River
36.88	-81.68	34	0.29	Tumbling Creek-North Fork Holston River
36.87	-81.71	41	0.287	Tumbling Creek-North Fork Holston River
36.9	-81.7	47	0.287	Tumbling Creek-North Fork Holston River

36.9	-81.7	48	0.165	Tumbling Creek-North Fork Holston River
36.69	-83.1	25	0.298	Wallen Creek-Powell River
36.68	-83.26	25	0.146	Wallen Creek-Powell River
36.66	-83.27	25	0.228	Wallen Creek-Powell River
36.67	-83.2	25	0.731	Wallen Creek-Powell River
36.71	-83.09	26	0.183	Wallen Creek-Powell River
36.69	-83.21	27	0.249	Wallen Creek-Powell River
36.67	-83.2	27	0.45	Wallen Creek-Powell River
36.68	-83.15	30	0.256	Wallen Creek-Powell River
36.64	-83.19	30	0.252	Wallen Creek-Powell River
36.68	-83.24	30	0.173	Wallen Creek-Powell River
36.66	-83.22	30	0.121	Wallen Creek-Powell River
36.73	-83.02	31	0.13	Wallen Creek-Powell River
36.62	-83.28	31	0.223	Wallen Creek-Powell River
36.69	-83.19	32	0.117	Wallen Creek-Powell River
36.71	-83.06	33	0.235	Wallen Creek-Powell River
36.67	-83.13	38	0.203	Wallen Creek-Powell River
36.61	-83.33	38	0.132	Wallen Creek-Powell River
36.65	-83.24	39	0.137	Wallen Creek-Powell River
36.7	-83.08	41	0.507	Wallen Creek-Powell River
36.67	-83.2	42	3.704	Wallen Creek-Powell River
36.63	-83.3	42	0.125	Wallen Creek-Powell River
36.69	-83.17	43	0.564	Wallen Creek-Powell River
36.62	-83.28	44	0.129	Wallen Creek-Powell River
36.63	-83.22	46	0.291	Wallen Creek-Powell River
36.66	-83.22	50	0.174	Wallen Creek-Powell River

Notably, CPs can provide benefits beyond achieving the greatest biotic response, and so other watersheds (e.g., those with high amounts of agriculture) need not be excluded from future conservation efforts. For example, some CPs increase agricultural production and may still have important benefits for biota even if resulting biotic indices do not match reference conditions. An alternative process for prioritizing watersheds for CP implementation might follow the same steps described above except focus on locations where CP density is currently too low to enhance water quality or instream habitat. This approach could serve as an initial step toward reaching density thresholds that benefit instream conditions and biota (Figure 5.2, Table 5.2).

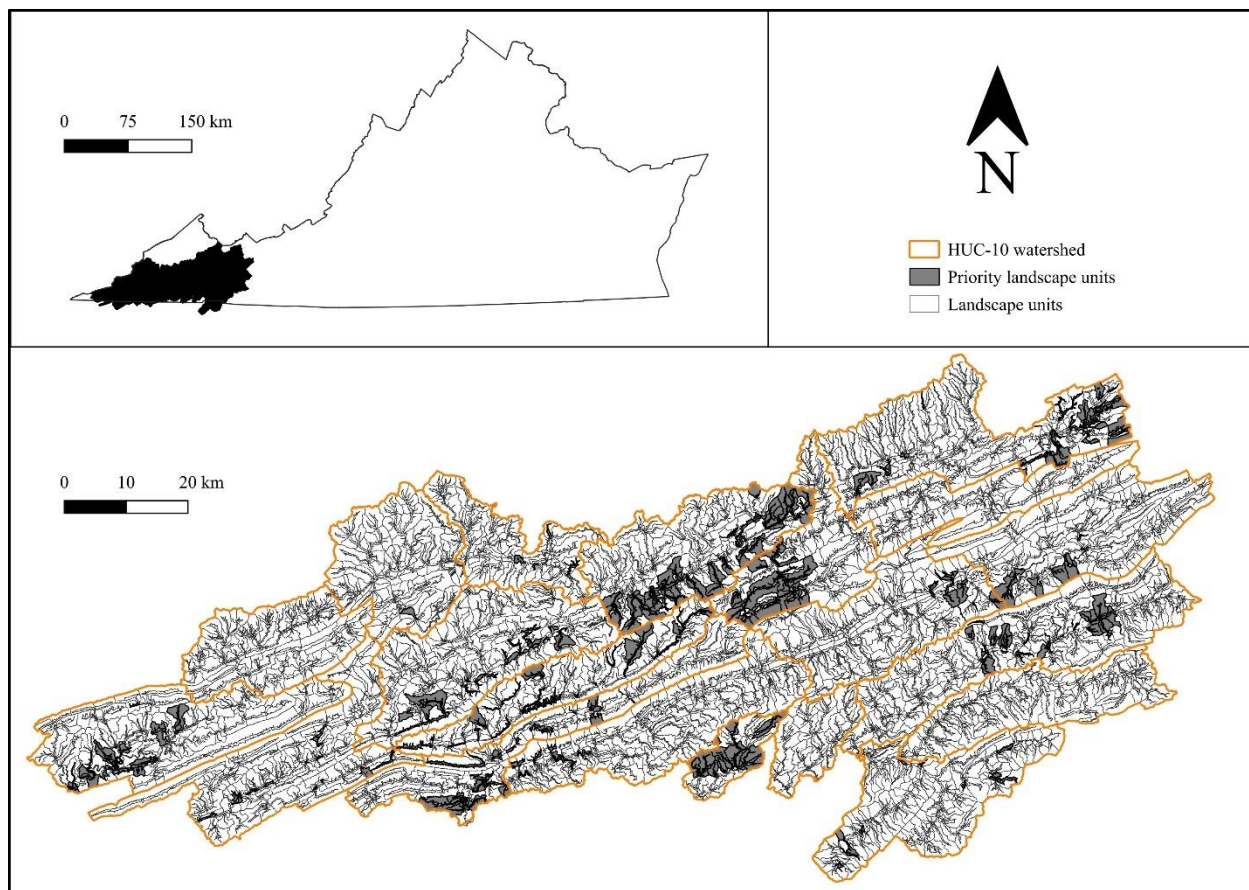


Figure 5.2. Landscape units where installing conservation practices could serve as an initial step toward reaching thresholds that benefit instream conditions and biota. See Table 5.2 for the coordinates of the landscape units.

Table 5.2. Landscape units where greater density (number/hectare) of conservation practices (CPs) could serve as an initial step toward reaching density thresholds that benefit instream conditions and biota. Ag = percentage agricultural land use.

Latitude	Longitude	Ag	CP	HUC-12
36.64	-82.44	25	0	Abrams Creek-North Fork Holston River
36.62	-82.52	25	0	Abrams Creek-North Fork Holston River
36.65	-82.49	26	0	Abrams Creek-North Fork Holston River
36.62	-82.51	28	0	Abrams Creek-North Fork Holston River
36.65	-82.45	30	0	Abrams Creek-North Fork Holston River
36.64	-82.53	30	0	Abrams Creek-North Fork Holston River
36.64	-82.52	31	0	Abrams Creek-North Fork Holston River
36.64	-82.42	34	0	Abrams Creek-North Fork Holston River
36.66	-82.46	37	0	Abrams Creek-North Fork Holston River
36.65	-82.45	38	0	Abrams Creek-North Fork Holston River
36.63	-82.42	38	0	Abrams Creek-North Fork Holston River
36.74	-82.04	41	0	Abrams Creek-North Fork Holston River

36.65	-82.39	43	0	Abrams Creek-North Fork Holston River
36.65	-82.4	38	0.09	Abrams Creek-North Fork Holston River
36.72	-82.11	25	0	Beaver Creek
36.63	-82.17	26	0	Beaver Creek
36.65	-82.12	29	0	Beaver Creek
36.64	-82.18	29	0	Beaver Creek
36.63	-82.2	29	0	Beaver Creek
36.73	-82.1	30	0	Beaver Creek
36.64	-82.09	32	0	Beaver Creek
36.74	-82.07	34	0	Beaver Creek
36.64	-82.12	37	0	Beaver Creek
36.64	-82.12	37	0	Beaver Creek
36.66	-82.21	38	0	Beaver Creek
36.64	-82.15	38	0	Beaver Creek
36.65	-82.22	39	0	Beaver Creek
36.67	-82.18	45	0	Beaver Creek
36.68	-82.13	47	0	Beaver Creek
36.64	-82.18	25	0.003	Beaver Creek
36.66	-82.13	37	0.019	Beaver Creek
36.66	-82.1	27	0.023	Beaver Creek
36.65	-82.15	50	0.036	Beaver Creek
36.64	-82.2	49	0.044	Beaver Creek
36.7	-82.06	50	0.053	Beaver Creek
36.69	-82.13	31	0.056	Beaver Creek
36.85	-82.11	26	0	Big Cedar Creek-Clinch River
36.85	-82.1	28	0	Big Cedar Creek-Clinch River
36.97	-82.04	33	0	Big Cedar Creek-Clinch River
36.95	-82.02	33	0	Big Cedar Creek-Clinch River
36.87	-82.07	33	0	Big Cedar Creek-Clinch River
36.86	-82.13	33	0	Big Cedar Creek-Clinch River
37.03	-81.98	34	0	Big Cedar Creek-Clinch River
36.86	-82.11	35	0	Big Cedar Creek-Clinch River
37.05	-82.02	36	0	Big Cedar Creek-Clinch River
36.85	-82.11	36	0	Big Cedar Creek-Clinch River
36.84	-82.13	36	0	Big Cedar Creek-Clinch River
36.92	-82.03	38	0	Big Cedar Creek-Clinch River
36.9	-82.01	41	0	Big Cedar Creek-Clinch River
36.88	-82.04	44	0	Big Cedar Creek-Clinch River
36.88	-82.03	45	0	Big Cedar Creek-Clinch River
36.88	-82.03	46	0	Big Cedar Creek-Clinch River
36.9	-82.02	49	0	Big Cedar Creek-Clinch River
36.88	-82.01	32	0.003	Big Cedar Creek-Clinch River
36.92	-82.01	43	0.004	Big Cedar Creek-Clinch River
36.9	-82.04	39	0.017	Big Cedar Creek-Clinch River
36.88	-82.13	45	0.017	Big Cedar Creek-Clinch River

36.92	-82.02	29	0.021	Big Cedar Creek-Clinch River
36.91	-82.05	37	0.032	Big Cedar Creek-Clinch River
36.89	-82.09	30	0.036	Big Cedar Creek-Clinch River
36.95	-82.07	42	0.05	Big Cedar Creek-Clinch River
36.96	-82.05	29	0.054	Big Cedar Creek-Clinch River
36.94	-82.04	44	0.063	Big Cedar Creek-Clinch River
36.93	-82.09	49	0.063	Big Cedar Creek-Clinch River
36.64	-82.59	25	0	Big Moccasin Creek-North Fork Holston River
36.62	-82.59	26	0	Big Moccasin Creek-North Fork Holston River
36.58	-82.59	26	0	Big Moccasin Creek-North Fork Holston River
36.61	-82.58	28	0	Big Moccasin Creek-North Fork Holston River
36.69	-82.5	29	0	Big Moccasin Creek-North Fork Holston River
36.6	-82.62	29	0	Big Moccasin Creek-North Fork Holston River
36.61	-82.58	29	0	Big Moccasin Creek-North Fork Holston River
36.59	-82.68	30	0	Big Moccasin Creek-North Fork Holston River
36.59	-82.63	30	0	Big Moccasin Creek-North Fork Holston River
36.6	-82.64	31	0	Big Moccasin Creek-North Fork Holston River
36.71	-82.42	32	0	Big Moccasin Creek-North Fork Holston River
36.63	-82.63	32	0	Big Moccasin Creek-North Fork Holston River
36.64	-82.57	32	0	Big Moccasin Creek-North Fork Holston River
36.72	-82.39	33	0	Big Moccasin Creek-North Fork Holston River
36.6	-82.58	34	0	Big Moccasin Creek-North Fork Holston River
36.57	-82.62	35	0	Big Moccasin Creek-North Fork Holston River
36.57	-82.63	35	0	Big Moccasin Creek-North Fork Holston River
36.67	-82.52	36	0	Big Moccasin Creek-North Fork Holston River
36.61	-82.56	36	0	Big Moccasin Creek-North Fork Holston River
36.59	-82.71	38	0	Big Moccasin Creek-North Fork Holston River
36.57	-82.62	38	0	Big Moccasin Creek-North Fork Holston River
36.69	-82.48	39	0	Big Moccasin Creek-North Fork Holston River
36.6	-82.59	39	0	Big Moccasin Creek-North Fork Holston River
36.57	-82.63	39	0	Big Moccasin Creek-North Fork Holston River
36.62	-82.57	43	0	Big Moccasin Creek-North Fork Holston River
36.65	-82.56	44	0	Big Moccasin Creek-North Fork Holston River
36.61	-82.58	46	0	Big Moccasin Creek-North Fork Holston River
36.58	-82.6	46	0	Big Moccasin Creek-North Fork Holston River
36.58	-82.62	47	0	Big Moccasin Creek-North Fork Holston River
36.59	-82.62	48	0	Big Moccasin Creek-North Fork Holston River
36.58	-82.61	48	0	Big Moccasin Creek-North Fork Holston River
36.74	-82.31	49	0	Big Moccasin Creek-North Fork Holston River
36.73	-82.39	34	0.007	Big Moccasin Creek-North Fork Holston River
36.58	-82.66	43	0.014	Big Moccasin Creek-North Fork Holston River
36.6	-82.54	27	0.015	Big Moccasin Creek-North Fork Holston River
36.71	-82.38	38	0.016	Big Moccasin Creek-North Fork Holston River
36.6	-82.59	28	0.017	Big Moccasin Creek-North Fork Holston River
36.65	-82.56	29	0.035	Big Moccasin Creek-North Fork Holston River

36.66	-82.54	28	0.044	Big Moccasin Creek-North Fork Holston River
36.69	-82.46	44	0.061	Big Moccasin Creek-North Fork Holston River
36.81	-82.37	25	0	Copper Creek
36.8	-82.27	25	0	Copper Creek
36.71	-82.51	26	0	Copper Creek
36.74	-82.42	27	0	Copper Creek
36.72	-82.57	27	0	Copper Creek
36.74	-82.48	28	0	Copper Creek
36.8	-82.27	29	0	Copper Creek
36.72	-82.5	29	0	Copper Creek
36.83	-82.19	30	0	Copper Creek
36.69	-82.54	30	0	Copper Creek
36.66	-82.64	31	0	Copper Creek
36.66	-82.63	32	0	Copper Creek
36.74	-82.32	33	0	Copper Creek
36.74	-82.46	34	0	Copper Creek
36.86	-82.2	39	0	Copper Creek
36.69	-82.59	40	0	Copper Creek
36.78	-82.26	41	0	Copper Creek
36.68	-82.59	42	0	Copper Creek
36.68	-82.56	43	0	Copper Creek
36.76	-82.31	44	0	Copper Creek
36.7	-82.54	44	0	Copper Creek
36.77	-82.28	46	0	Copper Creek
36.75	-82.38	47	0	Copper Creek
36.67	-82.68	50	0	Copper Creek
36.8	-82.32	50	0.004	Copper Creek
36.66	-82.71	32	0.005	Copper Creek
36.84	-82.24	45	0.009	Copper Creek
36.75	-82.33	28	0.01	Copper Creek
36.74	-82.53	44	0.024	Copper Creek
36.86	-82.18	31	0.027	Copper Creek
36.81	-82.25	31	0.028	Copper Creek
36.83	-82.23	43	0.036	Copper Creek
36.72	-82.48	35	0.037	Copper Creek
36.79	-82.36	46	0.037	Copper Creek
36.8	-82.31	47	0.049	Copper Creek
36.77	-82.33	35	0.061	Copper Creek
36.7	-82.6	32	0.07	Copper Creek
36.8	-82.35	45	0.082	Copper Creek
36.85	-82.21	41	0.085	Copper Creek
36.77	-82.5	31	0.088	Copper Creek
36.85	-82.23	36	0.09	Copper Creek
36.73	-82.45	33	0.098	Copper Creek
37.04	-82.1	25	0	Dumps Creek-Clinch River

36.94	-82.16	25	0	Dumps Creek-Clinch River
36.86	-82.34	25	0	Dumps Creek-Clinch River
36.91	-82.23	25	0	Dumps Creek-Clinch River
36.97	-82.12	26	0	Dumps Creek-Clinch River
36.91	-82.22	26	0	Dumps Creek-Clinch River
36.84	-82.32	27	0	Dumps Creek-Clinch River
36.92	-82.17	28	0	Dumps Creek-Clinch River
36.99	-82.06	29	0	Dumps Creek-Clinch River
37.03	-82.03	30	0	Dumps Creek-Clinch River
37.01	-82.05	30	0	Dumps Creek-Clinch River
36.99	-82.06	30	0	Dumps Creek-Clinch River
36.99	-82.05	30	0	Dumps Creek-Clinch River
36.98	-81.97	30	0	Dumps Creek-Clinch River
36.97	-82	30	0	Dumps Creek-Clinch River
36.96	-82.09	30	0	Dumps Creek-Clinch River
36.91	-82.3	32	0	Dumps Creek-Clinch River
37	-82.09	34	0	Dumps Creek-Clinch River
36.91	-82.24	34	0	Dumps Creek-Clinch River
37.02	-82	36	0	Dumps Creek-Clinch River
36.97	-82.02	36	0	Dumps Creek-Clinch River
36.93	-82.15	38	0	Dumps Creek-Clinch River
36.97	-82.14	40	0	Dumps Creek-Clinch River
36.88	-82.26	40	0	Dumps Creek-Clinch River
36.99	-82.05	41	0	Dumps Creek-Clinch River
36.98	-82.13	41	0	Dumps Creek-Clinch River
36.89	-82.28	41	0	Dumps Creek-Clinch River
36.92	-82.24	44	0	Dumps Creek-Clinch River
36.99	-82.11	45	0	Dumps Creek-Clinch River
36.89	-82.29	45	0	Dumps Creek-Clinch River
37	-82.09	47	0	Dumps Creek-Clinch River
36.89	-82.28	47	0	Dumps Creek-Clinch River
36.87	-82.27	49	0	Dumps Creek-Clinch River
36.91	-82.23	49	0	Dumps Creek-Clinch River
37.03	-82.03	50	0	Dumps Creek-Clinch River
37.02	-82.01	50	0	Dumps Creek-Clinch River
36.88	-82.29	50	0	Dumps Creek-Clinch River
36.9	-82.25	36	0.001	Dumps Creek-Clinch River
36.88	-82.24	36	0.004	Dumps Creek-Clinch River
36.89	-82.31	31	0.011	Dumps Creek-Clinch River
36.89	-82.25	46	0.016	Dumps Creek-Clinch River
37.02	-82.04	35	0.018	Dumps Creek-Clinch River
36.85	-82.35	47	0.019	Dumps Creek-Clinch River
37	-82.01	40	0.02	Dumps Creek-Clinch River
37.03	-82	43	0.022	Dumps Creek-Clinch River
36.86	-82.29	30	0.023	Dumps Creek-Clinch River

37.01	-82.07	29	0.027	Dumps Creek-Clinch River
36.89	-82.2	27	0.028	Dumps Creek-Clinch River
36.89	-82.17	32	0.028	Dumps Creek-Clinch River
36.93	-82.24	37	0.037	Dumps Creek-Clinch River
36.9	-82.26	41	0.041	Dumps Creek-Clinch River
36.93	-82.15	30	0.047	Dumps Creek-Clinch River
36.92	-82.17	25	0.052	Dumps Creek-Clinch River
36.88	-82.35	36	0.052	Dumps Creek-Clinch River
36.83	-82.29	46	0.067	Dumps Creek-Clinch River
36.96	-82.13	35	0.07	Dumps Creek-Clinch River
36.86	-82.32	33	0.078	Dumps Creek-Clinch River
36.94	-82.12	35	0.082	Dumps Creek-Clinch River
36.96	-82.09	31	0.083	Dumps Creek-Clinch River
36.96	-82.55	25	0	Guest River
36.97	-82.47	26	0	Guest River
36.93	-82.5	27	0	Guest River
36.92	-82.43	35	0	Guest River
36.93	-82.53	25	0.07	Guest River
36.98	-81.5	26	0	Laurel Creek-North Fork Holston River
36.93	-81.56	26	0	Laurel Creek-North Fork Holston River
36.93	-81.65	29	0	Laurel Creek-North Fork Holston River
36.97	-81.51	31	0	Laurel Creek-North Fork Holston River
36.95	-81.49	31	0	Laurel Creek-North Fork Holston River
36.95	-81.59	34	0	Laurel Creek-North Fork Holston River
36.95	-81.49	49	0	Laurel Creek-North Fork Holston River
36.93	-81.5	34	0.029	Laurel Creek-North Fork Holston River
36.96	-81.5	30	0.03	Laurel Creek-North Fork Holston River
36.92	-81.54	31	0.045	Laurel Creek-North Fork Holston River
36.92	-81.62	33	0.047	Laurel Creek-North Fork Holston River
36.9	-81.58	41	0.07	Laurel Creek-North Fork Holston River
36.93	-81.52	25	0.085	Laurel Creek-North Fork Holston River
36.9	-81.64	47	0.095	Laurel Creek-North Fork Holston River
36.62	-81.66	26	0	Laurel Creek-South Fork Holston River
36.54	-81.9	26	0	Laurel Creek-South Fork Holston River
36.67	-81.64	27	0	Laurel Creek-South Fork Holston River
36.62	-81.64	27	0	Laurel Creek-South Fork Holston River
36.65	-81.83	27	0	Laurel Creek-South Fork Holston River
36.5	-81.94	27	0	Laurel Creek-South Fork Holston River
36.63	-81.65	28	0	Laurel Creek-South Fork Holston River
36.66	-81.76	29	0	Laurel Creek-South Fork Holston River
36.49	-81.94	30	0	Laurel Creek-South Fork Holston River
36.64	-81.79	32	0	Laurel Creek-South Fork Holston River
36.72	-81.65	37	0	Laurel Creek-South Fork Holston River
36.61	-81.71	38	0	Laurel Creek-South Fork Holston River
36.66	-81.83	45	0	Laurel Creek-South Fork Holston River

36.63	-81.84	46	0	Laurel Creek-South Fork Holston River
36.53	-81.93	33	0.021	Laurel Creek-South Fork Holston River
36.55	-81.9	26	0.033	Laurel Creek-South Fork Holston River
36.51	-81.92	40	0.048	Laurel Creek-South Fork Holston River
36.8	-81.62	25	0	Middle Fork Holston River
36.81	-81.67	27	0	Middle Fork Holston River
36.79	-81.69	30	0	Middle Fork Holston River
36.78	-81.57	30	0	Middle Fork Holston River
36.85	-81.51	32	0	Middle Fork Holston River
36.81	-81.64	32	0	Middle Fork Holston River
36.83	-81.6	33	0	Middle Fork Holston River
36.85	-81.69	34	0	Middle Fork Holston River
36.78	-81.47	34	0	Middle Fork Holston River
36.82	-81.56	34	0	Middle Fork Holston River
36.81	-81.61	34	0	Middle Fork Holston River
36.88	-81.45	36	0	Middle Fork Holston River
36.81	-81.68	36	0	Middle Fork Holston River
36.79	-81.67	36	0	Middle Fork Holston River
36.84	-81.53	37	0	Middle Fork Holston River
36.8	-81.68	38	0	Middle Fork Holston River
36.85	-81.54	39	0	Middle Fork Holston River
36.84	-81.49	39	0	Middle Fork Holston River
36.81	-81.56	42	0	Middle Fork Holston River
36.83	-81.45	43	0	Middle Fork Holston River
36.8	-81.61	43	0	Middle Fork Holston River
36.82	-81.66	44	0	Middle Fork Holston River
36.8	-81.68	46	0	Middle Fork Holston River
36.86	-81.47	50	0	Middle Fork Holston River
36.83	-81.56	50	0	Middle Fork Holston River
36.85	-81.43	31	0.006	Middle Fork Holston River
36.84	-81.7	40	0.011	Middle Fork Holston River
36.84	-81.48	42	0.014	Middle Fork Holston River
36.83	-81.66	35	0.018	Middle Fork Holston River
36.86	-81.45	29	0.024	Middle Fork Holston River
36.85	-81.46	38	0.03	Middle Fork Holston River
36.86	-81.48	48	0.031	Middle Fork Holston River
36.86	-81.49	27	0.038	Middle Fork Holston River
36.86	-81.45	42	0.074	Middle Fork Holston River
36.88	-81.47	41	0.078	Middle Fork Holston River
36.86	-81.49	29	0.082	Middle Fork Holston River
36.83	-81.64	41	0.082	Middle Fork Holston River
36.83	-81.64	46	0.082	Middle Fork Holston River
36.81	-81.57	49	0.087	Middle Fork Holston River
36.85	-81.46	43	0.095	Middle Fork Holston River
36.61	-82.87	27	0	North Fork Clinch River-Clinch River

36.59	-83	27	0	North Fork Clinch River-Clinch River
36.55	-83.08	29	0	North Fork Clinch River-Clinch River
36.6	-82.89	31	0	North Fork Clinch River-Clinch River
36.54	-83.1	37	0	North Fork Clinch River-Clinch River
36.68	-82.88	38	0	North Fork Clinch River-Clinch River
36.63	-82.9	39	0	North Fork Clinch River-Clinch River
36.65	-82.75	40	0	North Fork Clinch River-Clinch River
36.55	-83.1	40	0	North Fork Clinch River-Clinch River
36.66	-82.89	43	0	North Fork Clinch River-Clinch River
36.64	-82.88	47	0	North Fork Clinch River-Clinch River
36.59	-83.01	48	0	North Fork Clinch River-Clinch River
36.58	-83.02	49	0	North Fork Clinch River-Clinch River
36.58	-83.03	50	0	North Fork Clinch River-Clinch River
36.63	-82.76	44	0.022	North Fork Clinch River-Clinch River
36.6	-82.97	25	0.062	North Fork Clinch River-Clinch River
36.58	-83.03	37	0.069	North Fork Clinch River-Clinch River
36.62	-82.79	27	0.089	North Fork Clinch River-Clinch River
36.65	-81.81	37	0	Rowland Creek-South Fork Holston River
36.85	-82.72	29	0	South Fork Powell River-Powell River
36.83	-82.5	25	0	Stony Creek-Clinch River
36.81	-82.49	25	0	Stony Creek-Clinch River
36.68	-82.72	25	0	Stony Creek-Clinch River
36.75	-82.6	30	0	Stony Creek-Clinch River
36.7	-82.69	32	0	Stony Creek-Clinch River
36.83	-82.46	34	0	Stony Creek-Clinch River
36.74	-82.61	35	0	Stony Creek-Clinch River
36.7	-82.66	36	0	Stony Creek-Clinch River
36.81	-82.53	37	0	Stony Creek-Clinch River
36.82	-82.54	41	0	Stony Creek-Clinch River
36.82	-82.47	42	0	Stony Creek-Clinch River
36.72	-82.68	42	0	Stony Creek-Clinch River
36.69	-82.69	42	0	Stony Creek-Clinch River
36.81	-82.49	44	0	Stony Creek-Clinch River
36.78	-82.55	44	0	Stony Creek-Clinch River
36.83	-82.44	48	0	Stony Creek-Clinch River
36.81	-82.5	48	0	Stony Creek-Clinch River
36.76	-82.61	49	0	Stony Creek-Clinch River
36.79	-82.53	37	0.021	Stony Creek-Clinch River
36.71	-82.69	41	0.024	Stony Creek-Clinch River
36.79	-82.55	33	0.038	Stony Creek-Clinch River
36.73	-82.68	36	0.039	Stony Creek-Clinch River
36.76	-82.57	44	0.053	Stony Creek-Clinch River
36.76	-82.59	35	0.061	Stony Creek-Clinch River
36.8	-82.51	39	0.061	Stony Creek-Clinch River
36.82	-82.44	33	0.071	Stony Creek-Clinch River

36.76	-82.63	39	0.079	Stony Creek-Clinch River
36.7	-82.73	45	0.079	Stony Creek-Clinch River
37.11	-81.58	25	0	Swords Creek-Clinch River
37.02	-81.96	25	0	Swords Creek-Clinch River
37.17	-81.52	26	0	Swords Creek-Clinch River
37.09	-81.82	26	0	Swords Creek-Clinch River
37.07	-81.86	27	0	Swords Creek-Clinch River
37.02	-81.87	27	0	Swords Creek-Clinch River
37.03	-81.91	29	0	Swords Creek-Clinch River
37.14	-81.52	30	0	Swords Creek-Clinch River
37.06	-81.91	30	0	Swords Creek-Clinch River
37.13	-81.5	32	0	Swords Creek-Clinch River
37.13	-81.49	32	0	Swords Creek-Clinch River
37.12	-81.6	32	0	Swords Creek-Clinch River
37.17	-81.79	32	0	Swords Creek-Clinch River
37	-81.93	32	0	Swords Creek-Clinch River
37.17	-81.54	33	0	Swords Creek-Clinch River
37.14	-81.47	33	0	Swords Creek-Clinch River
37.13	-81.55	33	0	Swords Creek-Clinch River
37.12	-81.55	35	0	Swords Creek-Clinch River
37.08	-81.61	36	0	Swords Creek-Clinch River
37.09	-81.86	36	0	Swords Creek-Clinch River
37.14	-81.48	37	0	Swords Creek-Clinch River
37.1	-81.54	37	0	Swords Creek-Clinch River
37.17	-81.47	38	0	Swords Creek-Clinch River
37.07	-81.85	39	0	Swords Creek-Clinch River
37.16	-81.48	41	0	Swords Creek-Clinch River
37.09	-81.83	41	0	Swords Creek-Clinch River
37.12	-81.49	42	0	Swords Creek-Clinch River
37.01	-81.9	43	0	Swords Creek-Clinch River
37.07	-81.49	44	0	Swords Creek-Clinch River
37.05	-81.81	44	0	Swords Creek-Clinch River
37.06	-81.59	46	0	Swords Creek-Clinch River
37.16	-81.47	47	0	Swords Creek-Clinch River
37.19	-81.45	48	0	Swords Creek-Clinch River
37.15	-81.54	48	0	Swords Creek-Clinch River
37.15	-81.48	50	0	Swords Creek-Clinch River
37.08	-81.85	50	0	Swords Creek-Clinch River
37.03	-81.85	25	0.008	Swords Creek-Clinch River
37.15	-81.49	42	0.009	Swords Creek-Clinch River
37.13	-81.51	34	0.012	Swords Creek-Clinch River
37.17	-81.45	39	0.014	Swords Creek-Clinch River
37.06	-81.88	34	0.026	Swords Creek-Clinch River
37.16	-81.5	32	0.035	Swords Creek-Clinch River
37.12	-81.44	25	0.038	Swords Creek-Clinch River

37.09	-81.55	35	0.039	Swords Creek-Clinch River
37.13	-81.56	47	0.041	Swords Creek-Clinch River
37.13	-81.56	39	0.048	Swords Creek-Clinch River
37.09	-81.55	50	0.056	Swords Creek-Clinch River
37.19	-81.47	40	0.064	Swords Creek-Clinch River
37.17	-81.44	26	0.083	Swords Creek-Clinch River
37.09	-81.58	50	0.096	Swords Creek-Clinch River
37.14	-81.44	36	0.099	Swords Creek-Clinch River
36.9	-81.77	27	0	Tumbling Creek-North Fork Holston River
36.93	-81.68	28	0	Tumbling Creek-North Fork Holston River
36.86	-81.75	29	0	Tumbling Creek-North Fork Holston River
36.88	-81.7	32	0	Tumbling Creek-North Fork Holston River
36.9	-81.72	34	0	Tumbling Creek-North Fork Holston River
36.92	-81.75	35	0	Tumbling Creek-North Fork Holston River
36.91	-81.72	38	0	Tumbling Creek-North Fork Holston River
36.89	-81.78	38	0	Tumbling Creek-North Fork Holston River
36.91	-81.74	39	0	Tumbling Creek-North Fork Holston River
36.92	-81.73	41	0	Tumbling Creek-North Fork Holston River
36.85	-81.73	41	0	Tumbling Creek-North Fork Holston River
36.91	-81.74	43	0	Tumbling Creek-North Fork Holston River
36.91	-81.75	44	0	Tumbling Creek-North Fork Holston River
36.89	-81.77	44	0	Tumbling Creek-North Fork Holston River
36.89	-81.72	36	0.02	Tumbling Creek-North Fork Holston River
36.88	-81.66	37	0.028	Tumbling Creek-North Fork Holston River
36.9	-81.75	26	0.037	Tumbling Creek-North Fork Holston River
36.88	-81.74	36	0.045	Tumbling Creek-North Fork Holston River
36.65	-83.25	25	0	Wallen Creek-Powell River
36.63	-83.17	27	0	Wallen Creek-Powell River
36.65	-83.22	27	0	Wallen Creek-Powell River
36.63	-83.29	27	0	Wallen Creek-Powell River
36.59	-83.32	29	0	Wallen Creek-Powell River
36.63	-83.17	30	0	Wallen Creek-Powell River
36.59	-83.33	35	0	Wallen Creek-Powell River
36.61	-83.33	40	0	Wallen Creek-Powell River
36.6	-83.35	40	0	Wallen Creek-Powell River
36.62	-83.2	41	0	Wallen Creek-Powell River
36.58	-83.33	45	0	Wallen Creek-Powell River
36.62	-83.25	47	0	Wallen Creek-Powell River
36.61	-83.27	47	0	Wallen Creek-Powell River
36.67	-83.14	48	0	Wallen Creek-Powell River
36.65	-83.23	50	0	Wallen Creek-Powell River
36.61	-83.3	29	0.008	Wallen Creek-Powell River
36.63	-83.26	49	0.017	Wallen Creek-Powell River
36.69	-83.14	25	0.036	Wallen Creek-Powell River
36.62	-83.2	29	0.036	Wallen Creek-Powell River

36.59	-83.32	29	0.038	Wallen Creek-Powell River
36.63	-83.24	35	0.039	Wallen Creek-Powell River
36.61	-83.24	34	0.066	Wallen Creek-Powell River
36.67	-83.17	27	0.073	Wallen Creek-Powell River
36.64	-83.27	38	0.082	Wallen Creek-Powell River
36.71	-83.22	35	0.087	Wallen Creek-Powell River
36.7	-83.14	25	0.088	Wallen Creek-Powell River
36.62	-83.26	26	0.089	Wallen Creek-Powell River
36.6	-83.3	33	0.096	Wallen Creek-Powell River

Acknowledgments

Under ordinary circumstances, Paul L. Angermeier (USGS, Virginia Cooperative Fish and Wildlife Research Unit, Virginia Tech) would have been a co-author on this report since he contributed significantly to the study design, editing, and administration. However, the USGS has imposed an onerous, lengthy process for approving final reports to sponsors of Unit projects; the process incurs excessive time and/or monetary costs. To avoid these costs, which would not improve the content, quality, or utility of the final report, he chose to withdraw his name from authorship.

References

- Barbour, M. T., J. Gerritsen, B. D. Snyder, and J. B. Stribling. 1999. Rapid bioassessment protocols for use in streams and wadeable rivers: Periphyton, benthic macroinvertebrates and fish, Second Edition. EPA 841-B-99-002. U.S. Environmental Protection Agency, Office of Water, Washington, D.C.
- Baker M., R. King, D. Kahle. 2023. TITAN2: Threshold indicator taxa analysis. R package version 2.4.2. <https://CRAN.R-project.org/package=TITAN2>
- Bates, D., M. Maechler, B. Bolker, and S. Walker. 2015. Fitting linear mixed-effects models using lme4. *Journal of Statistical Software* 67: 1–48.
- Bhandari, R., R. Thakali, G. A. Kandissounon, A. Kalra, and S. Ahmad. 2018. Effects of soil data resolution on the simulated stream flow and water quality: Application of watershed-based SWAT model. *World Environmental and Water Resources Congress 2018*, Minneapolis, MN.
- Bieger, K., J. G. Arnold, H. Rathjens, M. J. White, D. D. Bosch, P. M. Allen, M. Volk, and R. Srinivasan. 2017. Introduction to SWAT+, a completely restructured version of the Soil and Water Assessment Tool. *Journal of the American Water Resources Association* 53:115–130.

- Bieger, K., H. Rathjens, P. M. Allen, J.G. Arnold. 2015. Development and evaluation of bankfull hydraulic geometry relationships for the physiographic regions of the United States. *Journal of the American Water Resources Association* 51:842–858.
- Boomer, K. B., D. E. Weller, and T. E. Jordan. 2008. Empirical models based on the Universal Soil Loss Equation fail to predict sediment discharges from Chesapeake Bay catchments. *Journal of Environmental Quality* 37: 79–89.
- Buhr, D. X., R. W. Lammers, and B. P. Bledsoe. 2022. Global sensitivity analyses of key riparian nitrogen models. *Environmental Modelling and Software* 158:105542.
- Burton, J., and J. Gerritsen. 2003. A stream condition index for Virginia non-coastal streams. Tetra Tech Inc., Owings Mill, MD.
- Chesapeake Bay Program. 2020. Chesapeake Assessment and Scenario Tool (CAST) Version 2019. Chesapeake Bay Program Office, Annapolis.
- Dile, Y., R. Srinivasan, and C. George. 2023. QGIS interface for SWAT+: QSWAT+. Texas AM University, TX.
- Fong Y., Y. Huang, P. Gilbert, and S. Permar. 2017. chngpt: Threshold regression model estimation and inference. *BMC Bioinformatics* 18:454.
- Gassman, P. 2023. SWAT literature database for peer-reviewed journal articles. https://www.card.iastate.edu/swat_articles/
- Hamilton, S. K. 2012. Biogeochemical time lags may delay responses of streams to ecological restoration. *Freshwater Biology* 57:43–57.
- Her, Y., J. Frankenberger, I. Chaubey, and R. Srinivasan 2015. Threshold effects in HRU definition of the soil and water assessment tool. *Transactions of the ASABE* 58:367–378.
- James, C. 2022. SWAT+ Toolbox. <https://celray.github.io/docs/swatplus-toolbox/v1.0/index.html>
- Martin, Z. M. 2019. Relating fine sediment dynamics and best management practices (BMPs) to instream habitat conditions for priority fishes and mussels in the Copper Creek Watershed. Virginia Department of Game and Inland Fisheries, Blacksburg, VA.
- Meals, D. W., S. A. Dressing, and T. E. Davenport. 2010. Lag time in water quality response to best management practices: A review. *Journal of Environmental Quality* 39:85–96.

- Moriiasi, D. N., J. G. Arnold, M. W. Van Liew, R. L. Bingner, R. D. Harmel, and T. L. Veith. 2007. Model evaluation guidelines for systematic quantification of accuracy in watershed simulations. *Transactions of the ASABE* 50:885–900.
- Mouser, J. B. 2024. Using an interdisciplinary approach to improve efficacy of agricultural conservation practices for protecting stream health.
- Natural Resources Conservation Service. 2019a. Conservation practices. https://www.nrcs.usda.gov/wps/portal/nrcs/detailfull/-tio-l/technical/cp/ncps/?cid=nr143_026849.
- Natural Resources Conservation Service. 2019b. Web soil survey. <https://websoilsurvey.sc.egov.usda.gov/App/WebSoilSurvey.aspx>. Accessed 21 July 2020.
- Noe, G. B., K. G. Hopkins, P. R. Claggett, E. R. Schenk, M. J. Metes, L. Ahmed, T. R. Doody, and C. R. Hupp. 2022. Streambank and floodplain geomorphic change and contribution to watershed material budgets. *Environmental Research Letters* 17:064015.
- PRISM Climate Group. 2020. Data explorer: Download time series values in bulk. <https://prism.oregonstate.edu/explorer/bulk.php>. Accessed 4 August 2020.
- R Core Team (2023). R: A language and environment for statistical computing. R Foundation for Statistical Computing. <https://www.R-project.org/>
- Shimizu G. and L. Goncalves. 2023. *_AgroReg: Regression analysis linear and nonlinear for agriculture*. R package version 1.2.9. <https://CRAN.R-project.org/package=AgroReg>.
- Singh, S., S. Hwang, J. G. Arnold, and R. Bhattarai. 2023. Evaluation of agricultural BMPs' impact on water quality and crop production using SWAT+ model. *Agriculture* 13:1484.
- Tech, J. 2023. SWAT+ editor documentation. Texas AM University, TX.
- U.S. Environmental Protection Agency and U.S. Geological Survey. 2012. National hydrography dataset plus – NHDPlus. https://nhdplus.com/NHDPlus/NHDPlusV2_data.php. Accessed 10 January 2020.
- U.S. Geological Survey. 2019a. USGS NED 1 arc-second n37w082 1 x 1 degree ArcGrid 2019 Geospatial_Data_Presentation_Form: raster digital data. <https://viewer.nationalmap.gov/advanced-viewer/>. Accessed 18 June 2020.
- U.S. Geological Survey. 2019b. NLCD 2016 land cover conterminous United States. <https://www.mrlc.gov/>. Accessed 25 April 2020.

- U.S. Geological Survey. 2020. USGS current water data for Virginia.
<https://waterdata.usgs.gov/va/nwis/rt>. Accessed 4 December 2020.
- Virginia Department of Environmental Quality. (2004). Total Maximum Daily Load (TMDL) development for the Upper Clinch River Watershed.
- Virginia Department of Environmental Quality. (2009). Bacteria and benthic Total Maximum Daily Load development for Middle Fork Holston River.
- Virginia Department of Environmental Quality. (2014). Bacteria and sediment TMDL development Lower Clinch River Watershed, VA.
- Virginia Department of Conservation and Recreation. 2019. Virginia agricultural cost share manual. <http://consapps.dcr.virginia.gov/htdocs/agbmpman/agbmptoc.htm>.
- Virginia Department of Environmental Quality. 2021. DEQ environmental data mapper. <https://apps.deq.virginia.gov/EDM/> Accessed 10 December 2021.
- Wallington, K., and X. Cai. 2023. Updating SWAT+ to clarify understanding of in-stream phosphorus retention and remobilization: SWAT+P.R&R. *Water Resources Research* 59:e2022WR033283.
- Wallington, K., X. Cai, and M. Kalcic. 2024. Evaluating the longevity of in-stream phosphorus legacies: A downstream cascade of recovery following point source remediation. *Science of the Total Environment* 912:168711.
- Wang X., and A. M. Melesse. 2006. Effects of STATSGO and SSURGO as inputs on SWAT model's snowmelt simulation. *Journal of the American Water Resources Association* 42:1217–1246.
- Wei, X., R. T. Bailey, R. M. Records, T. C. Wible, and M. Arabi. 2019. Comprehensive simulation of nitrate transport in coupled surface-subsurface hydrologic systems using the linked SWAT-MODFLOW-RT3D model. *Environmental Modelling and Software* 122:104242
- Wolman, M. G. 1954. A method of sampling coarse river-bed material. *EOS, Transactions American Geophysical Union* 35:951–956.